DSPACE

https://dspace.org/

Gasification of high ash coal and chars from South African coals

Oboirien, Bilainu Obozokhai

2012-07-06
http://hdl.handle.net/10539/11625

Downloaded from a DSpace repository. https://dspace.org/

GASIFICATION OF HIGH ASH COAL AND CHARS FROM SOUTH AFRICAN COALS

Bilainu Obozokhai Oboirien

A Thesis submitted to the Faculty of Engineering and the Built Environment, University of the Witwatersrand, in fulfilment of the requirements for the degree of Doctor of Philosophy.

Johannesburg 2011

DECLARATION

I declare that this thesis is my own, unaided work. It is being submitted for the Degree of Doctor of Philosophy to the University of the Witwatersrand, Johannesburg. It has not been submitted before for any degree or examination in any other University.

Day of…….2011

ABSTRACT

This study seeks to explore the behaviour of several different South African bituminous coals currently used as feed in local power stations and to establish their technical performance and structural changes in a fluidised bed gasifier. It is anticipated that this would also assist in optimising gasifier operations for the gasification of fine high ash coals for power generation. The research was conducted by correlating the gasification performance of the selected coals and their derived chars against a range of chemical, physical and optical characteristics including mineral and maceral (and specifically inertinite) contents after testing in a pilot scale fluidised bed gasifier. Of specific interest were the changes in chemical microstructures during the transformation of the various coal macerals to their relevant chars following gasification. Raman spectroscopy and XRD analyses were used to examine the chemical carbon structures and the minerals associated in the coal. The relationship between the organic components and their gasified products (macerals-to-char) and the inorganic components to their gasified products (minerals-to-ash) including their physical structure and behaviour was determined by petrographic analysis.

A higher loss of coal reactivity was obtained from vitrinites-rich coals due to a higher degree of structural transformation of carbon in the coal. Inertinite-rich coals experienced a lower loss of coal reactivity and lower degree of structural transformation even with longer residence time. The structural transformation of the macerals is due to realignment of the carbon molecules leading to substantial swelling (enhanced plasticity) in some macerals. Further modification was found to be due to proximity to melted minerals. Furthermore, the gasification performance of low grade coals can be optimised by varying the oxygen content used for coal gasification.

ACKNOWLEDGEMENTS

First, I thank the almighty God for His mercies and protection during the planning and execution of this thesis.

I would like to express my sincere gratitude to my supervisor Prof Rosemary Falcon for her guidance, trust, encouragement and care.

I would also want to thank Mr Brian North for his informative discussion and support during course of this project. Mr Andre Engelbrecht for his help in char generation from pilot–scale gasification test. Mr Aston for the operation of the laboratory scale fluidised bed reactor. Mr Alphius Bokaba his help with coal preparation. Dr Sabine Verryn for her help with the XRD analysis, Ms Vivien du Cann for petrographic analysis, and Rudolph Erasmus for Raman mapping studies for their help in the characterisation

My gratitude is also extended to my colleagues who helped me during the research and writing of this dissertation. Also, I express my profound appreciation to all my friends for their support throughout the course of my study. My appreciation is expressed to Mr & Mrs Rabiu, Mr & Mrs Raji, Mr & Mrs Obayopo, Dr & Mrs Ibrahim, Dr & Mrs Salisu, Dr & Mrs Adeleke, Dr & Mrs Adebesin, Drs Odusote and Agboola.

I would like to thank the CSIR for their financial support for this project.

Finally I would like to thank my parents Mr and Mrs Oboirien, for their constant love and support and my brothers and sisters for their prayers. My most special thanks to my wife, Kafayat, and our kids for their patience, sacrifices, encouragement, love and support all these years.

Table of Contents

TITLE PAGE……i
DECLARATION……..ii
ABSTRACT……iii
ACKNOWLEDGEMENTS……....iv
TABLE OF CONTENT……...v
LIST OF FIGURES……..viii
LIST OF TABLES……...x
NOMECLATURE ……xi

CHAPTER 1 INTRODUCTION 1
1.1 Background and research motivation 1
1.2 Aims and objectives 5
1.3 Research questions 5
1.4 Hypothesis 6
1.5 Outline of the thesis 6

CHAPTER 2. LITERATURE REVIEW 7
2.1 Gasification: Introduction 7
2.2 Power generation from coal gasification of low grade coals 9
2.3 Fluidised bed gasification of low grade coals 11
2.4 Char deactivation in a fluidised bed gasifier 11
2.5 Coal properties 15
2.5.1 Maceral composition 15
2.5.2 Rank 18
2.5.3 Mineral matter content 19
2.6 Reaction conditions 25
2.7 Analytical techniques to study interaction char-mineral during gasification 26
2.7.1 General review of analytical techniques in the characterisation of coal char structure 27
2.7.1.1 Real density measurement 27
2.7.1.2 X-ray Diffraction technique (XRD) 27
2.7.1. 3 FTIR 28
2.7.1.4 Raman spectroscopy. 28
2.7.2 Review of analytical techniques of char-mineral matter interaction 29
2.8 Conclusion and work program of this thesis 30

CHAPTER 3 EXPERIMENTAL AND TOOLS 32
3.1 Introduction 32
3.2 Coal samples 32
3.3 Bench-scale fluidised bed experiment 34
3.3.1 Char Reactivity measurements 34
3.4 Pilot-plant experiments 34
3.4.1 Description of the test facility 35
3.4.2 Feeding system 35

3.4.3 Air and steam supply system 36
3.4.4 Gasifier 36
3.4.5 Test procedure 37
3.5 Char characterisation 38
3.5.1 Chemical analysis 38
3.5.2 Petrographic analysis 39
3.5.3 FT-IR spectrometry 40
3.5.4.Fourier Transform Raman Spectroscopy 40
3.5.6 X-ray Diffraction 41
3.5.7 Scanning Electron Microscopy 41
3.5.8 Specific surface area measurements 42
3.5.9 Carbon conversion 42

CHAPTER 4: CHARACTERISATION OF SOUTH AFRICAN COAL AND CHARS IN FLUIDISED BED GASIFICATION 43
4.1 Introduction 43
4.2 Experimental 43
4.3 Results and discussion 44
4.3.1Proximate and ultimate analysis 44
4.3.2 Petrographic analysis 48
4.3.2.1 Reflectance properties 48
4.3.2.2 Carbon form analysis 51
4.3.3 Structural characteristics of raw coals and chars 57
4.3.3.1 Aromaticity 57
4.3.3.2 Coke Forms 58
4.3.3.3 Raman Analysis 59
4.3.3.4X-ray diffraction Analysis (XRD) 62
4.3.3.5 FTIR Analysis 68
4.3.3.6 Surface area analysis (BET results) 70
4.4 Conclusions 71

CHAPTER 5 TEXTURAL PROPERTIES OF CHARS AS DETERMINED BY PETROGRAPHIC ANALYSIS: COMPARISON BETWEEN AIR-BLOWN, OXYGEN-BLOWN AND OXYGEN-ENRICHED GASIFICATION 73
5.1 Introduction 73
5.2 Experimental 74
5.2.1 Parent coal sample and gasification 74
5.3 Results and discussion 75
5.3.1 Reflectance properties and carbon forms 75
5.3 2 Inorganic mineral and organic maceral associations 79
5.4. Correlation to previous workers' concepts 82
5.5 Conclusions 82

CHAPTER 6 MINERAL-CHAR INTERACTION DURING GASIFICATION OF HIGH ASH COALS IN FLUIDISED BED GASIFICATION 85
6.1 Introduction 85
6.2 Experimental 85
6.3 Results and discussion 88
6.3.1 Carbon and ash analyses of char samples 88
6.3.2 Carbon structure of the chars samples 90

6.3.3 Characterisation of minerals phases in the char samples 92
6.3.4 Char-mineral interaction 95
6.3.5 Modelling of char-mineral interaction of high ash coals during fluidised bed gasification 102
6.4 Conclusions 107

CHAPTER 7 CONCLUSIONS AND RECOMMENDATIONS 109
7.1 Conclusions 109
7.2 Recommendations 113
References 114
Appendix A Char reflectance data 127
Appendix B Raman parameters used for the constrcution of Raman maps 131
Appendix C List of Publications 132

List of Figures

Figure 2.1 A schematic representation of the gasification process……..8
Figure 2.2 Mineral transformation in coal……..21
Figure 3.1 A schematic diagram of the FBG pilot plant……....35
Figure 3.2 Dimension and details of the FBG furnace……...37
Figure 4.1 Comparison of proximate analyses of Malta coal and its chars……....45
Figure 4.2 Comparison of fixed carbon content of parent coal and fixed carbon Conversion……46
Figure 4.3 Coal/Char total maceral reflectance histogram……50
Figure 4.4a Thin-walled isotropic coke……....52
Figure 4.4b Thick-walled isotropic coke……..52
Figure 4.5a Mixed porous from reactive coal particles……....53
Figure 4.5b Inerts-rich coal particle……53
Figure 4.6 Dense char from pure inertinite……53
Figure 4.7 Partially consumed carbon body with darker borders and zone……...55
Figure 4.8 "Slag" penerating carbon matrix in cracks and fissures.....56
Figure 4.9 Raman spectra of Matla char with corresponding curve fitted bands.....60
Figure 4.10 Raman spectra of Duhva char with corresponding curve fitted bands.....60
Figure 4.11 Raman spectra of Grootegeluk char with corresponding curve fitted bands 61
Figure 4.12 XRD pattern for the Duhva coal and char.....64
Figure 4.13 XRD pattern for the Matla coal and char.....65
Figure 4.14 XRD pattern for the Grootegeluk coal and char.....67
Figure 4.15 FT-IR spectra for Duhva coal and char.....68
Figure 4.16 FT-IR spectra for Matla coal and char.....69
Figure 4.17 FT-IR spectra for Grootegeluk coal and char.....69
Figure 5.1Char reflectance histogram for O_2-blown, O_2-enrinched and air blown derived form the gasification of Grootegeluk coal.....76
Figure 5.2a Thin-walled isotropic coke.....77
Figure 5.2b Thick-walled isotropic coke.....77
Figure 5.2c Relatively unchanged inertinite.....77
Figure 5.2d Partially consumed carbon.....77
Figure 5.3 Correlation between thin-walled highly porous isotropic coke and melted and melted minerals surrounding/penetrating carbon.....81
Figure 5.4a Melted "slag' minerals-penetrating /surrounding carbon.....82
Figure 5.4b Melted "slag' minerals as a separate body.....82
Figure 6.1 Raman spectra of Grootegeluk chars at 910 ^oC and 1000 ^oC.....90
Figure 6.2 Raman spectra of New Vaal chars at 910 ^oC and 1000 ^oC.....91
Figure 6.3 XRD diffractogram of Grootegeluk char at 1000 ^oC and 35mins.....92
Figure 6.4 Mineral matter in Grootegeluk char at different temperatures and residence Time.....93
Figure 6.5 Mineral matter in New Vaal char at different temperatures and residence time.....94
Figure 6.6 SEM images illustrating discrete agglomerate minerals distribution in a Grootegeluk char.....96

Figure 6.7 SEM images illustrating disseminated minerals distribution in a Grootegeluk char.....97

Figure 6.8 X-ray mapping of discrete agglomerates for Grootegeluk char generated at 960 ^{o}C and 30 mins under oxygen-enriched gasification conditions.....98
Figure 6.9 X-ray mapping of disseminated mineral distribution in a Grootegeluk char generated at 960 ^{o}C and 30 mins under oxygen-enriched gasification conditions.....99
Figure 6.10 I_D/I_G mapping of Grootegeluk char with minerals in disseminated Phases.....100
Figure 6.11 I_D/I_G mapping of New Vaal char with minerals in disseminated phase..101
Figure 6.12 I_V/I_G mapping of Grootegeluk char with minerals in disseminated Phases.....102
Figure 6.13 I_V/I_G mapping of New Vaal char with minerals in disseminated phases 102
Figure 6.14 Gasification rate vs carbon conversion of Grootegeluk coal and chars..105
Figure 6.15 Gasification rate vs carbon conversion of New Vaal coal and chars.....106
Figure 6.16 Estimation of reaction order of New Vaal coal.....106

List of Tables

Table 3.1 Properties of the different coals 33
Table 3.2 Details of test work performed in the pilot-plant.....38
Table 4.1 Gasification operating conditions.....44
Table 4.2 Proximate and ultimate analysis and calorific value of the parent coals.....46
Table 4.3 Proximate and ultimate analysis and calorific vale of bed char.....47
Table 4.4 Proximate and ultimate analysis and calorific value of cyclone chars.....47
Table 4.5 Summary of the major petrographic properties of the parent coals.....49
Table 4.6 Summary of the reflectance properties of the char samples.....50
Table 4.7 Relative proportions of the various char formed 51
Table 4.8 Petrographic composition of chars.....57
Table 4.9 Aromaticity of the different coals and chars.....58
Table 4.10 Raman spectroscopic parameters obtained after curve fitting the Experimental data points by using two-lorentzian bands (D and G).....62
Table 4.11 Surface area of the different coal ad char samples.....71
Table 4.12 Evolution of surface area for Grootegeluk char samples.....71
Table 5.1 Details of gasification tests carried out under air-blown, oxygen-blown and Oxygen-enriched conditions.....74
Table 5.2 Carbon form analysis.....77
Table 5.3 Organic/inorganic constituents.....81
Table 6.1a Proximate, ultimate and as chemistry data for New Vaal coal and Grootegeluk coal samples 86
Table 6.1b Proximate, ultimate and as chemistry data for New Vaal coal and Grootegeluk coal samples 87
Table 6.1c Coal mineralogy data for New Vaal coal and Grootegeluk coal samples87
Table 6.2a Test conditions for Grootegeluk coal.....87
Table 6.2b Test conditions for New Vaal coal.....88
Table 6.3 Organic/inorganic constituents of Grootegeluk char samples.....89
Table 6.4 Organic/inorganic constituents of New Vaal char samples.....89
Table 6.5 Comparison of intrinsic reaction rate of Grootegeluk coal chars and New Vaal coal chars.....107

NOMENCLATURE

CAPITALS

Fm	Fraction of the surface occupied by the melted minerals
R	Relative reactivity
S	Specific surface area
V_p	Volume of the particle

LOWER CASE

C_{daf}	Carbon on dry ash free basis
f_a	Aromaticity
k	Reaction constant
n	Reaction order
q_g	Global or overall rate
q_i	Intrinsic rate
$q_{0.5}$	Gasification rate at 50% carbon conversion
t_{50}	Time for fractional conversion of 0.5
x	Carbon conversion
V_{daf}	Volatile matter on air dry basis

GREEK SYMBOLS

ρ_c	Apparent density of carbon

ACRONYMS

BET	Brunaer Emmett Teller
CSIR	Council for Scientific and Industrial Research (South Africa)
FBG	Fluidised Bed Gasification
FTIR	Fourier Transform Infrared Resonance
IGCC	Integrated Gasification Combined cycle
ISO	International Standards Organisation
SEM	Scanning Electron Microscopy
XRD	X-ray diffraction
TGA	Thermo gravimetric

CHAPTER 1 INTRODUCTION

1.1 Background and research motivation

The electricity demand in South Africa is increasing at a rate of 1 000 MW per year (Inlgesi and Pouri, 2010). While there is increasing pressure to adopt non-fossil fuel electricity-generating technologies, the abundant reserves and low cost of coal makes it the preferred energy source to meet increasing demands for the foreseeable future. It is also foreseen that coal-based generation is likely to provide 50% of this demand (IRP 2010). The challenge in the future is to enhance both the efficiency and environmental acceptability of coal use by adopting clean coal technologies (CCTs). CCTs are defined as "technologies designed to enhance the efficiency and the environmental acceptability of coal extraction, preparation and use (Henderson, 2003). The increased efficiency of clean coal technologies results in reduced CO_2 emissions for a specified electric output (Androutsopoulos and Hatzilyberis, 2001). Also the emission of other environmental pollutants such as NO_x, SO_x and particulates are significantly reduced (Harris *et al.* 2003)

Coal is a heterogeneous material consisting of organic and inorganic matter (Taylor *et al.* 1998). The organic matter is referred to as macerals while the inorganic matter is known as minerals. The mineral matter either exists separately or it is associated within the carbonaceous materials (macerals) (Matsuoka *et al*. 2006). The mineral matter could account for 50 wt% and it is distributed in various forms (Shiraz *et al.* 1995).

One important coal utilisation process in the suite of clean coal technologies is coal gasification. Here solid coal is converted into gaseous fuel used to power a turbine and thereby to generate power. With gasification, power station generation efficiencies can be improved from 35%, using coal combustion, to between 45% and 55% (Schimmoller, 2005). The emissions of CO_2 into the atmosphere can also be reduced. During gasification, the organic and inorganic matter undergoes various chemical and physical transformations.

In order to maximise the gasification efficiency, it is essential to understand the mechanism for the chemical and physical transformation. This will assist in the reduction of carbon emissions in the process especially when gasifying low rank coals. Coal gasification is becoming an attractive alternative for power generation since it offers higher efficiency and improved environmental performance than conventional pulverised fuel technology carried out in combustion boilers (Cousins *et al*. 2007). The volume of gas produced from gasification is much less compared to that obtained from combustion systems. The reduced volume of gas will require smaller equipment for CO_2 capture and hence results in lower cost and lower emission (Collot, 2006).

Several options are used to control the feedrate of coal during gasification, namely fixed bed, fluidised bed and entrained–flow systems. Fluidised bed gasifiers have the potential advantage that low-grade coals rich in ash and inertinites can be processed more efficiently than in conventional pulverised coal boilers. (Cousin *et al*. 2007; Everson *et al.* 2008). The higher efficiency that coal gasification offers could be used as a strategy for carbon abatement in the future. A potential disadvantage of fluidised bed coal gasification is low carbon conversion in comparison to other types of gasifiers. This is due to its low operating temperature (900-1050 ^{o}C) and rapid loss of coal reactivity (Cousins *et al*. 2007; Collot, 2006). The rapid loss of coal reactivity reported by Cousins and his co-workers are for porous chars derived from relatively vitrinite-rich coals with low ash yield. There is little research reported on the change in reactivity during the gasification of high inertinite coals especially those with high ash yield in a fluidised bed gasifier. These coals are presently used as feed in local power stations in South Africa. The use of these coals is characterised by high ash content and rich in inertinites presents a (further) challenge as a result of the presence of dense chars formed from the non-reactive inertinites. The dense char structure will require a longer reaction time using low temperature gasifiers such as fluidised bed reactors. The long residence time could lead to structural reorganisation in the solid char and anneal it. This can further decrease the char reactivity due to the loss of carbon active site (Senneca *et al.* 1998; Cousin *et al*. 2007).

A viable solution for the gasification of high ash and other low quality coals is the use of oxygen-enriched air as a gasification agent (Belyaev, 2003). The use of oxygen enriched air can lead to higher reactivity of coal particles (Rathnam *et al.* 2009). This significantly increases the calorific value of the synthesis gas obtained. The use of enriched air reduces the nitrogen dilution effect in air blown gasification, thereby increasing the gasification temperature. This allows for the addition of higher quantity of steam to maintaining the thermal level in the gasifier (Campoy *et al.* 2009). The appropriate combination of temperature and steam leads to higher carbon conversion and gasification efficiency.

There is relatively little work on the fluidised bed gasification of inertinite rich, high ash coals using enriched-air-system mixtures as gasification agent. In this type of gasifier, a better understanding of the forms of chars derived from inertinites and their reactivities at different operating conditions is clearly necessary given the nature of South African coals especially under enriched air and steam gasification conditions.

The change in carbonaceous structure is stated to be one of the key factors that affect the rate of gasification (Sekine *et al.* 2006; Li, 2007). Also, given that the dispersion of mineral matter changes when there is a change in char structure and that minerals act as catalysts for coal gasification, these facts also impact upon the rate of gasification (Li, 2007; Zhang *et al.* 2008). The change in carbonaceous structure is due to the modification of the organic and inorganic constituents of coal (Senneca *et al*. 1998; Sekine *et al*. 2006; Sheng, 2007). The different organic components present in coal react differently when gasified. Senneca *et al.* (1998) investigated the microstructural changes and loss of gasification reactivity of two types of coal, namely Ruhr coal (Ru) and a South African coal (SA) at different temperatures (900-1400 ^{O}C). These coal samples were similar in rank but different in the maceral composition. The Ruhr coal was reported to be vitrinite-rich and the South African coal was inertinite-rich. The researchers observed that there were clear differences between the two coals and modification of their structures. They concluded that the cause could have been the difference in the inertinite and vitrinite content.

In addition to the organic component, the inorganic component of coal can also have an effect on the evolution of the char microstructure and reactivity (Linden *et al*. 1998; Sheng, 2007; Bai *et al*. 2009). Lunden *et al.* (1998) reported that mineral matter can interact with the carbonaceous matrix to decrease char reactivity either by blocking access to carbon active sites hence reducing the available carbon per unit area in the char or by increasing carbon crystallite growth. They hypothesised that the same molecular strain from the mineral particle that prevents or promotes carbon ordering may also resist penetration of oxygen into the carbon matrix. However they could not distinguish between the effects of mineral matter on carbon ordering and molecular–level reactivity due to inadequate experimental technique.

In another study, Zhang *et al*. (2009) studied the effect of included minerals on the reactivity of chars. They reported that included minerals facilitate the formation of pores within low ash chars but inhibits the formation of pores for high ash chars. They suggested this observation indicates different forms of interaction between the mineral matter. In the dense char with negligible metastable liquid phase, the included minerals cannot penetrate into the carbon atoms, thus have little influence on the ordering of the carbon. For porous chars with a high metastable liquid phase, the decomposed mineral will attract and adsorb the metastable liquid phase around it. A structurally more ordered carbon will thus be formed in the interaction part. A less ordered carbon is formed from the unaffected part (Zhang *et al.* 2009). Based on this, the degree of interaction between char and mineral could be used to predict the changes in reactivity during gasification of low grade coal.

Hence a study showing the relationship between the organic (maceral-to-char) and inorganic (mineral-to-ash) components in coal including their structure and behaviour under various conditions is likely to provide useful information on how to predict the behaviour of a particular coal/char submitted for fluidised bed gasification. Ultimately, it is anticipated that this would also assist in optimising gasifier operations for potential future gasification operations in South Africa, whether for power generation or coal to liquids production.

For the above reasons, the current research seeks to explore the behaviour of some South African bituminous coals currently used as feed in local power stations and to establish their technical performance and structural changes in a fluidised bed gasifier. It is anticipated that this would provide new insights into the evaluation of the typically high-ash inertinite-rich coals currently available on the South African domestic market.

1.2 Aims and objectives

The aim of this research is to investigate the fluidisation of fine, high ash-content South African coals in fluidised-bed gasifiers by studying the transformation of macerals and minerals and their interactions under various conditions. It is anticipated that this would provide new insights into the evolution of the typically high-ash inertinite-rich coals currently available on the South African domestic market. It is hoped that this information will be useful in maximising the efficiency and economics of a zero-emission systems in South Africa. In order to realise the aim mentioned above, this study will focus on the following activities:

- The investigation of chemical, structural and petrographic properties of some South African bituminous coals used as feed to power stations.
- Determination of the relationship between the organic (maceral-to-char) and inorganic (mineral-to-char) components in coal including their structure and behaviour.
- Investigation of the impact of different gaseous environments during the transformation of coal to char under similar fluidised bed conditions.
- Investigation of the different forms of mineral-char interaction during the gasification of high ash coals in fluidised bed gasification.

1.3 Research questions

- What microstructural changes occur in the organic (maceral) and inorganic (mineral) components of coal during low temperature gasification?

- How do these components and their microstructural changes affect the reactivity of coal chars in low temperature gasification?

1.4 Hypothesis

The relationship between the organic (maceral-to-char) and inorganic (mineral-to-ash) components in coal including their structure and behaviour can be used to predict the behaviour of a particular coal/char submitted for fluidised bed gasification.

1.5 Outline of the thesis

Chapter 2 reviews previous work on the impact of coal char properties on the carbon chemical microstructure and its influence on gasification reactivity at different reaction conditions. Also a brief review of various analytical methods used is detailed and their limitations highlighted.

Chapter 3 presents the experimental materials and procedures used in this study. This involves technical details of the analytical instruments as well as the pilot-scale test facility used for gasification.

Chapter 4 correlates the gasification performance of the selected South African coals and their derived chars against a range of chemical, physical and optical characteristics including mineral and maceral (and specifically inertinite) contents and their changes in chemical microstructures following gasification in a fluidised bed gasifier.

Chapter 5 presents textural properties of chars generated in a fluidised bed gasifier under air-blown, oxygen-blown and oxygen-enriched conditions were determined by detailed petrographic analysis. The char samples were assessed in terms of their microscopic characteristics (reflectance properties, carbon rich forms and basic forms of visible minerals).

Chapter 6 presents results on the impact of Al silicates clays on the modification of local carbon in a char matrix. An attempt was further made to model the impact of the interaction on char reactivity during gasification

Finally, conclusions and recommendations for future work are given in **Chapter 7.**

CHAPTER 2 LITERATURE REVIEW

2.1 Gasification: Introduction

Gasification is the reaction of solid fuels with air, oxygen, steam, carbon dioxide, or a mixture of these gases at a temperature exceeding 700 ^{o}C, to yield a gaseous product suitable for use either as a source of energy or as a raw material for the synthesis of chemicals, liquid fuels or other gaseous fuels (Collot, 2006). The amount of oxygen required in gasification is less than the amount stoichiometrically required for oxidation (Collot, 2006). This indicates that in a gasifier the air supply is only a fraction of the stoichiometric rate. The ratio of actual air fuel ratio to the stiochiometric air fuel ratio is called the equivalence ratio (ER). The quality of gas obtained from a gasifier depends strongly on the value used, which must be significantly lower than 1 to ensure a condition far from combustion. Operating at ER values lower than 0.2 can results in problems (Basu, 2006). These include incomplete gasification, excessive char formation and low heating value of the product gas. On the other hand, operating at higher ER values greater than 0.4 can result in excessive formation of products of complete combustion, such as CO_2 and H_2O at the expense of desirable products like CO and H_2 (Basu, 2006).

Collot (2006) reported that in industrial gasifiers, the value of ER is normally maintained at 0.20 to 0.30 leaving a reaction environment that is reducing instead of oxidising. The bed temperature of a gasifier increases with ER because the higher the amount of air, the greater the combustion and amount of heat released. One way of maintaining the thermal level (gasification temperature) in the gasifier is by the addition of steam (Campoy *et al*. 2009). The addition of steam can also lead to higher H_2 yield. The appropriate combination of temperature and steam leads to higher CO and H_2 yields, heating value, carbon conversion and gasification efficiency (Campoy *et al.* 2009).

In a typical gasifier, three major processes occur; they are drying and pyrolysis, combustion and gasification. This is illustrated in Figure 2.1. In drying and pyrolysis moisture in the solid fuel is evaporated and the water vapour, organic liquids and noncondensable gases are further separated from char (Basu, 2006).

Oxygen supplied to the gasifier reacts with the combustible substances present, resulting in the formation of CO_2 and H_2O, which subsequently undergo reduction upon contact with the char produced from pyrolysis. Gasification involves a series of endothermic reactions supported by the heat produced from the combustion reaction. These yield combustibles gases such as H_2 and CO_2. There is a need to make a balance between the endothermic reaction and exothermic reaction otherwise this could lead to a low carbon conversion in the gasifier (Bayarsaikhan *et al.* 2006). The endothermic reaction between char and gasifying agent such as steam during gasification is essential to convert the chemical energy of coal into that of the product gas. The reaction can also act as a chemical heat pump for recuperating the thermal energy, internally available or externally added to the gasifier into the chemical energy of the product gas. (Li and Li, 2006).

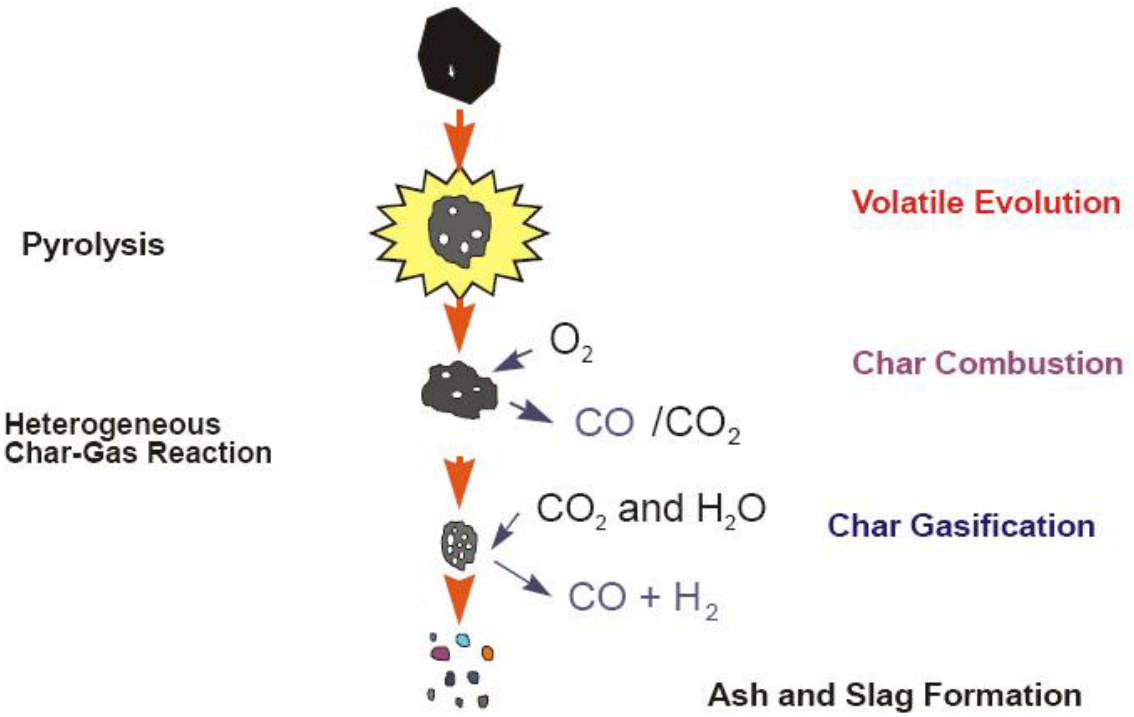


Figure 2.1 A schematic representation of the gasification process (Adapted, from Harris *et al*. 2003)

Gasification reactors are divided into three groups depending on how the feed is brought into contact with the gasification agent (flow geometry). They are

fixed/moving bed, fluidised bed or entrained flow gasifier (Basu, 2006; Collot, 2006). In a fixed bed gasifier the gasification medium flows through a fixed bed of lump solid coal (<51 mm). The flow can be concurrent or countercurrent. For a fluidised bed gasifier coal feed stock with a size range of 0.5-5 mm can be used (Basu, 2006). Coal particles are suspended in the gas flow. The result is turbulent mixing of gas and solids (coal) in the gasifier. Entrained-flow gasifiers are operated with pulverised coal with particles of less than 150 μm. The particles and gases flow concurrently at high speed. Collot (2006) reported that coal properties have an influence on gasifier design, operation and performance of a gasifier.

Based on their assessment**,** fluidised bed gasification is the most suitable option for the gasification of fine coals (0.5-5 mm) with high ash content. Recently, Beleyaev (2008) reported that the use of fluidised bed gasification is the most appropriate technology for the gasification of high ash Russian coal at commercial–scale. The gasification of high-ash coal with equivalent diameter of 3mm was carried out in a spouted fluidised bed reactor. Emerging economies such as that of South African and India are heavily dependent on the use of coals with high ash content for their electricity production. There is a need to balance their need for increased electricity output with efforts to control greenhouse gas emissions. Coal gasification is a promising clean coal technology that holds the potential to increase power generation efficiency and reduce carbon dioxide emissions.

2.2 Power generation from coal gasification of low grade coals

Coal gasification is becoming an attractive alternative for power generation since it offers higher efficiency and improved environmental performance than conventional pulverised fuel technology (Cousins *et al*. 2007). There is a significant reduction in the emissions of NO_x, SO_2 and particulates when compared with conventional coal-fired power stations.

Clean gas obtained from a gasifier can fuel a large combined cycle system for electricity generation, where the gasified fuel is first burnt in combustion turbine-generator unit and then the hot exhaust gas from its gas turbine is used for generating steam to produce further power in a steam turbine-generator unit (Basu, 2006).

The combination of a gasifier and a combined cycle is called Integrated Gasification Combined Cycle (IGCC) (Henderson, 2003). Such a system also offers the possibility of cogeneration of electricity and chemicals from the high quality syngas that is produced (Collot, 2006). IGGC plants are also in the best position for CO_2 capture and sequestration. They offer a high pressure, high concentration CO_2 stream which is amenable to separation and collection.

Low temperature gasification, if used for power generation potentially results in increased efficiency by allowing more of coal energy to be converted to chemical energy rather than sensible heat (Bhattacharya, 2006). However, at low temperatures hydrocarbons such as methane do form. This might limit the capture of carbon in the form of carbon dioxide. If power generation rather than chemical production is the primary focus and less than one hundred percent carbon capture is intended, then low temperature gasification has a cost and efficiency advantage over high temperature gasification (Holt, 2004).

Burning high ash coals for power generation is generally associated with problems such as slagging, fouling, corrosion and bed agglomeration (Yan *et al.* 2003). In addition coal utilisation efficiency is low (Iyengar and Haque, 1991). Iyengar and Haque (1991) reported a reduction in gasification efficiency during the gasification of high ash Indian coals for power generation when there was an increase ash yield. In a recent study, Belyaev (2008) found that an optimum ash content of 30% is required for the fluidised bed gasification of high ash Russian coals in power generation. Presently the most commonly used gasifier for power generation is the entrained flow gasifier and it is not suitable for high ash coal with high ash fusion temperatures. Fluidised-bed gasification technologies appear to be better suited to for high ash coals, as explained in the section. 2.3 below.

2.3 Fluidised bed gasification of low grade coals

Fluidised bed gasifiers are classified as low temperature gasifiers. These types of gasifiers have the potential advantage that low-grade coals, such as the South African coals, which are high in ash can, be processed more efficiently than in other types of coal gasifiers. They usually operate at temperatures well below ash fusion temperatures of such coals (900-1050 ^{o}C) to avoid ash melting**,** thereby avoiding clinker formation (Collot, 2006). However, low temperature gasification leads to a low carbon conversion in fluidised bed gasifiers. In order to achieve higher level of char conversion, the reactivity of the coal derived char must be sufficiently high (Collot, 2006; Bhattacharya, 2006). The use of enriched oxygen may significantly increase the burnout of lower reactivity coals (Rathnam *et al.* 2009). This is because, in oxygen-enriched environments, devolatilization and combustion of coal particles are likely to occur faster than with air (Borah *et al.* 2008). In addition, enhanced tar decomposition and char gasification will contribute to higher gasification efficiency.

Char particle temperature is one of the important factors that determine the gasification rate**.** The use of air oxygen enriched air reduces the nitrogen dilution effect, increase the gasification temperature. This allows for the addition of steam while maintaining the thermal level in the gasifier (Campoy *et al.* 2009). The use of enriched oxygen for air-steam gasification has been reported to lead to higher level of carbon conversion for high ash and other low quality coals (Belyaev *et al*. 2003). There are relatively few reported studies on the fluidised bed gasification of inertinite-rich; high ash coals using enriched-air-system mixtures as gasification agent.

2.4 Char deactivation in a fluidised bed gasifier.

The reactivity of coal chars under gasification conditions is a major determinant of the gasifier size and design. Highly reactive coals provide high carbon conversion at moderate temperatures. Char reactivity has a significant influence on the degree of char recycle and the volume of oxidant required for the gasifier. Higher char reactivity may lead to lower O_2 usage or less enrichment which may result in lower operational cost (Rathnam *et al*. 2009). For fluidised bed gasifiers, the reactivity of the derived char must be sufficiently high because of the low operating temperature and long residence time (Collot, 2006). The nature and reactivity of coal chars depends on the

properties of the coal and operating conditions such as temperature, pressure and residence time (Zhuo *et al.* 2000).

Char deactivation is one of the key factors that lead to char reactivity loss. According to Hurt *et al.* (1998) there are three main mechanisms involved in char deactivation. Firstly, the intrinsic heterogeneity of the solid fuel particles which results in a segregation of the least reactive components of the fuel into the fly ash. Secondly, the burning of the fuel which may give rise to the development of an ash layer that can act as a barrier against oxygen penetration and consequently reduce the rate of oxidation of the partially burned char. Thirdly, the exposure of fuel to high temperature can cause thermal annealing of particles, characterised by the loss of surface area and of reactivity of the active sites. In fluidised bed gasification of high ash coals, thermal annealing and ash effects are the main processes that could contribute to the decrease in char reactivity.

Char annealing involves a series of complex transformations in the char matrix that include the loss of hydrogen and oxygen and the elimination of edge carbon sites due to coalescence of aromatic rings (Hurt *et al.* 1998; Senneca *et al*. 1998). The structural rearrangement of carbonaceous component involves the change of carbon hybridization and aromatisation, and these prevail at low temperatures. The stacking and reordering of graphene layers dominates at moderate temperatures, while at higher temperatures, lateral growth of carbon crystallites have been observed (Rouzaud and Oberlin, 1989; Cai *et al.* 1996; Lu *et al*. 2001; Senneca *et al*. 2005). According to Rouzaud and Oberlin (1989), at temperatures below 700 ^{o}C, the main structural transformation process is the release of CH groups. Between 700 and 1500 ^{o}C, the main process is the release of interlayer defects. However, between 1500 and 2000 ^{o}C, there is removal of in-plane defects. Above 2000 ^{o}C, interlayer and in-plane defects disappear and crystal growth begins.

Using the Raman spectroscopy technique, Bar-Ziv *et al*. (2000) observed that the loss of carbon reactivity correlated fairly well with changes in aromatisation and carbon hybridisation at temperatures below 1200 ^{o}C only. This indicates that the change of carbon hybridisation and loss of aliphatic functionalities might be responsible for the reacting sites**.** Zhang *et al.* (2008) reported that during pyrolysis aliphatic carbon,

along with hydrogen and oxygen, are released and the relative concentration of aromatic compounds increases. At operating conditions below 1000 ^{o}C, the carbon structure consists of units of composed of no more than 10-12 condensed aromatic rings, stacked in layers of two or three. However, between 1000 ^{o}C and 1600 ^{o}C, the extent of parallel orientation increases and thus the char becomes progressively more ordered in structure. The two–dimensional growth of aromatic layers is followed by the orientation of the aromatic layers in a hexagonal graphite structure.

Investigation by Keown *et al.* (2008) showed that the transformation of smaller aromatic ring to larger aromatic rings occurs during the gasification of biomass. This leads to a decrease in reactivity. The enrichment of large aromatic ring system during gasification does not favour the dispersion of mineral matter that may act as catalyst on the char surface (Liu *et al*. 2006). This indicates that the loss of reactivity in char can occur at the early stage of the transformation of the carbonaceous structure .i.e. during aromatisation (at low temperatures) or stacking and reordering (at moderate temperature) before the lateral growth in crystallites. In addition, Cousins *et al*. (2007) observed the loss of reactivity in char at short residence time but didn't observe any significant graphitic material from their XRD patterns. They suggested a movement toward the graphitic structure could account for the loss in reactivity.

Also more severe heat treatment may lead to the modification of the mineral matter in the coal. The transformation of the mineral matter will depend on the chemical nature of the ash material and in turn on the nature of the carbon (Senneca and Salatino, 2002; Gupta *et al.* 2006). As a further motivation for this work, there is a need to evaluate the transformation of the turbostratic carbon structure at different temperatures in fluidised bed gasification. This will be useful in the development of structural model that involves aromatisation, stacking and reordering and the lateral growth of carbon crystallites in a fluidised bed gasifier for high ash and inertinite coals.

Char reactivity is dominated by active sites on the char surface. The active sites include carbon and catalytic active sites (Tran *et al.* 2008). The loss or decrease in char reactivity has been attributed to the change in carbonaceous structure and the loss of catalytic activity of mineral matter (Sharma *et al*. 2002).

During gasification, the organic and inorganic matter undergoes various chemical and physical transformations. The chemical transformation involves the change in the organic chemical structure while the physical transformation involves a change in the char morphology and porosity. Less ordered carbon has higher gasification reactivity than highly crystalline carbon. During gasification crystallites present in coal are consumed, which leads to changes in both the pore structure as well as the crystalline structure. It is expected that changes in the crystalline structure will be directly reflected in changes in the active parts of the carbonaceous structure, because the active sites are generally considered to reside mainly at the edge sites of the crystallites (Tran *et al.* 2008). The relative importance of the factors depends on the nature of the coal sample as well as on the reaction conditions (Messenbock *et al*. 2000; Cousins *et al.* 2007). Hence there is a need to investigate the interaction between coal properties and reaction conditions in relation to char reactivities.

As stated earlier, in addition to the carbon active sites, the char matrix also includes catalytic sites. The carbon crystallite growth could lead to the decrease in the amount of edge carbon atoms in char available for catalytic species bonding which then results in poor dispersion of catalytic species. Thus, carbon active sites and catalytic active sites are both influenced negatively by the carbon crystalline growth.

In addition mineral matter tends to lose its catalytic capability because of the decrease in the catalytic species dispersion caused by sintering, melting, or volatilising. Based on this, it's essential to distinguish between the contributions of the modifications of the organic and of the inorganic constituents of coal on char deactivation. The relative importance of the modifications of the carbon structure versus changes of allotropic form, sintering, melting or vaporisation of the inorganic matter in coal remains largely to be assessed (Salatino and Senneca, 2007).

For enriched oxygen gasification, a high concentration of oxygen can prevent or delay thermodeactivation of chars (Alvarez *et al*. 2003; Senneca *et al*. 2007). Exposure of char to oxygen promotes the formation of stable surface oxides which reduces the fluidity of molten carbonaceous matter (Street *et al.* 1969). This is attributed to the formation of oxygenated cross-links on the surface of the particles, with the net effect

of reducing the mobility of the polyaromatic rings which make up the molten ground mass and therefore preventing their rearrangement into larger units (Alvarez *et al*. 2003). Senneca *et al.* (2007) reported that the exposure of chars to oxygen at low-to-moderate temperatures promotes extensive formation of stable surface oxides which in turn prevent or delay the progress of thermodeactivation of char while exposure to oxygen at moderate-to-high temperatures give rise to limited formation of stable surface oxides. They suggested that diffusional limitations might prevent the formation of surface oxides so that beneficial effect of carbon surface oxidation on the hindrance of thermal deactivation would be ruled out.

In other reports (Guo *et al*. 2008; Dong *et al.* 2009), it was indicated that in addition to the role of enriched oxygen in the prevention of thermal annealing of some of the function groups e.g oxygen-containing groups, new functional groups could be formed at reactive sites. This can result in the variation of carbon structure as a result of the competition between elimination of amorphous materials and generation of new amorphous materials at reactive sites.

2.5 Coal properties

Some of the key coal properties that can affect chemical and physical transformation of coal and subsequently its reactivity during gasification include its maceral composition, rank and mineral composition (Lu *et al.* 2000; Alonso *et al*. 2001; Liu *et al.* 2003; Mendez *et al.* 2003 and Choudhury *et al.* 2008). These are explained in the following sections.

2.5.1 Maceral composition

Macerals are the organic components of coal. Three main macerals groups are recognised namely vitrinite, liptinite and inertinite. Each maceral has its own specific physical and chemical properties. They can be distinguished from one another under the microscope by differences in reflectance, morphology, colour, shape, size polishing hardness and fluorescence. Their optical, physical, chemical and technological characteristics alter as the coal is heated**.** The maceral composition of coal can be used to study the transformation of the carbonaceous structure because each of the macerals group reacts differently. Based on the different maceral

composition in coal, at a fixed temperature the evolution of the carbonaceous structure of some coals may have experienced growth in the crystallite size .while some other coals would have only experienced aromatisation and not a growth in crystallise size. This could have a corresponding impact on the variation of reactivity. X-ray diffraction (XRD) studies conducted on two different coals showed that the inertinite-rich coal had a more oriented structure than the vitrinite–rich coal (Sharma *et al.* 2000; Van Niekerk *et al*. 2008). The inertinite-rich coal has a larger layer and higher stacking number than the vitrinite-rich coals. Sharma *et al.* (2000) also studied the inertinite and vitrinite present in Pocahontas NO.3 coal, using high–resolution transmission electron microscopy (HRTEM) and obtained similar results. Van Niekerk *et al.* (2008) studied the structure of two South African coals which are vitrinite-rich Waterberg and inertinite-rich Highveld coal. Waterberg coals are mostly used domestically as a coking coal and a feed coal for power stations and inertinite-rich Highveld coals are mostly used for combustion and gasification processes in South Africa (Cairncross, 2001; Kruszewska, 2003). Niekerk *et al.* (2008) observed that the inertinite–rich Highveld coal had a higher degree of crystalline stacking than vitrinite-rich Waterberg coal. In addition, the inerntinite-rich coal has more aromatic and polycondensed content than the vitrinite-rich coal. Similar results were reported by Wang *et al.* (2009) for some Chinese coals. They found out that an increase in inertinite content leads to an increase in aromaticity and condensation. Based on different maceral structural characteristics, thermal stability and the extent of thermodeactivation upon heat treatment will also be different.

With regards to the impact of maceral compositions of coals, Senneca *et al*. (1998) investigated the microstructural changes and loss of gasification reactivity of two types of coal, namely Ruhr coal (Ru) and a South African coal (SA) at different temperatures (900-1400 ^{O}C) using carbon dioxide as the gasifiying agent. These coal samples were similar in rank but different in the maceral compositions. The Ruhr coal was reported to be vitrinite-rich and the South African coal inertinite-rich. The researchers observed that there were clear differences between the two coals and modification of their structures. They concluded that the cause could have been the difference in the inertinite and vitrinite content.

Beeley *et al.* (1996) reported that when inertinite rich coals are carbonised, the low hydrogen content precludes fluidity and limits long range structural rearrangement. The observed resistance of inertinite-rich coal chars to thermal deactivation has been linked to the role of inertinite in the production of unreactive and dense chars (Crelling *et al*. 1992). On the other hand, vitrinite-rich coals usually with high hydrogen content after the carbonisation process soften and the mobile carbon undergoes nanoscale rearrangements to approximately align layer sects. The aligned layers then coalesce readily upon heat treatment, leading to extended layers, loss of edge sites and loss of reactivity (Beeley *et al*. 1996; Zhang *et al*. 2008).

The difference in thermal stability due to maceral composition is only significant at low temperatures. Sun *et al.* (2003) reported that the difference of aromaticity between vitrinite-rich fractions (pure maceral) and inertinite-rich fractions (pure maceral) was larger at lower temperature, while it became smaller at higher temperature. When the temperature was increased from 25 to 500 ^{o}C, the aromaticity of vitrinite increased from 0.51 to 0.83, while that of inertinite only increased from 0.76 to 0.87. At 500 ^{o}C, the aromaticity of vitrinite and inertinite was very close. This may be due to the fact that inertinite-rich coals contain lots of stable aromatic rings which are not easy broken at lower temperature, yet could be decomposed further while temperature is over 500 ^{o}C. In a similar study, Kalkreuth *et al.* (2005), found that although the vitrinite-rich coals are intrinsically more active than the inertinite rich ones at 500 ^{o}C, the difference tended to diminish significantly at higher temperatures (e.g. at 1300 ^{o}C).

The degree of thermodeactivation of char has been correlated with the degree of reactivity of virtinite chars, for example in the recent study by Zhang *et al.* (2008). The reactivity of two chars derived from two vitrinite rich fractions was compared. The vitrinite samples were prepared from two bituminous vitrinite rich coals with different vitrinite constituents and they found that chars with higher reactivity experienced a higher degree of deactivation. For inertinite rich coals, there seems to be uncertainty on the variation of reactivity (Cai *et al.* 1998; Kalkreuth *et al.* 2005).

Also, Cai *et al* (1996) investigated the effect of inertinite concentration of two coal samples. Significant differences were found between the responses of the sets of

chars. There was a drop in char reactivity with an increase in inertinite concentration in one and there was no change in reactivity in the other. They suggested that the difference is due to the rank of the coal samples. In higher rank coal samples, char reactivities are independent of the inertinite concentration. However in another study carried out by Kalkreuth *et al.* (2005) they observed that char reactivity changed when inertinite concentration was increased. Three coal samples were used and they were all in the same rank. There was a decrease in reactivity for two coal samples ('coal 1' and 'coal 2') and no effect for the third sample. This was attributed to the association of macerals and the mineral matter. For 'coal 1' and 'coal 2', there was a close association of inertinite with mineral matter, whereas there was no such relationship for the third coal sample ('coal 3').

2.5.2 Rank

In addition to the maceral composition, the rank of coal can also influence the structure and the reactivity (Jones, 1985; Alonso *et al.* 2001; Mendez *et al*. 2003 and Choudhury *et al.* 2008). Coal rank refers to the degree of maturation of the coal in the coalification process, and this is often accompanied by structural changes. Jasienko *et al.* (1995) reported that an increase in rank results in increase in the coefficient of aromaticity, which may lead to an increase in the dimensions of crystallites. It was also observed that an increase in aromaticity further leads to the formation of new simple structures, rather than the condensation of rings to large aromatic molecules. The changes undergone by vitrinite groups during coalification involve the reduction in cross linked structure. This results in the formation of more ordered coal structure. Bend *et al*. (1991) investigated the molecular structure of chars derived from nine vitrinite-rich coals of different rank. They found that the thermoplasticity of the char can be related to the molecular structure of the original virinite and this varies as a function of rank. The fluidity of the molten char material results in the formation of bigger, more ordered structures. Higher ranks do not melt upon heating due to large polyaromatic units (high aromaticity).

There is little information on the molecular arrangement of inertinite fractions and its variation with rank (Alonso *et al*. 2001; Fermoso *et al*. 2010)**.** This is due to the inherent heterogeneity of these macerals, hence difficult to characterise the variation

in morphology and plastic behaviour of inertinite-derived material in char particles (Fermoso *et al.* 2010).

Fermoso *et al*. (2010) studied the effect of different macerals on thermoplastic properties and particle morphology of five different rank coals:. They are lignite (LT), three bituminous coals with low (DI) and high (SA and DT) volatile matter contents respectively and a semi-anthracite (HV). With regards to maceral composition, coals DT and SA have high contents of have high inertinite contents. The inertinite in DT underwent a smooth process of oxidation and high porosity while in the SA coal, the inertinite-derived char particle tend to be massive. Vitrinite behaved similar in both coals yielding highly swollen isotropic particles. The low-volatile bituminous coal, DI, has a lower inertinite content of 25.7%. Its inertinite-derived char particles have a massive and isotropic appearance. Its char vitrinite-derived particles experience substantial swelling (enhanced plasticity), as occurred in SA and DT coals. In contrast, vitrinite-derived char particles show an exclusively anisotropic optical texture. This indicates that vitrinite-derived particles in DI coal present anisotropy not because of its thermoplasicity but because of an enhancement of the anisotropy inherent in the higher rank coal. Similar results were obtained with vitrinite derived particles in the anthracite.

Alonso *et al*. (2001) reported that the presence of inertinite derived materials in high rank coal chars enhanced their reactivities, whereas the opposite was observed for low rank coal chars. This was attributed to the fact that inertinite macerals yield both isotropic and anisotropic materials: inertinite in low rank coals increases the amount of anisotropic, less reactive char, but reduces it in high rank coals.

2.5.3 Mineral matter content

The mineral matter associated with coal included a wide range of minerals, the most abundant forms being clays, quartz, carbonates, pyrites and other forms of oxides. During gasification minerals can either transform or recombine to form new phases. The new phases can melt and become a liquid or liquid-solid mixture (Ninomiya and Sato, 1997).

Also, amorphous aluminiosilicate has been reported to be the dominant phase in chars generated from the fluidised bed gasification of coals (Kosminski *et al.* 2006). Decomposition of clays such as kaolinite, montmorillonite, illite and chamosite produced the amorphous aluminiosilicate phase.

With regards to South African coals, it has been reported that clays (kaolinite and illite) are the dominant mineral matter (Gaigher, 1980). Gaigher (1980) used XRD to determine the mass-percentage mineral matter proportions, the clay distribution and the mineralogy of 35 commercial grade South African coals. It was estimated that the average clay composition of South African coals are 54.1% kaolinite, 29.2% illite and 16.7% expandable clays (mixed layered clays and smectite clays). Other mineral matter that are found in South African coals are silicates, pyrite and carbonate minerals (Pinetown et al. 2007).

The mineral matter content of coals is known to influence gasification reactivity because of the presence of catalytically active compounds. During coal utilisation, the mineral matter undergoes structural and chemical changes. The structural changes involve the expansion of meta-clays, swelling and balling of aluminosilicates, while the chemical changes include mineral phase deformation and the formation of new crystalline and glass phases (Bryers, 1986; Kerkkonen, 1997). The crystal structure of kaolinite, for example, breaks down in a solid-state dehydroxylation reaction at around 450 ^{o}C to form a solid amorphous material referred to as metakaolin. Illite breaks down at a slightly higher temperature with similar results. Oxidation of pyrite and/or siderite would be expected to form hematite at similar or even lower temperatures, but only if plenty of oxygen is available. With more limited oxygen (i.e. more reducing conditions), magnetite and/or maghemite would be expected to form instead. Pyrrhotite would also be expected to form from pyrite in limited-oxygen conditions. This is illustrated below in Figure 2.2.

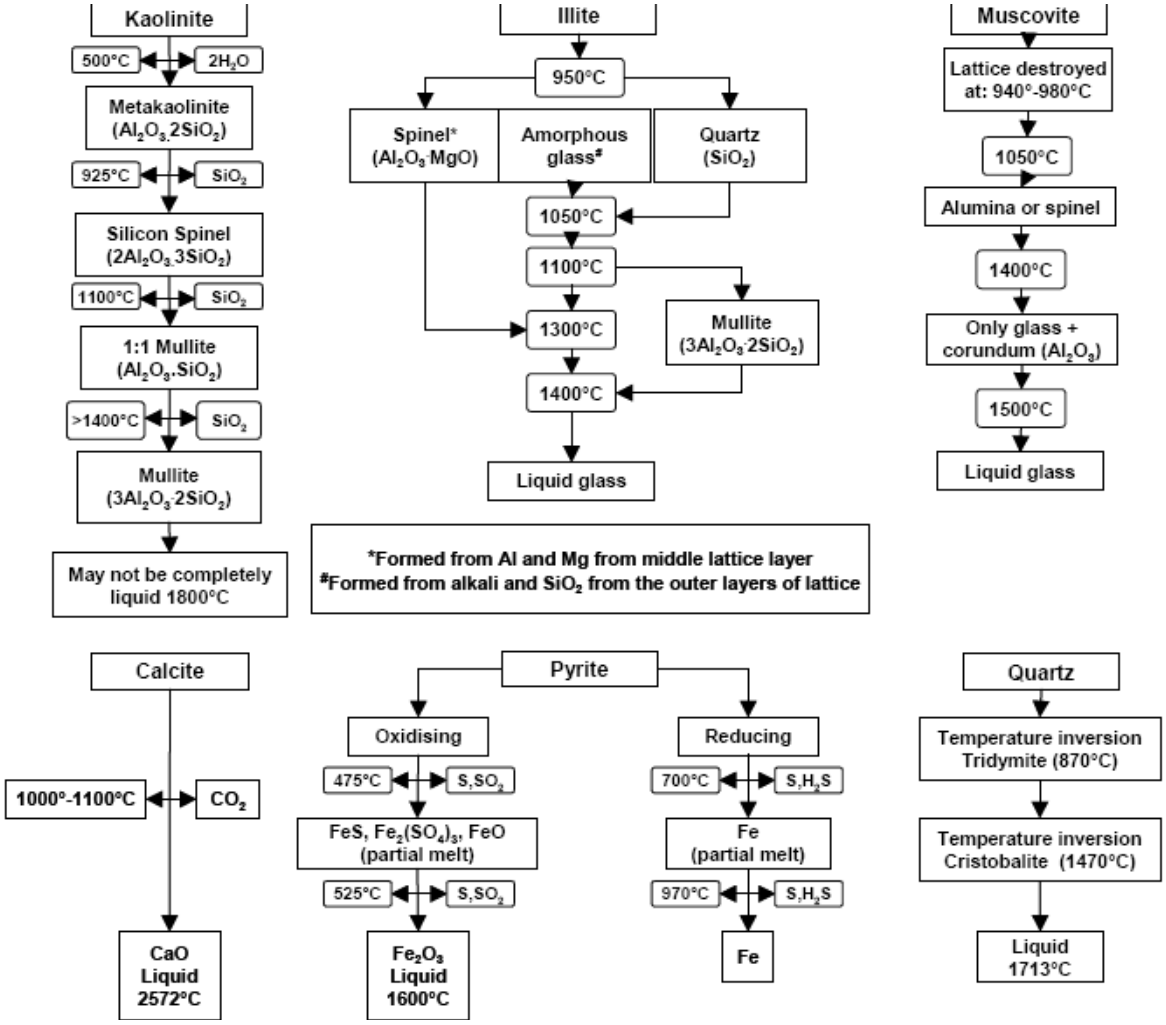


Figure 2.2 Mineral transformation in coals (Taken from Bryers, 1986)

The dominant phase after mineral transformation during fluidised bed gasification of low-grade coal is amorphous aluminosilicates (Kosminski *et al.* 2006). As illustrated in Figure 2.2 (taken from Bryers, 1986), this amorphous mineral matter is the result of the decomposition of kaolinite and illite. Gigore *et al*. (2008) reported that the type of association of mineral matter in coals has an important role in how clays are decomposed. The decomposition of kaolinite (the most abundant clay minerals in coal) intimately associated with silica bearing minerals favoured mullite formation, and in the absence of close associations, alumina was formed. These changes that occur during the mineral matter transformation can influence gasification reactivity. Liu *et al.* (2006) reported that the evolution of char reactivity can be correlated with incipient melting of mineral matter. The structural alteration of melted minerals has a direct influence on carbon conversion.

When minerals melt, they cover the surface of the chars thereby hindering carbon conversion (Lin *et al.* 1994; Bai *et al.* 2009). Melts with different structures have a different polymerisation degree which leads to different surface tension. The surface tension can be used to determine the contact of the melt and the char. High polymerisation represents a large surface tension and little effects by melts in gasification. Bai *et al.* (2009) used FT-IR analysis to study the alteration of aluminoslilicates melts and found that the shift in IR bands was caused by the alteration of melt structure. The shift of the Si-O-Si band at 1000 cm^{-1} and the Si-O band at 845cm^{-1} represents the degree of polymerisation of the aluminosilicates.

In addition to aluminosilicate melts preventing oxygen from reacting with the carbon phase, catalytic minerals can be encapsulated in the amorphous phase and further reduce the gasification rate (Li, 2007; Grigore, *et al.* 2008). Different proportions of catalytic minerals (Fe, Ca, Na and K) have been reported in the amorphous phase during coke gasification (Grigore *et al.* 2008). These can decrease the contact surface area between the catalytic mineral phase and coke/char during gasification. The nature of the mineral phase can be used to determine to what extent the minerals affects the gasification rate (Grigore *et al.* 2008). Hence there is a need to ascertain to what degree catalytic minerals formed from the decomposition of clay minerals affects gasification rate. This factor can be used to evaluate the variation in char reactivity during gasification.

Matjie *et al* (2011) studied mineral matter behaviour of South African coals in fixed bed gasification. They reported that mineral-mineral association and carbon-mineral association may also play a role in the formation of melted minerals. Also in 2006 Gupta *et al.* (2006) reported that a strong mineral-carbon interaction can increase the amount of melted minerals during coal combustion. In their study, a strong carbon association with the illite phase led to a reduction in melt temperature during combustion of coal. This is a result of a strong reducing environment provided by the carbon phase. Furthermore the organic composition of the carbon phase found in carbon-mineral association (i.e., the relative proportions of the macerals) could have a different effect on the proportion of melted mineral formation. In our preliminary studies, it was observed that higher proportions of inertinite macerals and inertinitic chars resulted in higher proportions of melted minerals. Char samples with low

proportions of organic matter resulted in higher proportion of melted minerals covering the char surface. Gaigher (1980) noted that there was a strong positive association between clay minerals and inertinite, and negative association between clay minerals and vitrinite for South African coals. However, there is currently a lack of understanding of what roles the different macerals could be on the decomposition of clays during gasification. Matijie et al.(2011) reported that mineralogical changes can be delayed during gasification when reactive minerals such as dolomite occur with organic fractions.

For melted minerals with similar structure, the content of iron oxides could reduce or prevent the mineral melt from covering the surface of the char (Bai *et al*. 2009). Higher iron oxide content leads to an increased pore size as a result of carbon thermal reaction with iron oxides (Wang *et al*. 1995). The expanding pore effect of iron oxides hinders the contact between melting minerals and char surface (Bai *et al*. 2009). In other reported studies (Li and Wikky, 2009) it was suggested that the amount of residual carbon in char plays a role in the proportion of included minerals that covers the surface of the char. The lower the residual carbon in the char, the more included minerals that cover on the char surface. The study of interaction between mineral and char will enable understanding of the effect of mineral on char reactivity and coal conversion.

Lunden *et al.* (1998) reported that mineral matter can interact with the carbonaceous matrix to decrease char reactivity either by blocking access to carbon active sites hence reducing the available carbon per unit area in the char or by increasing carbon crystallite growth. They hypothesised that the same molecular strain from the mineral particle that prevents or promotes carbon ordering may also resist penetration of oxygen into the carbon matrix. However they could not distinguish between the effects of mineral matter on carbon ordering and molecular–level reactivity due to inadequate experimental measurement.

Sekine *et al*. (2006) reported that the presence of silicon and aluminium compounds close to carbonaceous structure tends to suppress the gasification reaction at the coal char surface. Based on laser Raman spectroscopy and an EDX mapping technique developed, they observed that the location of silicon and aluminium are in good

accordance with the location of non-graphitic carbon and covered the carbon surface. They suggested that mineral matter inhibited catalytic activity by blocking carbon sites. However they did not report on the location of other elements such as calcium and iron which have a catalytic effect on gasification. Earlier reports have shown that coke in the vicinity of iron possessed a much more ordered graphitic structure than coke far away from iron (Wang *et al.* 1995). The following mechanism was proposed for the process.

The iron melt at first penetrates the surrounding carbon matrix through carbon dissolution-precipitation sequences leaving behind the well ordered graphitic carbons. As the penetration front moves further into the carbon the coke sample transforms into well ordered graphitic carbon. Since the penetration of iron melt follows the graphitisation front, the precipitated small graphite crystals would be transformed in later recrystallisation steps into large flakes. Eventually, as the iron particles become progressively smaller, the extent of graphitisation appears to decrease.

In another study, Zhang *et al*. (2009) studied the effect of included minerals on the reactivity of chars. They observed that included minerals facilitate the formation of pores for low ash chars but inhibits the formation of pores for high ash char. They suggested this observation indicates a different form of interaction between the mineral matter and the organic component in the char matrix and can be explained by the liquid-phase-and-mineral-matter interaction theory (Rusell *et al.* 1988). For the bituminous coal they studied, they reported low ash fractions soften and swell during devolatlisation and result in a porous and thin-walled char structure. The high ash fractions with lower organic content and relative low vitrinite content resulted in the formation of dense char. For this type of char (dense), there is no or negligible metastable liquid formation during char preparation. They suggested that in the dense char the included minerals can not penetrate into the carbon atoms, thus have little influence on the ordering of the carbon. The carbon in the dense char is homogenous and their carbon ordering is determined by their parent coals. For porous chars there is a high metastable liquid phase during char formation, the decomposed mineral will attract and adsorb the metastable liquid phase around it. A structurally more ordered carbon will thus be formed in the interaction part. A less ordered carbon is formed from the unaffected part (Zhang *et al*. 2009). Hence the carbons in the char can be

grouped into two parts; pure carbon and catalysed carbon. Accordingly, there is expected to be a high change in the reactivity of low ash and porous char and no or low change in the reactivity of high ash and dense char. To verify this hypothesis an adequate experimental technique must be developed to determine exactly which part of the carbon in char where interaction occurs. These would be useful in the development of a model of mineral-char interaction, to understand and predict the effect of mineral matter on char reactivity during gasification.

2.6 Reaction conditions

In addition to the properties of the coal, the conditions of char formation such as temperature, pressure, particle size, residence time and gaseous environment affect the nature and reactivity of char (Zhuo *et al.* 2000; Cousins *et al.* 2007). The interaction between coal properties and operating conditions can result in the variation of gasification reactivity of solid char (Chen *et al.* 2008).

The effect of temperature evolution of microstructure of coal and its corresponding effect on reactivity is well documented (Alavarez *et al*. 1995; Senneca *et al.* 1998; Sharma *et al*. 2002; Liu *et al*. 2003; Sekine *et al.* 2006; Sheng, 2007; and Cousins *et al*. 2007). An increase in temperature results in the reorganisation of the carbon matrix which could lead to a loss of char reactivity. Although the majority of the studies reported are at high temperature, structural reorganisation can also occur in low temperature gasification (Sharma, *et al*. 2002; Guo *et al*. 2009; Dong *et al*. 2009). Dong *et al*. (2009) reported that thermal annealing of coal char normally occurs at gasification temperatures greater than 800 ^{o}C. This temperature range falls within fluidised bed gasification range (800-1000 ^{o}C).

Guo *et al.* (2008) reported thermal decomposition of char and changes in the char structure resulted in the variation of gasification rate during the gasification of Victorian brown coal in steam and oxygen at 800 ^{o}C in a fluidised bed reactor. Cousins *et al*. (2007) varied the gasification temperature from 700-900 ^{o}C and observed a decrease in reactivity and only observed structural reorganisation at a residence time of 1 hour. This indicates that thermal annealing at a given temperature takes place over multiple time scales. The presence of dense chars formed from inertinites will require a long reaction time in a fluidised bed gasifier. Cousins *et al.*

(2006) observed a significant decline in char reactivity at 950 ^{o}C within about 10 seconds and further loss of reactivity over a longer residence time of 1 hour. Further analysis also showed that the loss of char reactivity is a function of the conditions of formation. A higher decline in char reactivity was observed under steam at constant temperature when compared with that obtained in CO_2 gasification. However there was no significant variation for larger particle sizes (600-850 micron). This indicates that differences in char reactivity are apparent when using small particles and not when using larger particles. They suggested that reactive tar precursors were able to crack further and recondense inside the pores of larger particles, forming increased quantities of unreactive secondary char. This coats surfaces and effectively masks the underlying char structure, slowing down the reaction of underlying char. In a recent study, Zhu *et al.* (2008) reported in addition to enhancement of secondary reactions of volatile matter inside larger particles, mineral segregation in coal particles will also affect the changes in char reactivity during gasification. They observed that there was an increase in inherent minerals (containing Na, K and Ca) in chars when particle size was decreased for the different size fractions of coal. The increase in inherent minerals in chars from smaller particle sizes was associated with mineral segregation in different size fractions of coal. In the gasification of lower rank coal char the catalytic effect of inherent minerals can increase the reactivity of chars, hence higher reactivity of chars and also higher variation in reactivity from smaller size fractions could be expected.

Another study showed that particle size and density can affect coal particle phase formation during coal gasification (Shannon *et al.* 2009). Mineral fractions are higher in denser particles than less dense particles. Smaller particles have lower fractions of minerals than larger. The distribution of minerals across particle size and density fractions can affect the melting behavior and subsequently the reactivity of the minerals in the char. Hence the effect of particle size and density on the interaction of the secondary char (liquid phase) and mineral matter on char structure and char reactivity could be useful in predicting char reactivity during coal gasification**.**

2.7 Analytical techniques to study char-mineral interaction during gasification

A number of techniques have been employed to characterize the influence of carbonaceous structural change and mineral matter during coal gasification. These

sections aim to present the advantages and limitations of the techniques. It is necessary to combine information gained from various techniques to provide a better understanding of the interaction between mineral-char of high ash coals during fluidised bed gasification and its effect on gasification.

2.7.1 General review of analytical techniques in the characterisation of coal char structure

2.7.1.1 Real density measurement

A real density measurement by the helium pycnometry technique provides a simple and quick way to study changes in solid structure. This is because helium can penetrate the submicropore range down to a size of about 3 Å (Tran *et al.* 2008). Tran *et al.* (2009) used this technique to study the crystalline structure of carbon anodes during gasification. Carbon anodes are a special type of carbon-carbon composites made from a combination of calcined petroleum coke and coal tar pitch and have a partially graphitized carbon structure (Tran *et al*. 2008). Pusz *et al.* (2010) also measured the apparent density of coke and used it to evaluate the changes in the coke structure upon reaction with CO_2. An increase in the helium density of coke samples after reaction with CO_2 was associated with an increase in the degree of structural order of coke. In another study, Alvarez and Borrego (2007) measured the apparent density of coal chars to investigate changes in the physical structure during combustion. They reported that density measurements in high-ash chars are subject to higher uncertainties due to the diluting effects of ash. This technique may not be adequate to study char structure especially at late stage of carbon burnout when the char contains a small proportion of carbon and has a high ash yield.

2.7.1.2 X-ray Diffraction technique (XRD)

The XRD technique has been used to evaluate stacking structure of highly crystalline carbon materials such as graphite. However its application is limited for coal char. One of the difficulties of using XRD techniques for characterisation of coal chars especially those derived from low temperature gasification such as from fluidised bed gasifiers is the absence or broadness of key peaks (Li, 2007; Maity and Choudhury, 2008). This could be due to a lack of well-oriented carbon structure in the derived coal char (Li, 2007). According to Maity and Choundry (2008) one way to solve the problem is to perform a slow-scan XRD analysis on char and this will increase the

resolution of the diffractograms. They classify the carbon-related peak around 20-26^{o} basically into two categories: one derived from aromatic stacking around 26^{o} called the π band and the other is named the γ band around 20^{o} which is believed to be derived from aliphatic chains. Also, Wu *et al*. (2008) separated the XRD peaks of char structure into two components with a broad peak assigned to the poor crystalline (P component) and narrow peak assigned to crystalline structure (G component).

2.7.1.3 FTIR

Quantitative IR analysis is useful for providing detailed structural information such as aromaticity and aromatic hydrogen content. Ibarra *et al.* (1996) carried out an FTIR study of the evolution of coal structure during the coalification process. They defined a few ratios of integrated absorbance areas of curve-fitted bands, to quantify the structural changes. For example, the CH_3/CH_2 (2955 cm^{-1} band /2920 cm^{-1}) ratio can be considered as an estimate of the length of aliphatic chains of coal and a branching index. The ratio of aromatic C-C to carboxylic groups appeared as a suitable index for assessing the degree of maturation of organic matter. However, Painter *et al.* (1994) pointed out that the extinction coefficients, used from converting integrated absorbance areas to concentration units, are very difficult to calculate for materials as complex as coals, due to the fact that the coefficients depend on a series of parameters such as coal structure, coalification stage, origin, etc. The choice of average absorption coefficients is an inherent deficiency of the IR methods in the analysis of coal structure. Often combination of the information obtained from FTIR spectroscopy and Raman spectroscopy is used to study changes in carbon structure during gasification (Dong *et al.* 2009).

2.7.1.4 Raman spectroscopy.

Raman spectroscopy is a powerful technique that has been used to characterise carbon structures (Tunisra and Koenig, 1970; Bar- ziv *et al.* 2000; Sadezky *et al*. 2005). It can be used to evaluate both the crystalline and molecular structures of carbon. (Li, 2007; Sheng, 2007). For very ordered carbonaceous material such as graphite, the Raman band is very intense and sharp with rather weak base-line signal. When the carbonaceous materials become more disordered, their Raman bands become broader and less well-defined. A number of methods have been reported on the evaluation of

less ordered carbons using FT-Raman spectra. Kawakami *et al*. (2005) used a four-peak curve fitting method to derive parameters from Raman spectra of charcoals. In this way, the original spectrum is represented by a combination of G, D, R1 and R2 bands. The G band corresponds to the graphitic and the D band to the graphitic defect fractions of the coke samples. The two other bands R1 and R2 are random structures can be used to determine the intensity of minimum point (valley) between the G band (graphitic) and the D band (graphitic defect fractions). However, this method does not suit disordered samples, e.g. mildly-pyrolyzed coal char, very well, because the valley between the G and D bands becomes very broad and intense. Consequently, more peaks need to be fitted into the raw spectrum. Most recently, Li *et al.* (2006) developed a deconvolution method of fitting 10 Gaussian bands into the Raman spectra of chars gasified from iron-exchanged Australian brown coals. The 10 peaks were assigned to various possible structures expected to exist in coals. However, the random shift of band positions and the interference of different bands during curve-fitting were found to occur when increasing the number of peaks fitted. Furthermore, the approach is time consuming and sometimes gives apparently incorrect results. Other methods include employment of the intensity ratio of raw (without deconvolution) D band to G band (I_D/I_G), the ratio of half-width of D peak to G band, the ratio of the minimum point of the valley between D and G band to G(I_V/I_G). A combination of both ratios can be used to carbon structure of coal char derived from low ash coals (Dong *et al.* 2009).

2.7. 2 Review of analytical techniques of char-mineral matter interaction

Lunden *et al.* (1998) examined the interaction between char-mineral matter during combustion of coal. They used a field-emission scanning electron microscope (FESEM) equipped with an energy-dispersive X-ray spectroscope(EDS) for chemical speciation and High Resolution Transmission Electron Microscope (HRTEM) for the carbon structure.EDS spectra performed in the HRTEM on the char samples showed an increase in the local concentration of mineral species at the pore surface when compared to further inside the char matrix. The local concentration of mineral specie at the pore surface was about 20% of the total local mass. They also reported that the high concentration of mineral matter on the surface of the char particle is expected at higher levels of conversion. The HRTEM images also show the development of varying amounts of crystalline material within the char matrix. The presence of

inorganic matter in solution in and around the turbostratic carbon may affect the extent of ordering in the carbon matrix, however from their measurements this experimental technique couldn't adequately distinguish between the potential effect of mineral matter on carbon ordering and the prevention of the penetration of oxygen into the carbon matrix.

Sekine *et al.* (2005) developed another method that can be used to study char-mineral interaction. This method employed an overlaying of results of laser Raman spectroscope (LRS)-mapping and the results of EDS mapping just on the same location of coal char. LRS mapping demonstrated the carbonaceous structural change of coal char and EDS mapping depicted the location of the ash-forming component. From the two mapping patterns, the location of Si and Al were in good in accordance with the location of non-graphitic carbon. They suggested that carbon located near the Si and Al compounds tended to resist gasification, since the carbon surface was covered with Si and Al compounds. Hence the reactant gas was unable to contact the carbon. However the effect of other elements such as Ca, Mg and Fe was not investigated. The method used in the evaluation of FT-Raman spectra is not well suited for disordered carbon structure. This involves calculating the ratio of the half-width of G-band to D-band (I_D/I_G). This does not account for the valley between the G and D bands which reflect the amorphous region in coal char (Dong *et al.* 2009). The increased reordering of the amorphous regions would lead to an intensity of the valley (I_V/I_G). In this study, a combination of both ratios I_D/I_G vs. I_V/I_G mapping will be used to evaluate carbon structure of chars. Also the EDS mapping will be extended to cover other elements such as Fe, Mg, Ca and K.

2.8 Conclusion and work program of this thesis

This study is motivated by the need to obtain a better understanding of coal reactivity during the gasification of high inertinite coals especially those with high ash contents in a fluidised bed gasifier under enriched air and steam fluidised bed gasification conditions. The use of these coals presents a (further) challenge as a result of the presence of dense chars formed from the inert inertinites. The dense char structures will require a long reaction time when using low temperature gasifiers such as fluidised reactor.

The most commonly recognized processes that contribute to decrease in reactivity are:

- Thermal annealing of the carbonaceous material particularly at longer residence times of gasification
- Mineral effects by locally displacing the char surface as a result of decomposition of clays in the coal.

The relative importance of the modifications of the carbon structure versus changes of allotropic form, sintering, melting or vaporisation of the inorganic matter in coal to char reactivity/deactivation needs to be investigated. The maceral composition and mineral distribution can be used to determine the relative modifications of the carbon structure versus changes of allotropic form, sintering, melting or vaporisation. Furthermore the interaction between the decomposed minerals on the carbonaceous matrix could affect reactivity. Molecular strain from the mineral particle can affect reactivity by blocking access to carbon active sites or promoting carbon ordering. This interaction could also be influenced by maceral composition. When there is no or little liquid phase (swelling), the mineral matter acts as a pore producer in the char matrix. Otherwise, the included minerals dilute and absorb the liquid phase, leading to the formation of a char structure with few voids and more ordered structure.

Hence the development of a complex model of mineral-char interaction is required to accurately predict and understand the effect of mineral matter on char reactivity during gasification. This study aims to correlate the gasification performance of the selected coals and their derived chars against a range of chemical, physical and optical characteristics including mineral and maceral (and specifically inertinite) contents and their changes in chemical microstructures following gasification in a fluidised bed gasifier. Raman spectroscopy and XRD analysis will be used to examine the chemical carbon structure and minerals associated in the coal. FT-IR has been used to determine the degree of polymerisation hence the contact between the chars and molten minerals. The relationship between the organic (maceral-to-char) and inorganic (mineral-to-ash) components in coal including their structure and behaviour will be determined by a petrographic analysis.

CHAPTER 3 EXPERIMENTAL AND TOOLS

3.1 Introduction

This chapter describes the coal samples, experimental apparatus and techniques used to investigate the interaction between the char matrix and mineral matter with specific focus on the evolution of char structure and reactivity. General methods for each apparatus are given, followed by specific details of the experiments performed in this work and the calculations used to analyse the data. Coal samples from three different mines were used in bench-scale experiment, and in the pilot scale gasifier work. Bench-scale experiments, including an atmospheric fluidised bed reactor and a thermogravimetric analyser were used to measure the char reactivity. The pilot-plant test facility consists of a coal feeding system, an air and steam supply and preheater system, a fliudised bed gasifier equipped with a cyclone and a particle recirculation system , a gas clean up and gas sampling system, and data acquisition system.

3.2 Coal samples

Three South African coals were used for the majority of the experimental work. Coal samples used in the gasification tests are some of the coal types used for power generation plants in South Africa. The selected coals are currently used as fuel for the Matla, Matimba (Grootegeluk coal) and Duhva power stations. The coal samples were crushed and sieved into different size fractions. Standard proximate, ultimate and maceral analyses for these coals are given in Table 3-1.

Table 3.1: Properties of the different coal samples

Sample	**Matla**	**Duhva**	**Grootegeluk**
Coal Proximate (wt%)			
Ash	44.00	39.20	35.70
Moisture	3.50	2.00	2.00
Volatile matter	19.90	19.60	27.30
Fixed Carbon(Calculation)	32.10	39.10	35.00
Coal Ultimate (wt%)			
C	39.09	46.93	49.20
H	2.90	2.87	3.87
N	0.92	1.10	0.97
O(Calculation)	8.60	6.38	6.79
S	0.66	1.42	1.47
Ash analysis			
SiO_2	58.91	53.08	68.60
Al_2O_3	28.76	20.18	20.05
Fe_2O_3	2.13	7.41	5.59
TiO_2	1.33	1.35	0.72
CaO	2.99	4.65	0.71
Na_2O	0.35	0.12	0.12
K_2O	0.76	0.89	1.25
SO_3	1.17	3.31	0.57
P_2O_5	0.22	0.73	0.08
Macerals analysis			
Vitrinite content %	36	24	83
Liptinite content %	4	4	5
Inertinite content %	59	71	12
Total reactives macerals %	56	55	96
Mean reflectance %	0.64	0.76	0.67
Microlithotype analysis			
Vitrite %	10	7	24
Liptite %	0	0	0
Inertite %	14	29	8
Intermediates %	24	23	22
Carbominerite %	24	18	29
Minerite %	28	23	17

3.3 Bench-scale fluidised bed experiment

Char samples were prepared in the fluidised bed reactor under pryolysis and gasification conditions. The experiments were carried out in a fluidised bed reactor with a height of 600 mm and a diameter of 52 mm. The vertical tubular fluidised bed reactor is made of high-grade stainless slab. The bed was externally heated via four electrical elements and the bed temperature was measured by means of a thermocouple. Air flow to the reactor is controlled with a rotameter. Coal was injected batch wise into the reactor. Once the coal had been in the reactor for the desired residence time, the char was drained into a cooled catch pot. Chars were prepared under a wide range of experimental conditions. Temperatures in the reactor were varied between 850 and 1000 ^{o}C; residence time was studied from 2-30 min. Particle size ranges were 200-500 micron, 500-1000 micron, 1-1.7 mm and 1.7-2.4 mm. Experiments were repeated 3-5 times for each condition. Reactivity measurements were carried out on the generated char.

3.3.1 Char Reactivity measurements

The reactivity of char was determined by the isothermal method. This involves tracking the weight loss as a function of time at a constant temperature. Char reactivity was carried out in a thermogravimetric analyser Perkin-Elmer TGA 7, coupled with a 1090 processor for continuous measurement of weight loss during oxidation. Char samples were reacted in air or pure carbon dioxide. The reaction conditions used were 21% O_2 at 500 ^{o}C and 100% CO_2 at 900 ^{o}C. About 5mg of char sample was placed in a platinum pan and purged with nitrogen. This is to allow complete removal of moisture. Then the purge gas was switched from N_2 to air. The weight loss was used to compare the reactivities of the different chars generated.

3.4 Pilot-plant experiments

The objective of the pilot–scale experiments was to gasify different high ash South African coals at the different conditions.

3.4.1 Description of the test facility

The fluidised bed gasifier consists of six main parts: (1) Coal feeding system (2) air and steam supply and preheated system (3) cyclone (4) gas sampling system (5) furnace; (6) gas distributor. A schematic diagram of this pilot plant is shown in Figure 3.1.

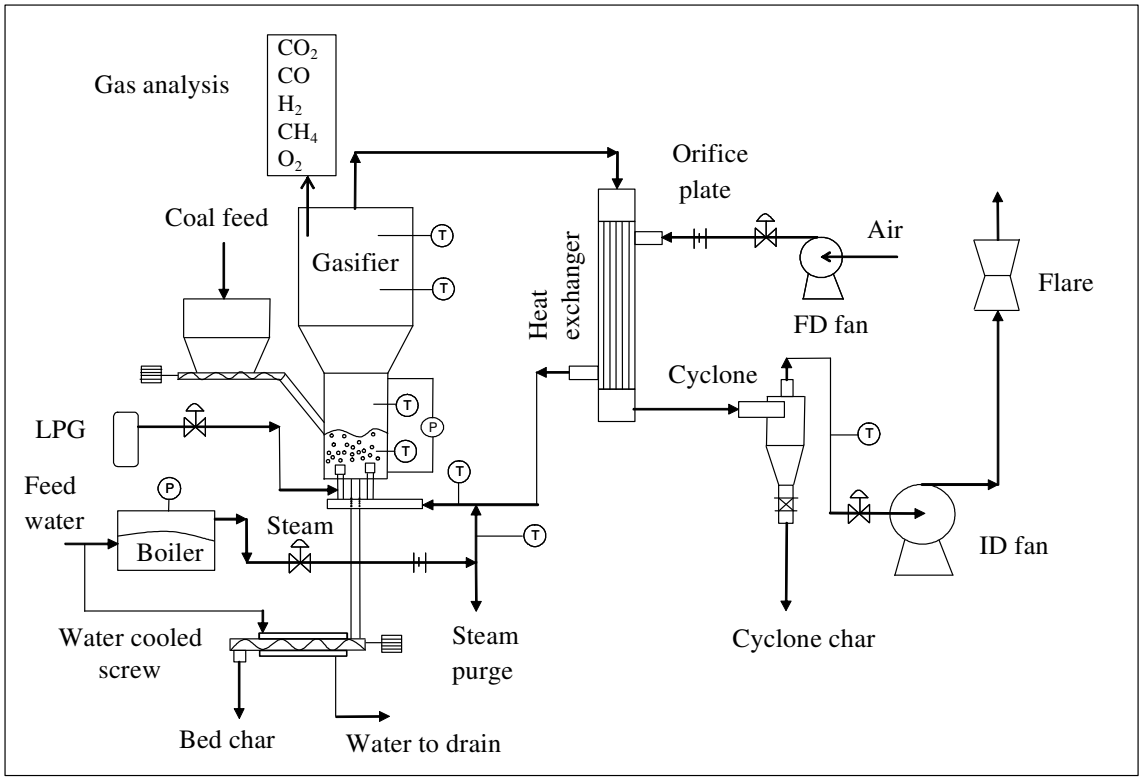


Figure 3 1. A schematic diagram of our FBG pilot plant

3.4.2 Feeding system

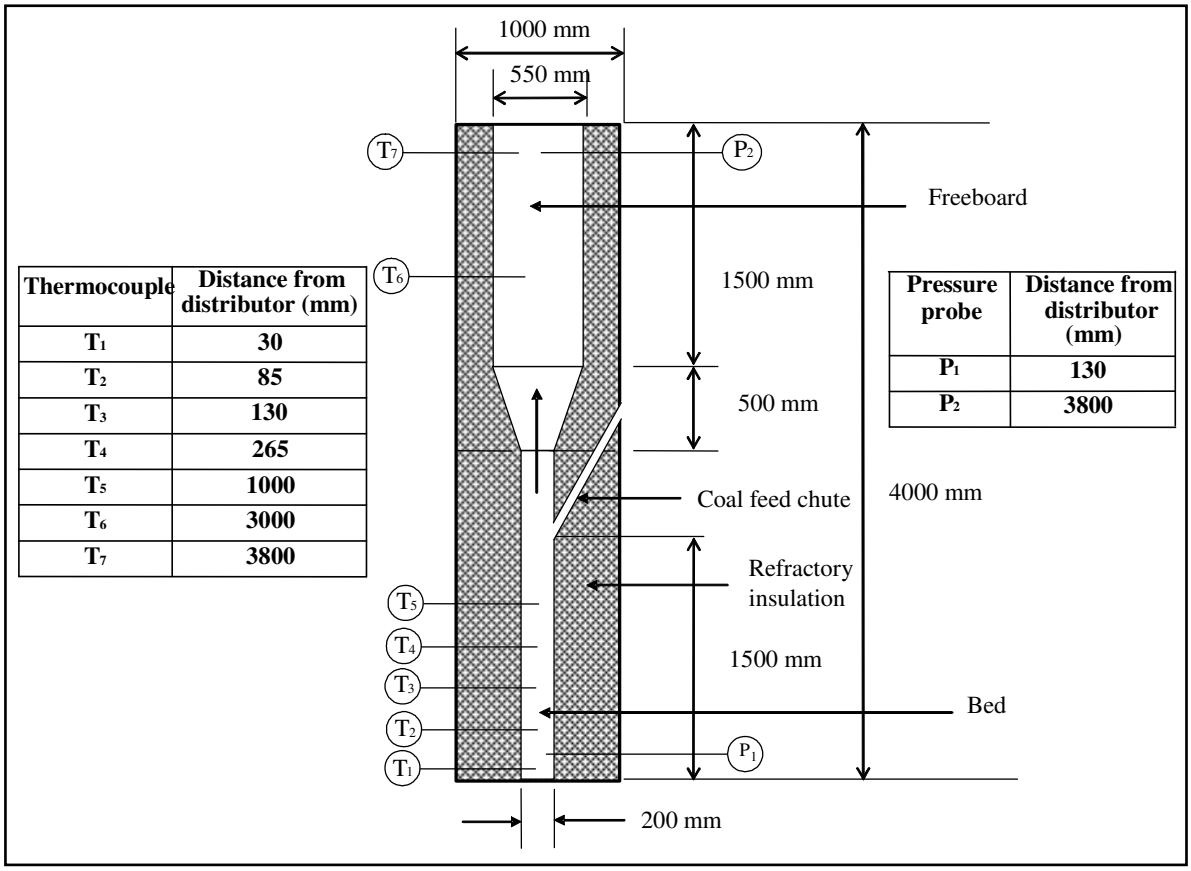
The feeding system consists of one lock hopper by which the feedstock is brought down to process pressure. The coal feedstock is conveyed from the hopper into the gasifier by a screw feeder. A variable rotating motor on the basis of the calibration curve control the feedstock feed rate.

3.4.3 Air and steam supply system

An air supply system provides primary and transporting air. This unit consists of one compressor, four electric valves to control the air flow rates and four flow meters. Primary gasification air is introduced into the gasifier via a spouting nozzle and a 60_ conical distributor to fluidize the bed materials. Primary air is preheated up to 270–300 ^{o}C by the flue gas generated from the gas combustor. Steam is generated in an electrode boiler. Steam and a part of primary air are mixed and introduced to the reactor through the distributor as fluidizing gases. Steam flow rate is controlled and measured by a valve and a mass steam flow meter, respectively.

3.4.4 Gasifier

The gasifier is a refractory-lined reactor with inside diameter of 200 mm in the dense bed, and expands to inside diameter of 550 mm in the freeboard. The total height of the gasifier is 4 m. The refractory is made up of two concentric cylinders with different thermal conductivity and wearing properties. The solids recirculation part consists of a cyclone. Seven temperature probes (from T1 to T7) measure the temperature variations along the gasifier. The probes T1–T5 monitor the temperature at the gasification reaction zone, and the probes T6 –T7 monitor the upper part. The distances of these probes from the distributor are shown in Figure 3.2. Two pressure taps were mounted at the bottom and exit of the reactor to monitor the fluidisation state in the reactor. The gasifier is equipped with an oil-fired start-up burner to heat the bed material to desired temperature at the start-up of each experimental test. The bottom ash is discharged via a water-cooled screw to two lock hoppers. After leaving the gasifier, the produced gas enters a cooler where the gas exchanges heat with water.



Thermocouple	Distance from distributor (mm)
T_1	30
T_2	85
T_3	130
T_4	265
T_5	1000
T_6	3000
T_7	3800

Pressure probe	Distance from distributor (mm)
P_1	130
P_2	3800

Figure 3.2: Dimension and details of the FBG Furnace (Engerbrelcht, 2008).

3.4.5 Test procedure

At the very beginning of each test run, approximate by 15 kg of bed materials (silica sand) was conveyed to the gasifier and the bed was heated with the start-up burner. After a few hours of heating, the bed temperature reached 650 ^{o}C, coal was fed into the gasifier using a carefully controlled feed rate that ensured the complete combustion of the coal. In such a combustion atmosphere, the coal was combusted and the reactor rapidly heated to about 925 ^{o}C. After the gasifier temperature was steady, the other feeder starts to feed the bed materials to the gasifier to the desired static bed height. The transition from combustion to gasification was done by increasing feeding of coal, decreasing the air flow rate, and introducing steam to the gasifier. The computer- based data acquisition system was activated to monitor and record the temperature, the pressure drop and the feed rate value during the start-up process. When the operation of the gasifier was stable, i.e. the temperature profile was steady, gas and ash samplings are taken for analysis. The bed temperature is controlled by increasing or decreasing the steam flow. If the steam flow drops below a minimum value (determined by the air/steam ratio), the air/coal ratio is adjusted. A minimum steam flow is required in order to prevent hot spots in the bed. Meanwhile,

the bottom ash was continuously discharged via the bed extraction screw to maintain the bed height. The cyclone ash was also discharged. After each test cyclone bin and extraction ash bin were sampled and analysed. The gasification tests were carried out under air-blown condition, oxygen blown and oxygen-enriched air blown condition. The flow rate of air and oxygen determine the oxygen content in the enriched inlet. For air-blown gasification air was used as oxygen supplier, so the oxygen percentage of the enriched air (OP) was 21% v/v for all the tests and the oxygen flow rate was nil. For oxygen-enriched gasification, the OP of the enriched air was 30%. For oxygen blown gasification the air flow rate was nil and only oxygen and steam where used as gasification agents. Full details of the test programme are given in Table 3.2.

Table 3 2: Details of test work performed in the pilot-plant

	Air blown	**Oxygen-enriched**	**Oxygen blown**
Coal feed rate (kg/h)	25-30	25-30	25-30
Air flow rate(Nm^3/h)	45-50	30-35	0
Oxygen flow rate (kg/h)	0	5-10	14-15
Steam flow rate (kg/h)	8-10	10-20	35
Bed temperature (^oC)	925-950	910-1000	950

3.5 Char characterisation

The changes in the characteristics of the char produced during the course of every test were assessed using a number of different techniques.(as described below)

3.5.1 Chemical analysis

The chemical analysis carried out on coal and char samples include proximate, ultimate and sulphur analyses**.** The proximate analysis is the method used to determine the percentages of moisture, volatile matter, fixed carbon (by difference), and ash. Moisture was measured by drying the sample in a platinum crucible at 105 ^oC in a hood for two hours (ASTM). The difference in weight before and after the drying procedure gives the moisture content of the sample. Ash content was determined by placing the dried sample into the oven, and the oven temperature was ramped up to 500 ^oC in one hour.

The sample was flooded with air every 30 mins by briefly opening the oven door. The temperature was then ramped up to 750 ^{o}C in another hour. Finally, the sample was soaked at 750 ^{o}C for at least 12 hours before the sample was cooled down and weighed again. The weight loss was used to calculate the ash content of the sample.

Volatile matter was estimated by placing one gram of coal was placed in a small (about 10 ml) tared ceramic crucible and dried for 1 hour at 105 °C. Then the crucible was cooled, weighed, and covered with a loose fitting cover. The covered crucible was placed inside a larger crucible to allow manipulation with tongs. Finally the crucibles were placed in a 950 °C muffle furnace for exactly 7 minutes and then cooled for 15 minutes before weighing. The weight loss from this analysis was used to calculate the volatile matter of the sample

Ultimate analysis was used to obtain the mass fraction of carbon, hydrogen, nitrogen and sulfur of the coal, char and residue samples. Each sample was weighed in a tared silver crucible before being totally burned by pure oxygen in the oxidation furnace in the analyzer. The products of combustion in the CHNS analyzer are CO_2, H_2O, N_2, and SO_x.

3.5.2 Petrographic analysis

The main purpose of this investigation was to assess the char samples in terms of their microscopic characteristics (reflectance properties, carbon form types, occurrence of visible minerals and char form size). This can provide some insight on the behaviour of carbon particles during gasification. The chars received were milled to a particle size of 2.5 mm for organic petrology analysis. A petrographic block of each sample was prepared and polished by the South African Bureau of Standards in accordance with the ISO Standard 7404-2, 1985 and then examined under the microscope at Petrographics SA, Pretoria. Random reflectance measurements were taken on each char in accordance with the ISO Standard 7404-5, 1994. A total random reflectance scan was undertaken on each sample. 250 reflectance readings were obtained on all carbon forms over the polished surface of each petrographic block, except in the case of the Matla char where it was only possible to obtain 100 measurements on char fragments of suitable size due to the very low occurrence of organic matter in this

particular sample. Quantitative analyses of the component types present were undertaken.

The microscopic constituents of the 3 chars were assessed by virtue of their colour, reflectance, degree of anisotropy, size, morphology and extent of devolatilization and general response to heating. The relative proportions of the carbon-rich constituents/inorganic materials and char form size ranges were established on the bases of 500 point-counts according to the method set out in the ISO Standard 7404 - 3, 1994.

3.5.3 FT-IR spectrometry

The infrared spectra of the samples were acquired by Fourier transformed infrared spectroscopy (FTIR), using a Nicolet Magna IR-560 spectrometer equipped with a mercury–cadmium telluride detector operating at 4 cm^{-1} by averaging 256 scans. The diffusion reflectance spectra were converted to the Kubelka–Munk function. The coal samples were well mixed with dried KBr (sample/KBr ratio 1/100), and then pressed into very thin pellets. Two pellets of each sample were used to derive the averaged spectra, in order to minimize experimental errors. Spectra were corrected from scattering using two baselines (4000–1800 cm^{-1} and 1800–400 cm^{-1}).

3.5.4. Fourier Transform Raman Spectroscopy

Raman spectroscopy was used to examine the chemical carbon structure. The Raman spectra of coal chars were obtained in air at room temperature using a Bruker Equinox 55 Fourier Transform Equinox 55 spectrometer with an FRA 106 Raman module equipped with a Ge detector and a 1064 nm Nd: YAG laser. The laser power was selected between 10 and 140 mW, depending on the samples tested; the spectral resolution was 4 cm^{-1}. For each sample, three measurements were made on a random fraction of the sample. 2000 scans were carried out in each measurement to obtain spectra with acceptable noise-to-signal ratio. The averaged spectrum of each sample from the three measured spectra were used to derive spectra parameters.

3.5.6 X-ray Diffraction

The X-ray diffraction patterns of coal and char particles have been recorded by a PANalytical X'Pert Pro powder diffractometer with X'Celerator detector and variable divergence- and fixed receiving slits with Fe filtered Cobalt (Co) K-alpha radiation. The phases were identified using X'Pert Highscore plus software. Coal and char samples were placed on a single crystal silicon disc sample holder. The sample holder did not give an amorphous halo and because the crystal was cut along a plane that did not diffract within the angular range of the diffractometer, no peaks could be seen in the background. This can therefore be described as a "zero background substrate". The samples were then loaded into the X-ray cavity and scanned in a step-scan mode (0.040/step) over the angular range from 10^{o} to 60^{o}. The qualitative XRD analysis was carried out using the Graphics and Identification programme. The percentages of the individual crystalline phases (minerals) in each sample were determined using the reference intensity ratio (RIR). RIR values were determined from PDF-2 date base (JCPDS-ICDD PDF-2, 2003. In order to determine the proportion of amorphous material in the samples, calcium fluoride was used as internal standard.

X-ray diffraction was used to evaluate more fully the nature of the clay minerals in the feed coal samples. The clay fractions(less than 2 effective diameters) of each sample were isolated by ultrasonic dispersion in sodium hexametaphosphate (Calgon) and subsequent settling. The clay fraction was further investigated by X-ray diffraction of oriented aggregates using, glycol and heat treatment. The relative proportions of the different clay minerals for each sample were determined by the method of Griffin (Carver, 1971).

3.5.7 Scanning Electron Microscopy

SEM coupled with energy dispersive X-ray analyser was used for image and chemical analysis. Coal char morphology and cross-sections were examined using high-resolution field emission scanning electron microscopy (FESEM). A small amount of each coal char samples was mounted on an adhesive tape and examined under the FESEM. Cross sections of char samples were mixed with resin in 30 mm mount and allowed to cure, and then cross sections of the char particles were obtained by polishing each mount as indicated. The internal structure of char was inspected under

the FESEM. Elemental mapping was also undertaken using the EDAX facility on selected particles.

3.5.8 Specific surface area measurements

Internal surface areas of coal and char samples were measured via isothermal gas adsorption using a Micromeritics Tristar 3000 instrument with either N_2 adsorption gas. N_2 adsorption is conducted at 77 K (the normal boiling point of N_2). The small micropores cannot be adequately accessed at this temperature because the activation energy of diffusion is too high, and because of thermal shrinkage of pores at this temperature.Therefore N_2 surface area is a measure of the surface area of larger pores only. N_2 adsorption isotherms are used to calculate surface area by the BET equation.

$$\frac{P}{V(P_0 - P)} = \frac{1}{V_m c} + \left(\frac{c-1}{V_m c}\right)\left(\frac{P}{P_0}\right) \qquad 4.2$$

Where P is the pressure of a given data point, P_0 is the saturation vapour pressure of the adsorbate, V is the volume absorbed at a given pressure, V_m is the monolayer volume, v and c is a constant. Surface area can be calculated by linearising the data by plotting P/ (V (P_0-P) vs. 1/ (V_mc) and using a linear regression analysis to calculate the values for V_m and c. The surface area can be calculated by using the density to determine the number of moles in the monolayer and assuming that each molecule covers 0.162 nm^2.

3.5.9 Carbon conversion

Carbon conversion was calculated using analyses of the feed coal and the char produced using ash as a tracer component as follows

$$\text{Conversion} = 100 - \left(100\frac{C_{char} / A_{char}}{C_{coal} / A_{coal}}\right) \qquad 4.3$$

Where Ccoal or Char is the carbon in coal or char (dry basis) and Acoal or Achar is the ash in the coal or the char (dry basis)

CHAPTER 4: CHARACTERISATION OF SOUTH AFRICAN COAL AND CHARS IN FLUIDISED BED GASIFICATION

4.1 Introduction

This chapter seeks to explore the behaviour of three South African bituminous coals currently used as feed in local power stations and to establish their technical performance and structural changes in a fluidised bed gasifier. It is anticipated that this will provide new insights into the evolution of the typically high-ash inertinite-rich coals currently available on the South African domestic market. This was achieved by correlating the gasification performance of the selected coals and their derived chars against a range of chemical, physical and optical characteristics including mineral and maceral (and specifically inertinite) contents and the changes in chemical microstructures following gasification in a fluidised bed gasifier. Raman spectroscopy and XRD analysis were used to examine the chemical carbon structure and minerals associated in the coal. FT-IR was used to determine the degree of polymerisation hence the contact between the chars and molten minerals. The relationship between the organic (maceral-to-char) and inorganic (mineral-to-ash) components in coals including their structure and behaviour was determined by a petrographic analysis.

4.2 Experimental

Char samples were prepared from the parent coal samples in the pilot-scale gasifier as described in Chapter 3. The coal samples were gasified at 950 ^{o}C in oxygen blown conditions. The operating conditions for the gasification tests are summarised in Table 4.1. A detailed characterisation of the char was carried out using various experimental techniques earlier mentioned.

Table 4.1: Gasification operating conditions

	Matla	Duvha	Grootegeluk
Pressure (kPa)	90	90	90
Bed temperature(^{o}C)	950	950	950
Coal feeding rate (kg/h)	24	26.4	23
Mean particle size (mm)	1.6	1.9	1.9
Mean residence time (min	36 – 37	35 -36	45 – 46
Fluidising velocity(m/s)	1.9 - 2.2	1.9 - 2.2	1.9 - 2.2
Gasification agents	O_2 & steam	O_2 & steam	O_2 & steam

4.3 Results and discussion

4.3.1Proximate and ultimate analysis

The results of proximate and calorific values of the parent coals and bed char and cyclone are presented in Tables 4.2-4.4. The bed char especially for Matla has n ash yield of almost 100 %, while the cyclone char still contains some organic matter, mainly fixed carbon (non-volatile) form. The Duhva char particles show similar trends but not the Grootegeluk char particles. This indicates Matla coal had the highest carbon conversion. A comparison of proximate analyses of Matla coal and its chars is presented in Figure 4.1.

One of the key factors that determine the formation of char is the amount of volatile matter released. The evolution of escaping volatiles affects char porosity and reactivity, since high porosity in chars have been attributed to high devolatilisation (Mendez *et al.* 1993). As observed in this study, there was no significant difference in the total volatile yield for the three chars (94-96%); however, there was a significant difference in the morphology of the chars. Two of the selected coal samples produced a solid/dense char; while only one of the coal samples produced porous char. Similar results were obtained for loss of fixed carbon. This indicates that the gasification reactivity cannot be correlated with coal property using only volatile matter released.

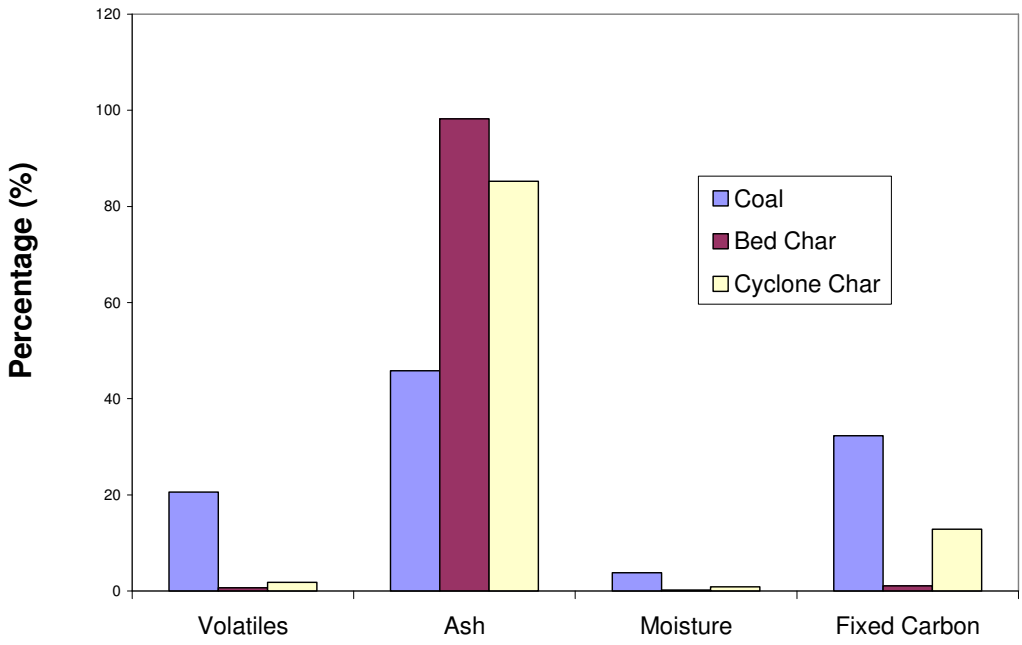


Figure 4.1: Comparison of proximate analyses of Matla coal and its chars

The fixed carbon conversion for the different coals varied between 66-89% with Matla coal having the highest conversion (89%). However, there was no direct relationship between fixed carbon content of coal and the carbon burnout values for the different coal (Figure 4.2). Similar results have been reported for combustion by Mendez *et al*. 2003 and Choudhury *et al*. (2008) for some selected coals of different rank. They suggested that key properties that influence the burnout behaviour of coal are coal rank, maceral composition and mineral matter content. In this study, the selected coals were similar in rank. The effect of maceral and mineral composition on conversion will be discussed in the petrographic analysis in the next section.

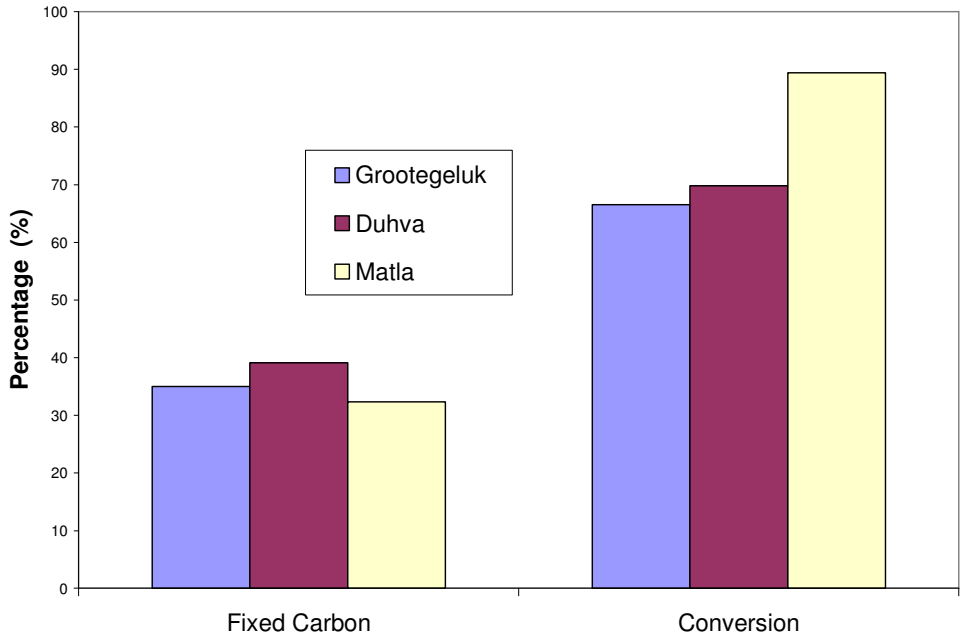


Figure 4.2: Comparison of fixed carbon content of parent coal and fixed carbon conversion

Table 4.2: Proximate and ultimate analysis and calorific value of parent coals

Coal		Matla	Grootegeluk	Duvha
Proximate analysis (as determined on air-dried basis)	Standard			
Ash content (%)	ISO 1171	44.00	35.70	39.20
Inherent moisture (%)	SABS 925	3.80	2.00	2.10
Volatile matter (%)	ISO 562	19.9	27.30	19.60
Fixed carbon (%)	By diff.	32.30	35.00	39.10
Calorific value				
Calorific value (MJ/kg)	ISO 1928	18.60	19.80	21.10
Ultimate analysis(as determined on air-dried basis)				
Carbon (%)	ISO 12902	39.09	49.20	46.93
Hydrogen (%)	ISO 12902	2.90	3.87	2.87
Nitrogen (%)	ISO 12902	0.92	0.97	1.10
Sulphur (%)	ISO 19759	0.66	1.47	1.42
Oxygen (%)	By diff.	8.63	6.79	6.38

Table 4.2: Proximate and ultimate analysis and calorific value of bed chars

Bed Char		**Matla**	**Grootegeluk**	**Duvha**
Proximate analysis	Standard			
Ash content (%)	ISO 1171	98.00	73.10	93.10
Inherent moisture (%)	SABS 925	0.2	2.10	0.60
Volatile matter (%)	ISO 562	0.7	0.90	1.00
Fixed carbon (%)	By diff.	1.1	23.50	5.30
Calorific value				
Calorific value (MJ/kg)	ISO 1928	0.62	6.06	1.36
Ultimate analysis				
Carbon (%)	ISO 12902	1.66	22.60	5.90
Hydrogen (%)	ISO 12902	0.07	0.35	0.11
Nitrogen (%)	ISO 12902	0.00	0.25	0.07
Sulphur (%)	ISO 19759	0.06	0.63	0.20
Oxygen (%)	By diff.	0.01	0.57	0.02

Table 4.4: Proximate and ultimate analysis and calorific value of cyclone chars

Cyclone Char		**Matla**	**Grootegeluk**	**Duvha**
Proximate analysis	Standard			
Ash content (%)	ISO 1171	84.4	68.10	52.90
Inherent moisture (%)	SABS 925	0.9	1.70	2.40
Volatile matter (%)	ISO 562	1.80	1.50	2.30
Fixed carbon (%)	By diff.	12.9	28.80	42.40
Calorific value				
Calorific value (MJ/kg)	ISO 1928	3.86	9.10	14.60
Ultimate analysis				
Carbon (%)	ISO 12902	13.70	27.77	41.24
Hydrogen (%)	ISO 12902	0.20	0.41	0.61
Nitrogen (%)	ISO 12902	0.15	0.36	0.70
Sulphur (%)	ISO 19759	0.57	0.70	0.88
Oxygen (%)	By diff.	0.08	1.06	1.27

4.3.2 Petrographic analysis

The reflectance and type of macerals present in the parent coal have been reported to have an effect on the char properties (Jones *et al.* 1985). One of the key challenges to this analysis is the analysis of fine coal particles less than $30\,\mu m$, hence the cyclone char was not analysed. The results of reflectance measurments and the petrographic composition for the selected coals and their chars are presented in Tables 4 .5 and 4.6.

4.3.2.1 Reflectance properties

The vitrinite random reflectance data showed that, according to the ISO 11760 - 2005 Classification of Coals, the three original parent coals were characterized as bituminous, Medium Rank C coals, with mean random reflectance values within the range of 0.64% up to 0.76% Rv_{rand}. In order to assess the reactivity of the organic constituents during the char forming process, reflectance measurements were taken on the all the organic char components. The scan raw data are presented in Appendix A.

The results are presented in histograms and shown in Figure 4.3. Significant shifts were displayed in the levels and ranges of the reflectance in the char samples. The mean reflectance increased from 0.67 to 4.96% for the Grootegeluk char, it increased from 0.64 to 4.77 % for the Malta Char, and from 0.76 to 5.08% for the Duhva char.

The wide range of char reflectances will reflect variation in ignition temperature, time for burn-out of char and carbon content. High reflectances indicate more mature chars and high temperatures in the vicinity of the char. The lowest reflectance level of all the chars was greater than reflectance levels in the range of their parent coals. This suggests that no unreacted coal macerals were left. Approximately 15% to 30% of carbon particles exhibiting substantially lower levels of reflectance in the range of between 1-4% Rv_{rand} representing partially consumed char were encountered. Approximately 73-85% of the carbon particles displayed reflectance levels greater than 4% indicating highly reflecting 'clean' char. Duvha and Matla possess 15.2 and 16.0% of chars at reflectances over 6% Rv_{rand} respectively (and 3 and 5% over 7% Rv_{rand}), thereby indicating the likelihood of very high temperatures. However, Grootegeluk only has 11.6% at over 6% Rv_{rand} and 1.2% over 7% Rv_{rand}), as shown in Table 4.5.

This is a very high reflectance value which may indicate that the coal particle was burning at temperatures of over 1000 ^{o}C (Falcon, 2011). This is significant, as the fluidised bed temperatures are usually kept around 900 ^{o}C, but some char forms do burn at higher temperatures. Such high temperatures can have a large impact on the nature of the minerals which can melt, stick together (agglomerate) and form ash deposits, if the operations are not carefully controlled.

Table 4.5: Summary of the major petrographic properties of the parent coals

	GROOTEGELUK	MATLA	DUHVA
PARENT COAL			
RANK (degree of maturity)	**Bituminous**	**Bituminous**	**Bituminous**
ISO 11760-2005 Classification of Coals	**Medium Rank C**	**Medium Rank C**	**Medium Rank C**
Mean random reflectance of vitrinite %	**0.67**	**0.64**	**0.76**
Vitrinite-class distribution	**V 5 to V 8**	**V 5 to V 9**	**V 5 to V 10**
Standard deviation	**0.067**	**0.078**	**0.090**
Abnormalities	**None observed**	**None observed**	**None observed**
PETROGRAPHIC COMPOSITION (% by volume)			
Maceral analysis (mineral matter-free basis)			
Total reactive macerals %	**91**	**56**	**55**
Vitrinite content %	**83**	**36**	**24**
Liptinite content %	**5**	**4**	**4**
Total inertinite %	**12**	**59**	**71**
Heat altered (coke, char etc.) %	**0**	**1**	**1**
Maceral analysis - Total %	**100**	**100**	**100**
Microlithotype analysis (mineral matter basis)			
Vitrite %	**24**	**10**	**7**
Liptite %	**0**	**0**	**0**
Inertite %	**8**	**14**	**29**
Intermediates %	**22**	**24**	**23**
Visible minerals			
Carbominerite %	**29**	**24**	**18**
Minerite %	**17**	**28**	**23**
Microlithotype analysis - Total %	**100**	**100**	**100**
Condition analysis			
"Fresh" coal particles %	**84**	**78**	**83**
Cracks and fissures %	**14**	**19**	**15**
Severely weathered %	**2**	**2**	**1**
Heat altered (e.g., coke/char) %	**0**	**1**	**1**
Condition analysis - Total %	**100**	**100**	**100**

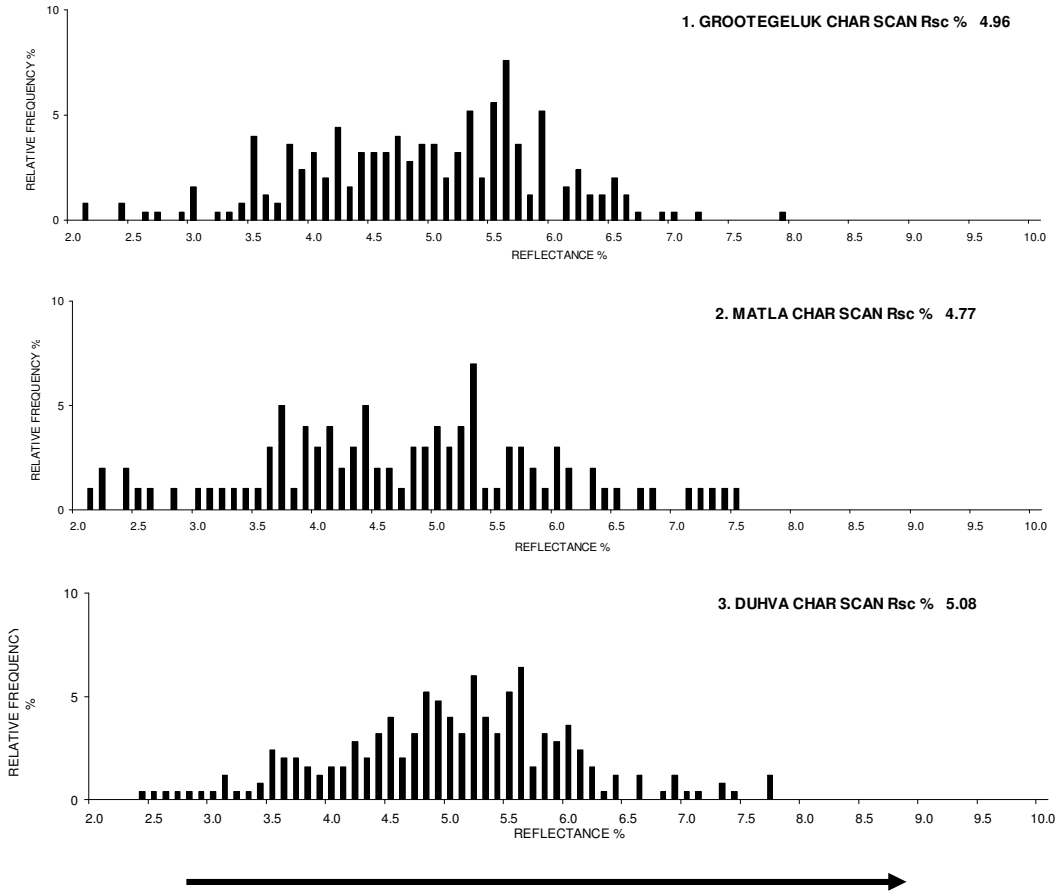


Figure 4.3: Reflectance histogram for char particles from each coal**. :** Increasing reflectance, decreasing volatiles, expected increase in ignition temperature and time for burn-out

Table 4.6: Summary of the reflectance properties of the char samples

Sample	**Mean random reflectance (Parent Coal)**	**Mean random reflectance (Chars) Rr%**	**Non-reacted Macerals >1%Rr**	**Partially consumed Char 1-4% Rr**	**Highly reflecting char 4-7 % Rr**		
					>4%	>6	>7
Grootegeleuk	0.67	4.96	0.0	18.0	82.0	11.6	1.2
Matla	0.64	4.77	0.0	27.0	73.0	15.2	3.0
Duvha	0.76	5.08	0.0	14.8	85.2	16.0	5.0

4.3.2.2 Carbon form analysis

Carbon form analysis has been used to estimate the various types of char formed and determine the changes in the carbon and mineral contents in char.

Types of char formed

The carbon form analysis revealed that the char samples represented different mixtures of partially reacted coal, 'char', coke and visible minerals. Some photomicrographs showing the different types of chars are presented in Figure 4.5-4.10. The relative proportions of the various char types and the occurrence of visible minerals are shown in Table 4.7.

Table 4.7: Relative proportions of the various char particles formed

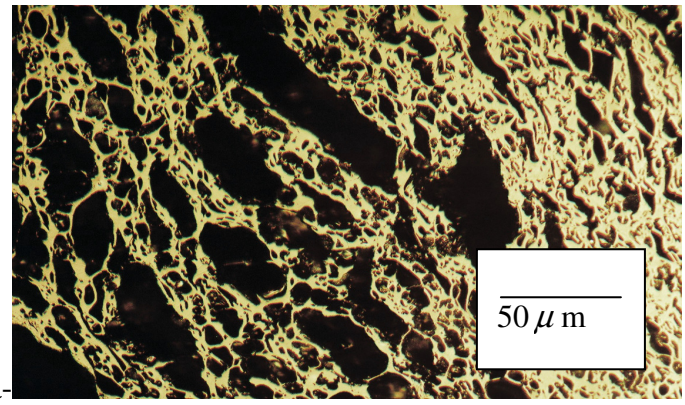
PETROGRAPHIC COMPOSITION (% by volume)			
Types of char formed	**GROOTEGELUK 903°C**	**MATLA 935°C**	**DUHVA 918°C**
Isotropic coke - thin walled, very porous %	**22**	**18**	**16**
Isotropic coke - thick walled, porous %	**28**	**10**	**6**
Mixed porous %	**14**	**16**	**21**
Relatively unchanged inertinite %	**12**	**27**	**33**
Partially consumed carbon %	**18**	**20**	**11**
Organic/inorganic associations % (minerals 25%-50%)	**6**	**9**	**13**

- **COKE FORMS**

These are derived mainly from "pure" vitrinite, i.e., vitrite, in the parent coal. The "coke" in these samples was represented by isotropic forms, sometimes pitted with very fine–sized open pores. Some coke particles were thin-walled and very porous, displaying well-developed devolatilisation vesicles, while others had quite thick coke walls with relatively smaller gas pores. These are shown in Figure 4.4a and 4.4b respectively. From the carbon form analysis presented in Table 4.7, Grootegeluk coal formed a higher proportion of isotropic coke (50%), as compared to Matla and Duhva coals (28% and 22% respectively). Also the porous isotropic coke form had the highest percentage in the Grootegeluk char. The predominance of porous isotropic coke forms in the Grootegeluk char can obviously be related to the high reactive

maceral content of 91% (mmf) in the parent coal. When coal is heated during the gasification process, the vitrinites and other reactive coal macerals soften and degasify, thereby creating pores. As the released gases within the pores increase in volume, the softening walls expand and the material increases in volume and surface area.

a-



b-

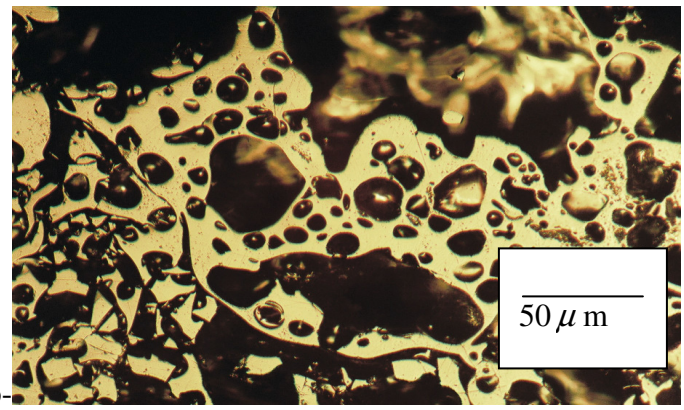
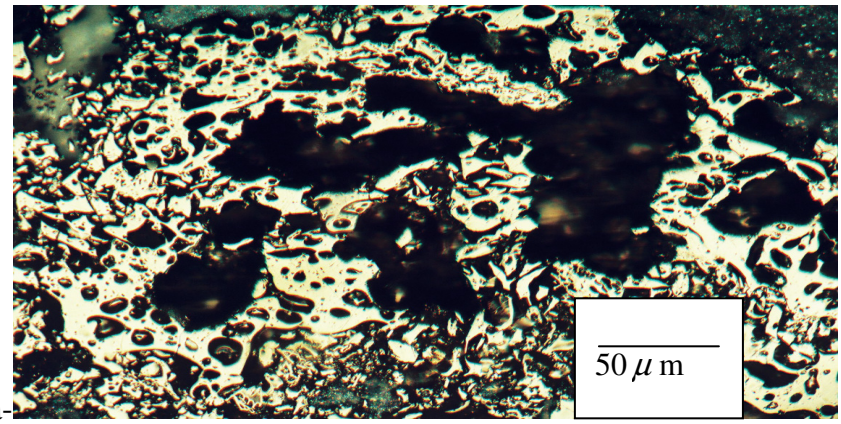


Figure 4.4: (a) Thin-walled Isotropic coke (b) Thick-walled Isotropic coke

- **CHAR FORMS**

Photomicrographs of mixed porous chars from reactive-rich coal particle and inert-rich coal particle are shown in Figures 4.5a and b. Dense char derived from pure inertinite is presented in Figure 4.6.

a-



b-

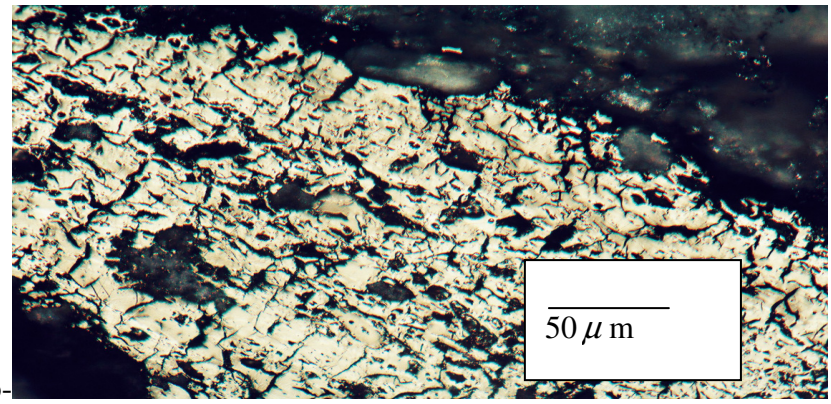


Figure 4.5 (a) Mixed porous from reactives-rich coal particle and (b) inerts-rich coal particle

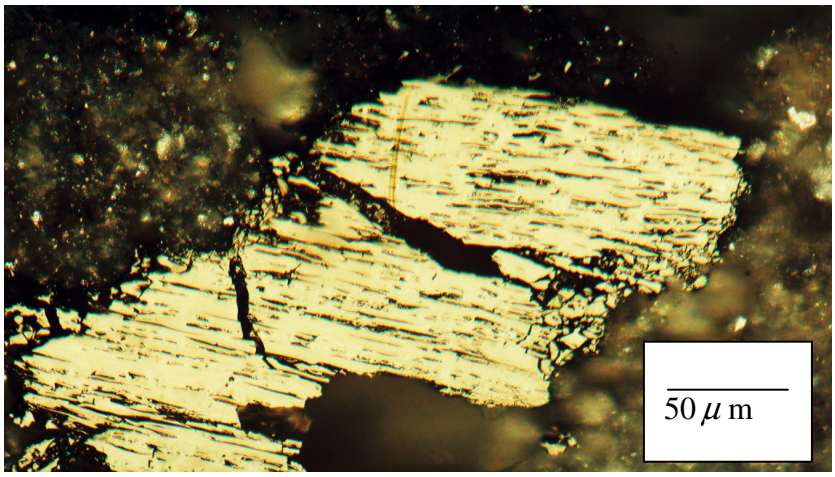


Figure 4.6. Dense char from pure inertinite

a) Mixed porous – derived mainly from intermediate microlithotypes in the parent coal. Those networks which had developed from reactive-rich coal were fine-walled and had "opened up" to varying extents, thus providing high internal surface areas. Thicker-walled and less porous networks had formed from inerts-rich parent coal particles. From the carbon form analysis, Duhva coal had the highest proportion of

mixed porous chars with a value of 21% while Matla and Grootegeluk coals had 16% and 14% respectively. The results indicate that inertinite macerals with variable reactivities are the main precursors for the mixed char forms.

b) Relatively unchanged Inertinites – also called dense chars, are derived from inert coal macerals in the parent coal which had not softened, expanded and "opened up" to any appreciable extent on processing. They largely retained their original coal maceral shape and form. Extensive cracking and disintegration of the inertinite materials were observed. Although some small pores are visible, the inertnitic–coally materials had increased in reflectance but have not devolatilised sufficiently to form porous char. Dense chars were predominately formed in high coals with proportions of inertinitic coals such as in Matla and Duhva (27 and 33% respectively. Grootegeluk on the other hand has very low inertinite (12% relative to 59 and 71%) in Matla and Duvha respectively) and very low dense char form (12% relative to 27 and 33% in Duvha and Matla respectively).

- **PARTIALLY CONSUMED CARBON**

Photomicrographs of partially consumed carbon are presented in Figure 4.7. This material was of reflectance levels above those of the original parent coal vitrinites, but substantially lower than those of the bright "clean" carbons. The edges appear darker, and inner zones had been partially "eaten away". Approximately 11 to 20% of carbon particles exhibiting substantially lower levels of reflectance representing partially consumed char were encountered.

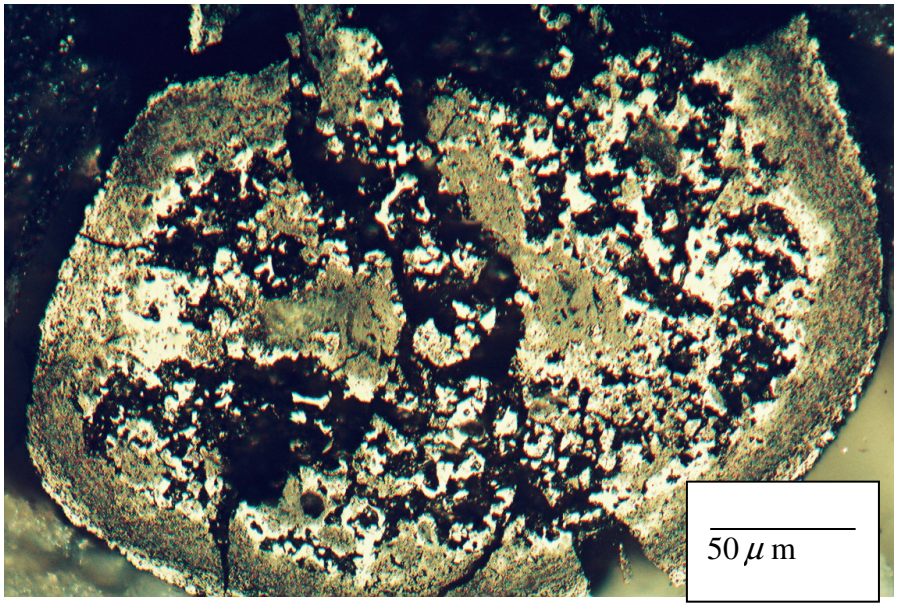


Figure 4.7**:** Photomicrograph of partially consumed carbon body with darker borders and zones

- **VISIBLE MINERALS**

The total mineral matter content varied substantially within the set of three chars (around 36% in the Grootegeluk char, 94% in the Matla and 84% in the Duhva). Greatly varying quantities of mineral "slag" bodies were observed in the char. Sometimes this "slag" had formed borders against the organic char or melted around carbon fragments. Occasionally, "slag" had penetrated into the carbon matrix. This is presented in Figure 4.8. The proportion of melted minerals covering the carbon matrix was 15 to 20% in the Matla and Duhva chars, and 4% in the Grootegeluk (~5%). Such inert mineral boundaries would severely reduce the ability of the carbon to further react.

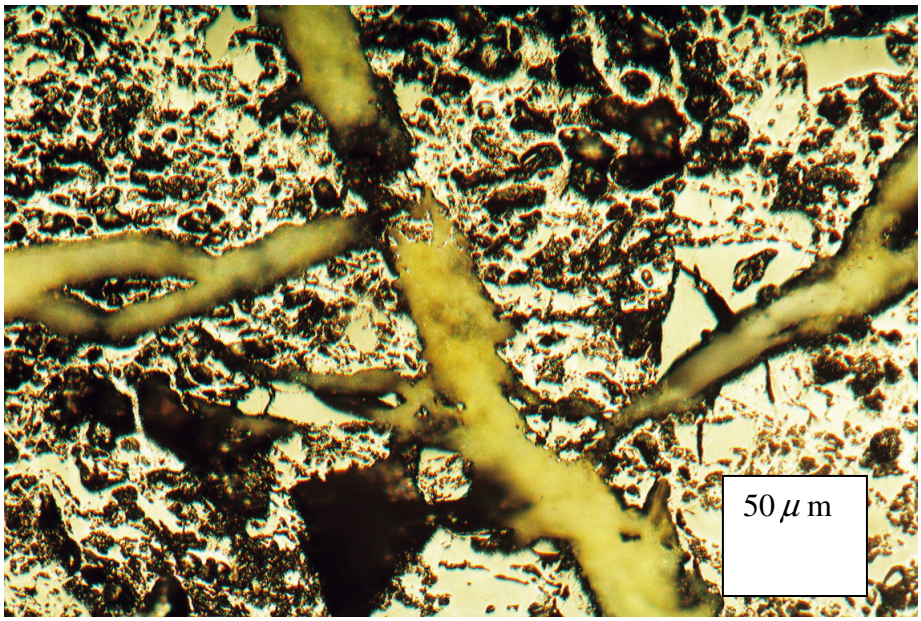


Figure 4.8: Photomicrograph of "Slag" penetrating carbon matrix in cracks and fissures

Consumed particles and mineral

The total carbon conversion of the particle was determined by the estimation of organic constituents/visible mineral matter in the char**.** The results of the petrographic composition of char are presented in Table 4.8. The petrographic analyses conducted on the chars indicated that there is a far higher organic-matter-derived carbon content in the Grootegeluk char with little or no indication of melted minerals whilst the reverse is the case in the other two samples. Both Matla and Duvha chars showed low carbon contents and high proportions of melted minerals. The char-to-mineral matter proportions (organic constituents versus visible mineral matter as determined by volume in percentage terms) indicate that Grootegeluk has 64% organic matter (char) and only 20% melted/sintered minerals with 16% unchanged minerals. The other two samples, Duvha and Matla both have very low proportions of organic matter (chars, 16% and 6% respectively) and very high proportions of melted/sintered minerals (74 and 75% respectively), with 10-19% of unchanged minerals. Borrego *et al.* (1997) and Wang *et al.* (2010) reported similar results for inertinite-rich coals when exposed to higher temperatures during pyrolysis and combustion tests undertaken between the temperatures of 600-1100 ^{o}C. The gasification temperature (900-950 ^{o}C) used in this study falls within this range.

Further analysis showed much higher proportions of melted minerals found in the two coals having higher inertinite contents (Duvha and Matla). Grootegeluk on the other hand has very low inertinite (12% relative to 59 and 71% in Matla and Duvha respectively) and showed very low melted minerals (20% relative to 74 and 75% in Duvha and Matla respectively). These results indicate a close correlation between the inertinite content and amount of melted minerals in the relevant chars.

From the petrographic compositions in Table 4.8, an attempt was made to correlate the proportion of the melted minerals in the various chars to the type of minerals in the parent coal. The results indicated a trend between melted mineral and kaolinite greater than 50% proportion i.e. clays. This may suggest that clays in concentrated form, either in high-ash carbonaceous particles as shales or mudstones, give rise to the highest proportion of melted minerals.

Table 4.8: Petrographic Composition of Chars

CHAR	GROOTEGELUK 903°C	MATLA 935 °C	DUHVA 918 °C
Carbon form analysis - Total %			
Organic constituents/visible mineral matter			
Total organic material %	64	6	16
Relatively unchanged visible minerals %	16	19	10
"Melted" minerals % - penetrating/surrounding carbon	4	19	16
"Melted slag" minerals % - separate bodies	16	56	58
Total %	100	100	100
Quartz + Clays > 50% per particle	12	33	26

4.3.3 Structural characteristics of raw coals and chars

4.3.3.1 Aromaticity

The active site concentration in the molecular structure of chars depends on the aromaticity and the degree of molecular ordering in the parent maceral structure (Borrego *et al.* 1997). The aromaticity factor was obtained from the expression in Equation 1 reported by Wang *et al*. (2009).

$$f_a = \frac{1200x(100 - V_{daf})}{1240xC_{daf}}, \qquad \textbf{(1)}$$

where f_a is aromaticity, V_{daf} is volatile matter on air dry basis and C_{daf} is carbon on dry ash free-basis. Table 4.9 showed that Matla and Grootegeluk coals had the highest and the lowest aromaticity factor, respectively. The results also showed there was an increase in aromaticity after gasification. This result correlates with the conversion level reported as total organic material in the chars in Table 4.9. These results are in agreement with those published for coal combustion by Lu *et al.* (2000). The results also indicate that inertinite-rich coals are more aromatic than vitrinite-rich coals. Similar results have been reported by Sun *et al*. (2003) and Wang *et al*. (2010). However, Duhva coal with higher inertinite contents (71%) had a lower conversion and lower aromaticity factor (1.66) in its' chars than the Matla derived char (1.98), with 59% inertinite content and an aromaticity factor of 1.98. This might be due to difference in rank, although it was assumed that all coals were similar in rank, their mean random vitrinite reflectances (Rv_{rand}) were not exactly equal but spanned over the interval 0.64-0.76%. This further suggests that for Matla and Grootegeluk with similar Rv_{rand} values of 0.64% and 0.67% respectively, the high inertinite contents is the main factor that contributed to the higher aromaticity and high burnout level. However, for Matla and Duhva with 0.64% and 0.76% Rov values, both the rank and inertinite content play an important role in the carbon conversion with the rank reducing the level of burnout.

Table 4.9: Aromaticity of the different coals and chars

Samples	Parent Coal	Char
Matla	1.98	57.88
Duhva	1.66	16.23
Grootegeluk	1.42	4.24

4.3.3.2 Coke Forms

The formation of coke indicates changes in the carbon structure of the coal/chars where coke is defined as a graphitised ordered carbon. From the petrographic analysis carried out to determine the various types of chars, Grootegeluk coal formed a higher proportion of isotropic coke (50%), as compared to Matla and Duhva coals (28% and 22% respectively).

4.3.3.3 Raman Analysis

The Raman spectra of the chars produced from the three different coal samples are presented in Figures 4.9-4.11. In all the Raman measurements the G and D bands were dominant and a weak 1124 cm^{-1} band was apparent. Qualitatively, the spectra for Duvha and Grootegeluk char are similar, while spectra of the Matla char are different. The G band for both Duvha and Grootegeluk char is weaker than the D band, in contrast to that for the Matla char. A comparative study of the peak position, the bandwidth of the three bands obtained after curve fitting (two-lorentzian bands) is presented in Table 4.10. The fitting parameters were used to evaluate the changes in the microstructure of the coal during gasification.

The D bandwidth of the three coal samples decreased after gasification, thereby suggesting an increase in reordering of the amorphous carbon (Dong *et al*. 2009). The most significant change was observed in Grootegeluk char. The D bandwidth decreased by 72 cm^{-1}, while that of the Duhva and Matla chars decreased by 20 cm^{-1} and 5 cm^{-1} respectively. These results indicate that increased ordering of the amorphous region can be correlated to the proportions of inertinite and vitrinite macerals in the coals. The Grootegeluk coal sample with high vitrinite content had the highest degree of ordering while the Duhva and Matla coals with high inertinite contents had low degrees of ordering. These results are in agreement with earlier studies (Sun *et al.* 2003; Wang *et al.* 2010) where it was reported that inertinite macerals have higher thermal stability than vitrinite.

The G-band width which is related to the crystalline component in the coal showed a decrease in the G-band width of Grootegeluk coal after gasification but relatively no change for Duhva and Matla coal. This indicates that there was no significant growth in the crystalline component for Duhva and Matla chars however there was an increase in the crystalline component for the Grootegeluk coal.

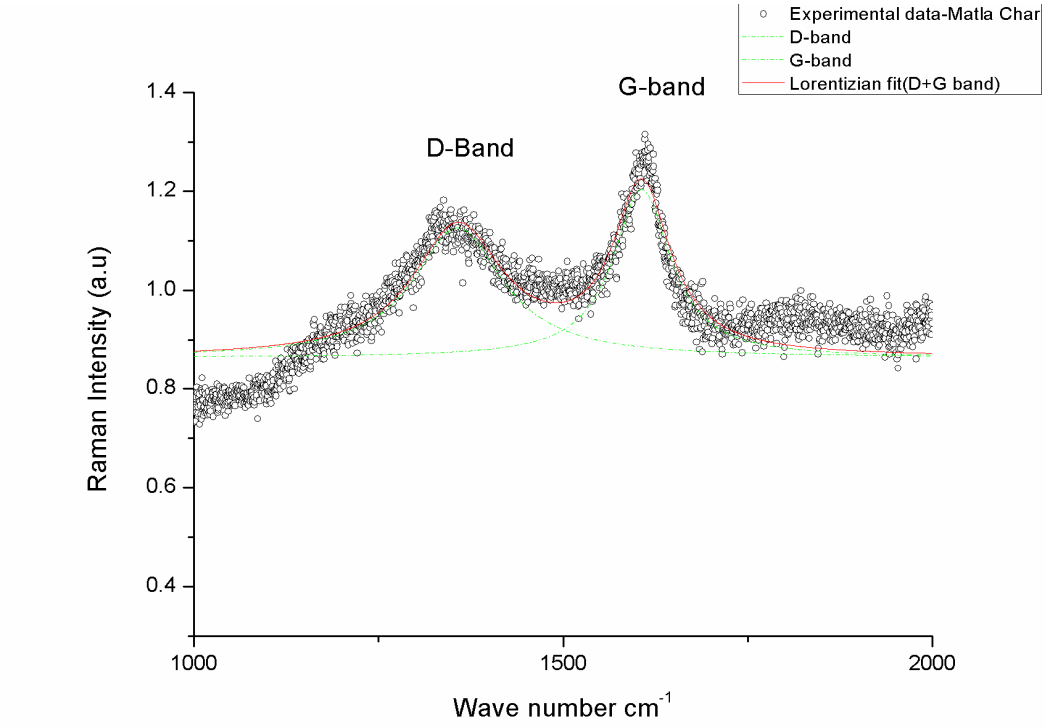


Figure 4.9: Raman spectra of Matla char with corresponding curve fitted bands

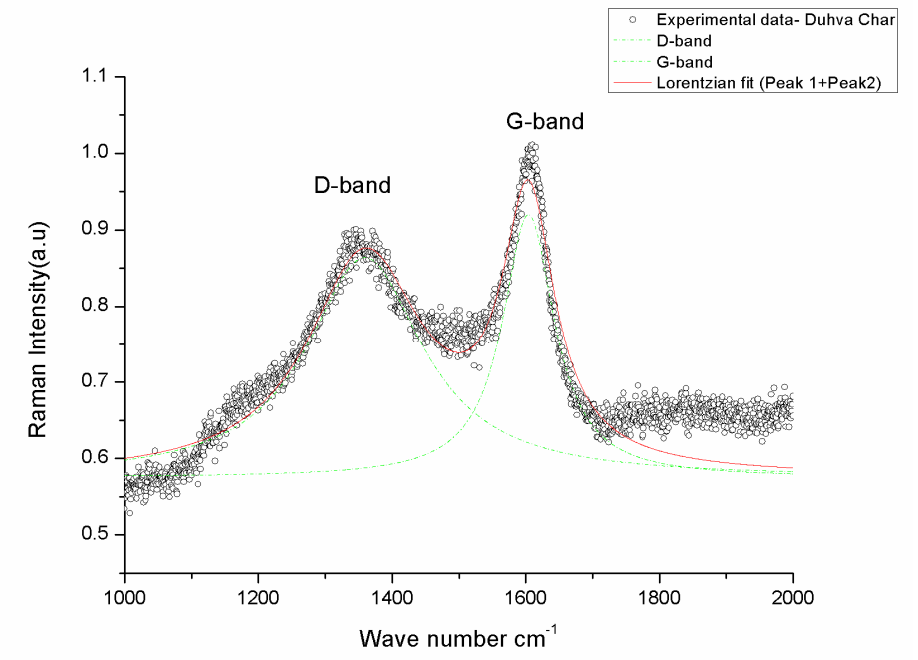


Figure 4.10: Raman spectra of Duhva char with corresponding curve fitted bands

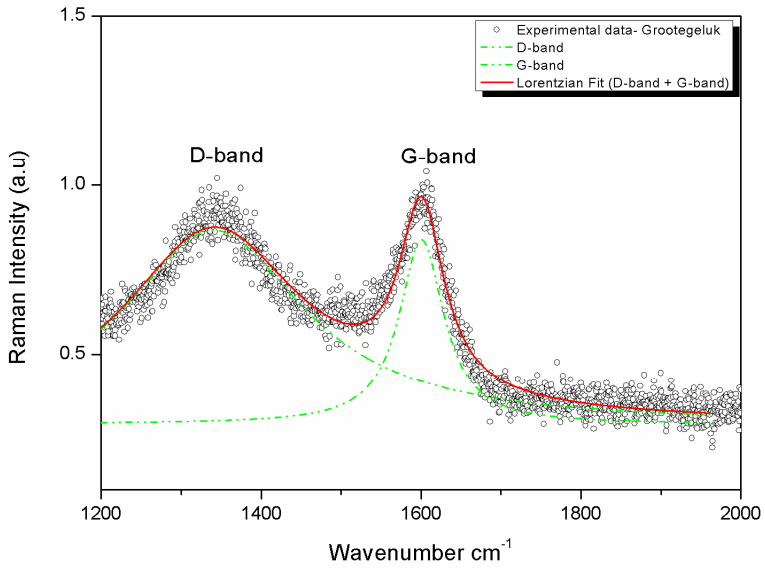


Figure 4.11: Raman spectra of Grootegeluk char with corresponding curve fitted bands

Table 4.10: Raman spectroscopic parameters obtained after curve fitting the experimental data points by using two-lorentzian bands (D and G).

Samples	Peak position (cm^{-1})	Band width (cm^{-1})
Matla Coal		
D	1363	153.71
G	1604	92.39
Char	1357	149.09
D	1606	94.57
G		
Grootegeluk Coal		
D	1370	260.56
G	1597	87.10
Char		
D	1349	188.32
G	1600	69.54
Duhva Coal		
D	1348	224.61
G	1598	84.15
Char		
D	1359	204.42
G	1603	92.61

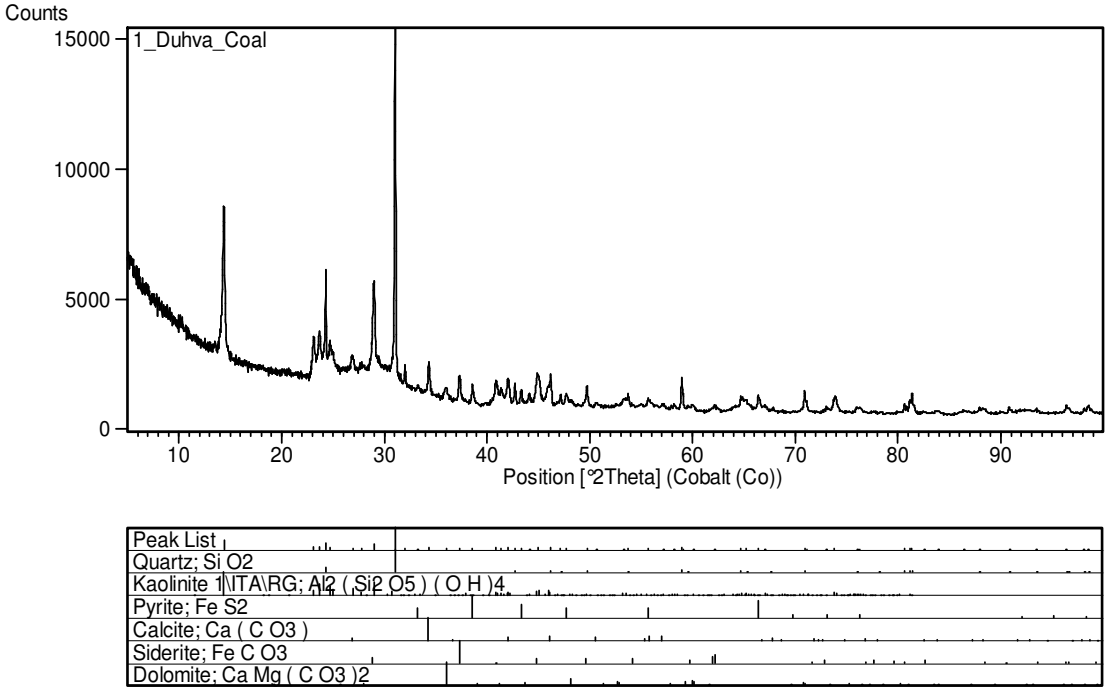
4.3.3.4 X-Ray Diffraction Analysis (XRD)

XRD diffractograms reveal that the three selected coals, two rich in inertinite (Matla and Duhva coal) and one rich in vitrinite content (Grootegeluk coal), contain a specific graphite-like structure as indicated by a graphite peak at 2θ of about 26^{o}. However, Matla and Duvha coals also show a variety of other peaks of lesser intensity whereas Grootegeluk has little or no variation. These features are illustrated in Figures 4.12-4.14. A sharper peak indicates a larger crystalline size and a greater degree of ordering. The change in the degree of carbon crystallinity in the chars relative to their initial coals following gasification may also be observed in Figures 4.12-4.14.

The difference in change before and after gasification is reflected in the intensity of the graphite peak.

For the vitrinite rich coal there was a significant change in the disordered bonding or crystalline carbon structure. At two theta of 26 degree in the Grootegeluk char, there is a very thick double line; the left hand line (line A) is approximately equal to the length of the right hand line (Line B). In the Matla char, however, the left hand line (line A) is about three quarters the length of the right hand line (Line B). In the Duvha char it is less than a quarter of the right hand line (Line B). This relates to the proportion of vitrinite in the original coals which may have graphitised during gasification. These observations indicate that the left hand line appears to relate to the vitrinite contents (true graphitisation in the vitrinite material) whilst the right hand line, appears to correlate to the inertinite contents. This right hand line is therefore likely to relate to increased disordered aromatisation in the inertinite – inertinite does not "graphitise''.

In addition to the bands of carbon, peaks related to crystalline inorganic phases were observed. The minerals identified in all the three coals included quartz (2θ =20.76 and 26.66^{o}), kaolinite (2θ =12.5 and 25.5^{o}) and dolomite (2θ = 31.0^{o}). After gasification, the latter two minerals disappeared whilst the peak relating to quartz remained in the spectra. The major transformation would appear to be the decomposition of the crystalline aluminosilicate minerals such as kaolinite to amorphous aluminosilicates. This observation is in agreement with Grigore *et al*. (2008) who stated that amorphous aluminosilicates are produced from the dehydroxylation of kaolinite. Bai *et al*. (2009) reported that the determination of the alteration of crystalline minerals to their melted forms can be used to indicate the amorphous phase of minerals after gasification. The mineral particle embedded in the amorphous material can be used to estimate the proportion of the melted minerals that covers the surface of the char. In this study, FTIR analysis was used to determine the degree of polymerisation hence the contact between the chars and molten minerals.



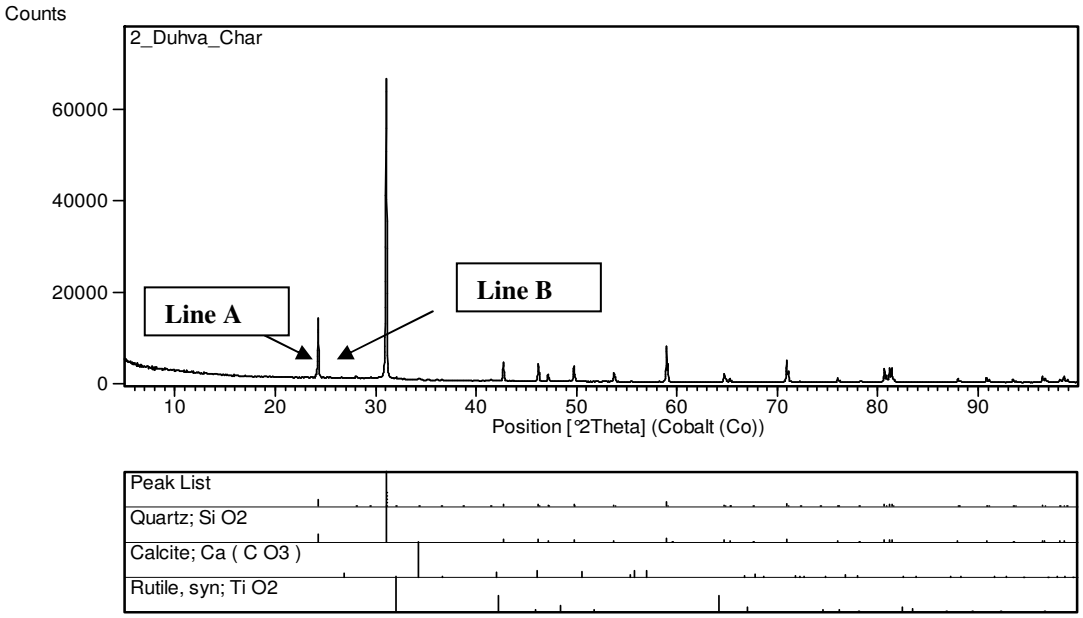


Figure 4.12: XRD pattern for the Duhva coal and their char

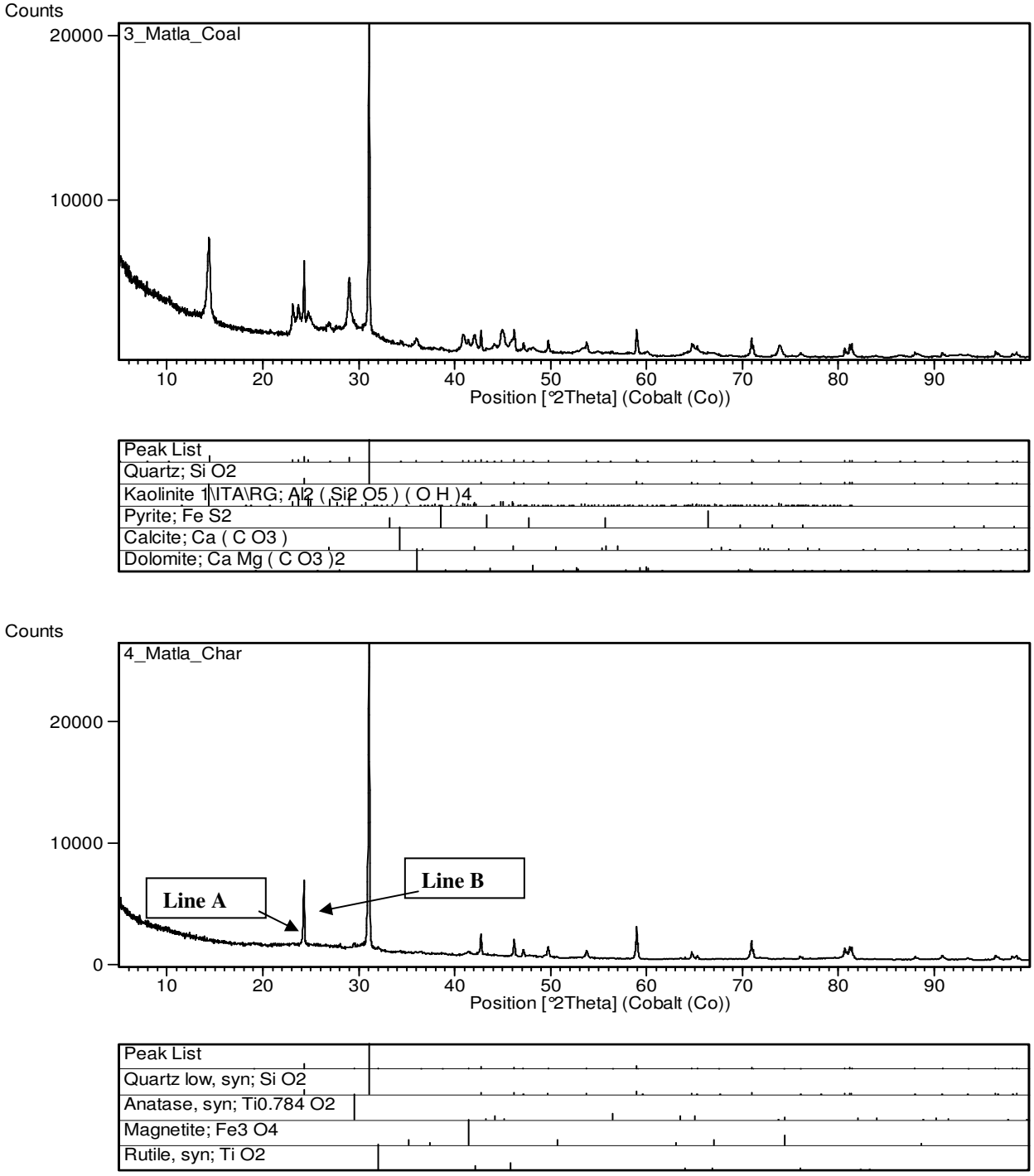
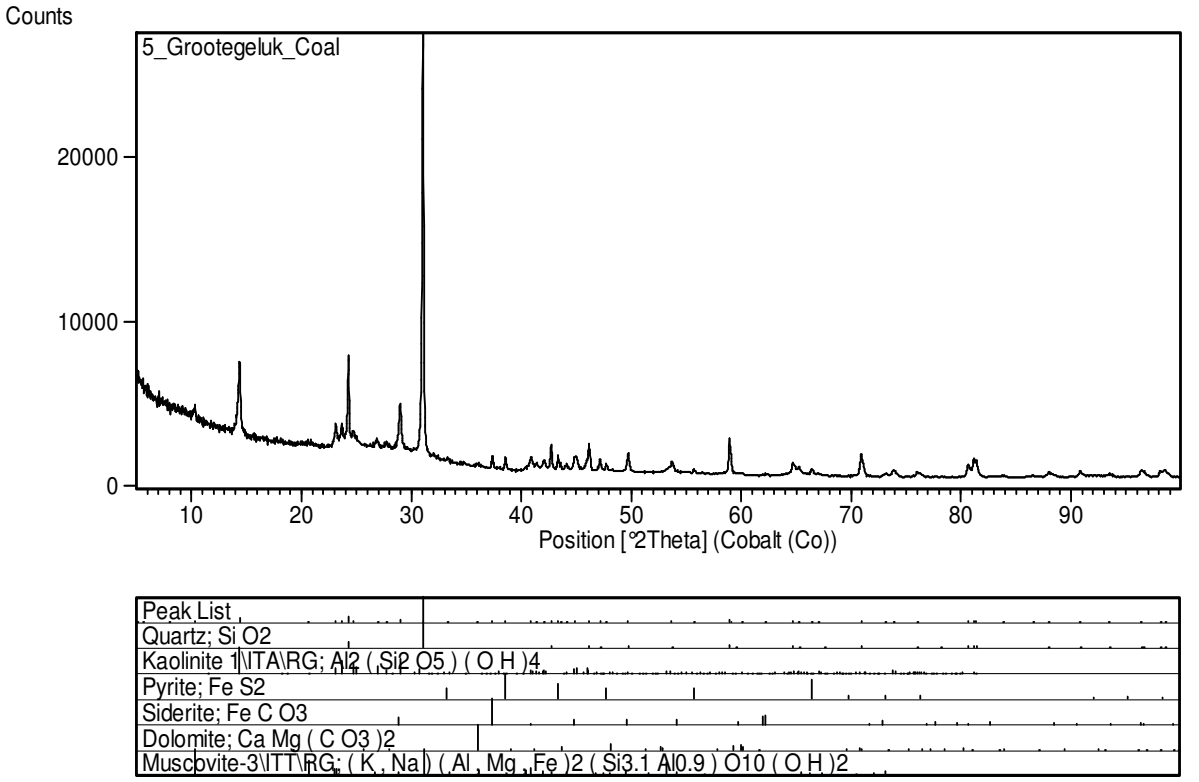
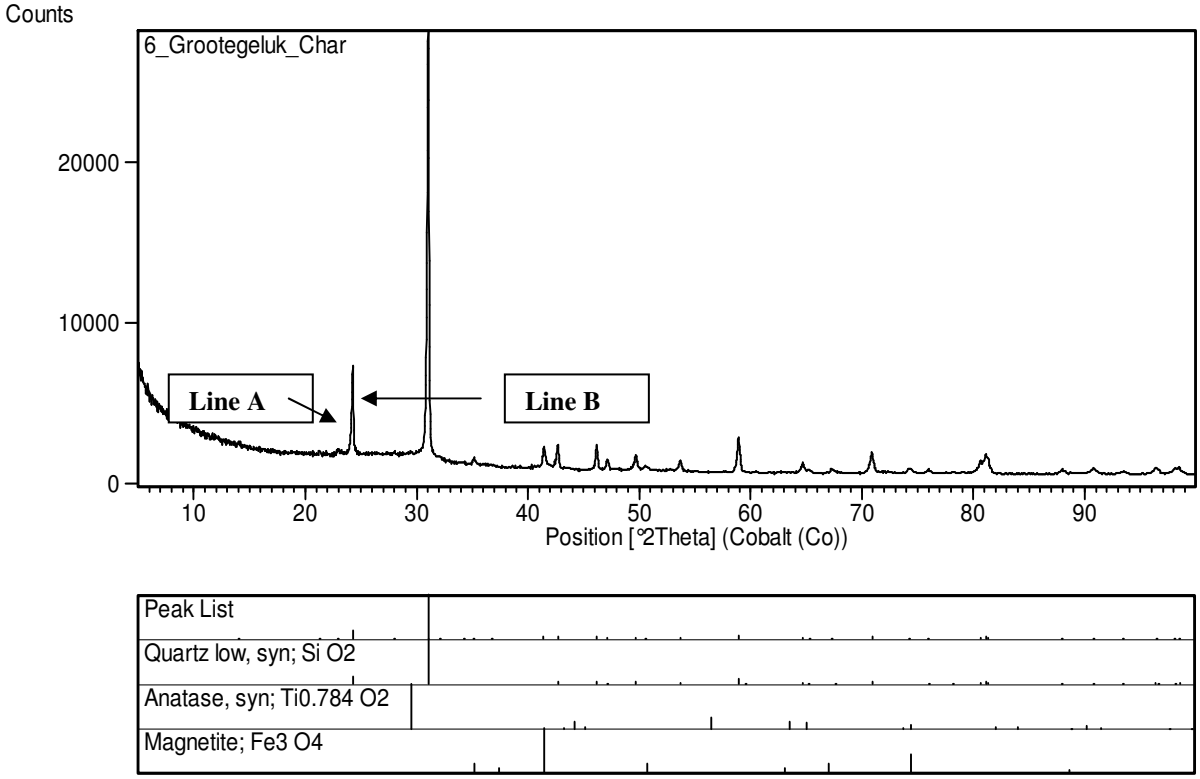


Figure 4.13: XRD pattern for the Matla coal and their char


Counts
5_Grootegeluk_Coal
20000
10000
0
10
20
30
40
50
60
70
80
90
Position [°2Theta] (Cobalt (Co))
Peak List ,
Quartz; Si O2
Kaolinite 1\ITA\RG; Al2 (Si2 O5) (O H)4
Pyrite; Fe S2
Siderite; Fe C O3
Dolomite; Ca Mg (C O3)2
Muscovite-3\ITT\RG; (K , Na) (Al , Mg , Fe)2 (Si3.1 Al0.9) O10 (O H)2


Counts
6_Grootegeluk_Char
20000
10000
0
Line A
Line B
10
20
30
40
50
60
70
80
90
Position [°2Theta] (Cobalt (Co))
Peak List
Quartz low, syn; Si O2
Anatase, syn; Ti0.784 O2
Magnetite; Fe3 O4

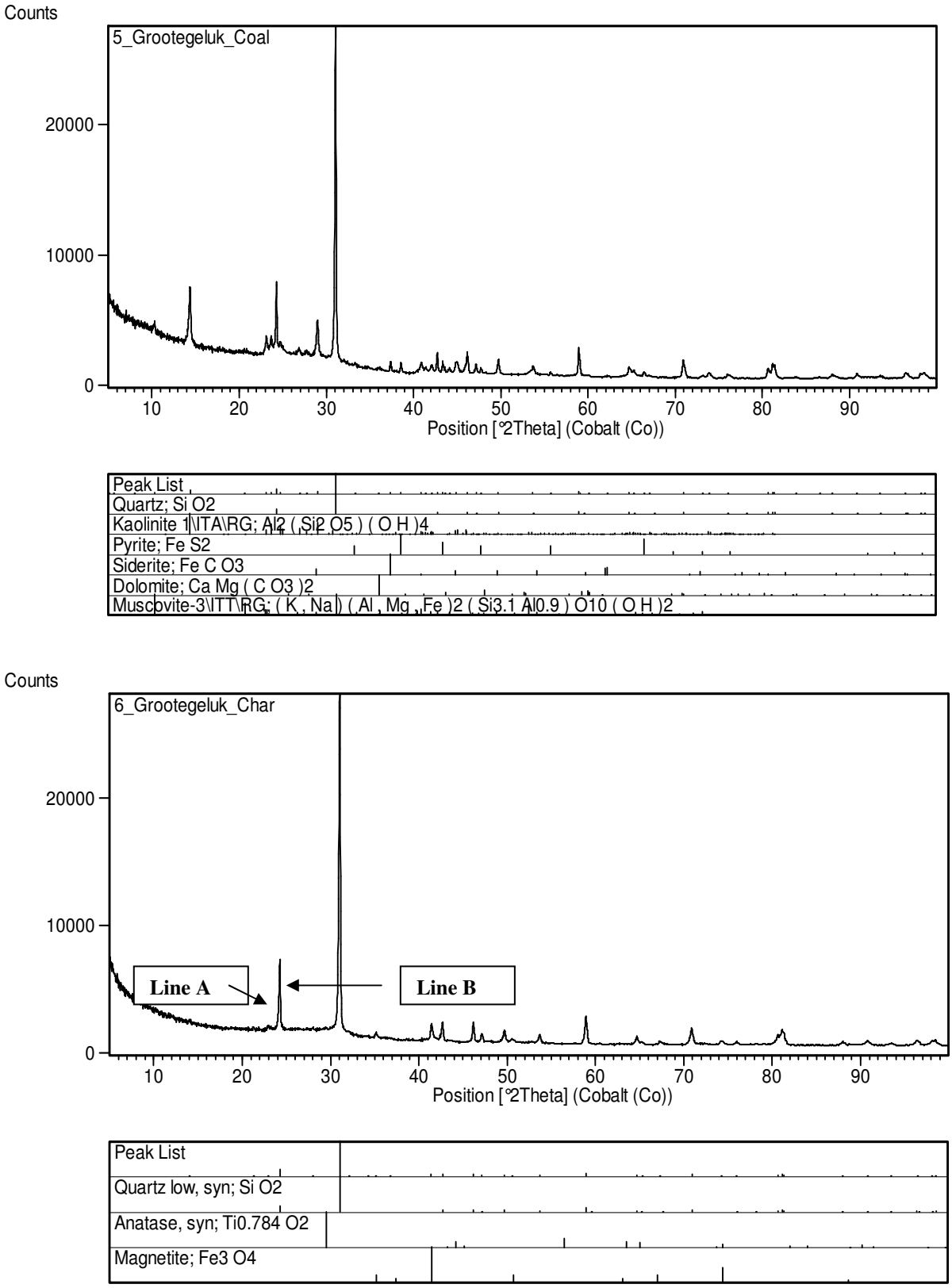


Figure 4.14: XRD pattern for the Grootegeluk coal and their char

4.3.3.5 FTIR Analysis

The alteration of the molten mineral structure can be determined by the FTIR technique. Minerals in an amorphous phase have a higher degree of polymerisation and increased surface tension of the molten form. This determines the degree of interaction between the char and the molten minerals (Bai *et al*. 2009). The FTIR spectra of the coals under investigation and their chars are shown in Figures 4.15-4.17. The shift of the Si-O-Si band at 1000 cm^{-1} and the Si-O band at 845cm^{-1} represents the degree of polymerisation of the aluminosilicates. The graphs illustrate that the fine crystalline structure of the aluminosilicate minerals (between 1000-600cm^{-1}) weakened after gasification due to polymerisation and the presence of a non-crystalline phase. The Si-O symmetric vibration band moves to lower wave number and the Si-O-Si asymmetric stretching band moves to a higher wave number.

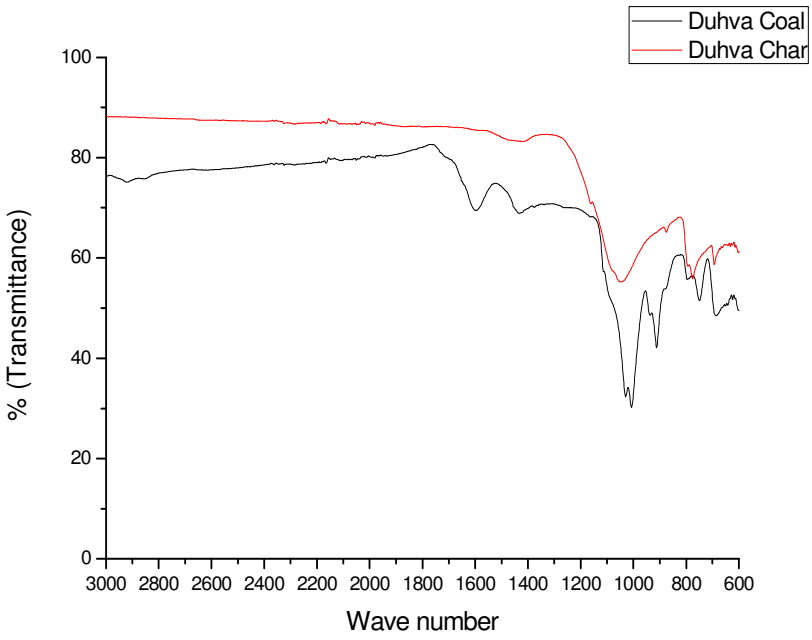


Figure 4.15: FT-IR Spectra for Duhva coal and char

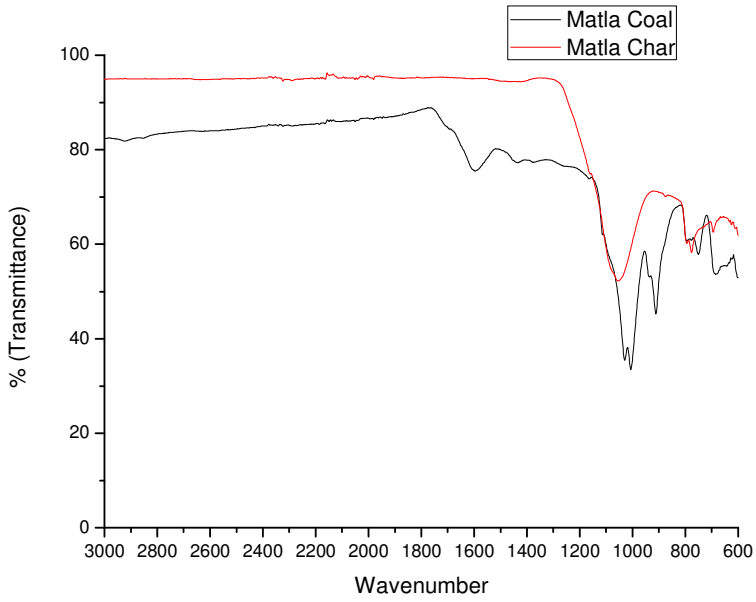


Figure 4.16: FT-IR Spectra for Matla coal and char

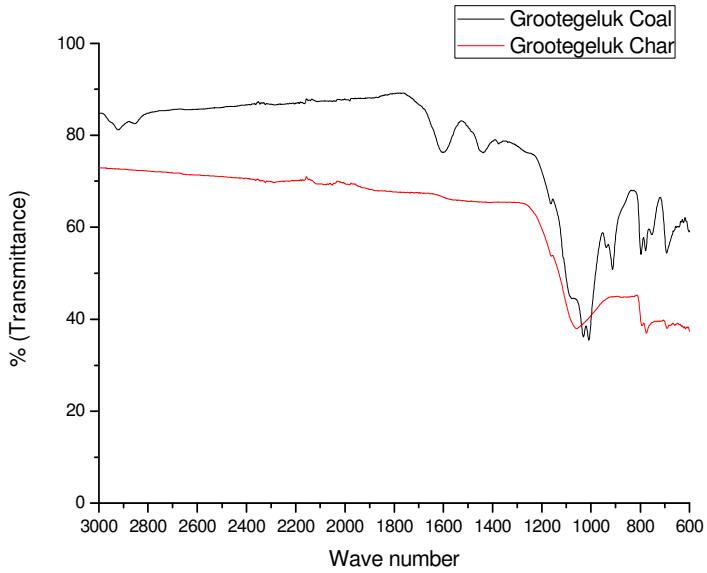


Figure 4.17: FT-IR Spectra for Grootegeluk coal and char

These observations indicate that the degree of polymerisation is higher (intensity virtually unchanged and therefore remains the same) in the Grootegeluk char than in Matla and Duhva char, suggesting that the amount of molten minerals spreading on the char surfaces is lowest in the Grootegeluk char.

These observations are in agreement with the petrographic analyses of the chars as reported earlier, i.e. the petrographic analysis showed that certain minerals had melted and been transformed into molten ash with some molten matter penetrating into cracks and pores in the chars. The presence of such mineral matter or "slag" which bordered penetrated or engulfed carbon fragments accounted for 15% to 20% in the Matla and Duhva chars respectively, whereas only 5% was observed in the Grootegeluk char. Such inert mineral boundaries may be expected to severely reduce the ability of the carbon to further react (Sekine *et al.* 2006; Bai *et al*. 2009)

The role of residual carbon in the spread of melted minerals on the surface of the char may be stated as follows: the lower the residual carbon in the char, the more included minerals becomes exposed on the surface of the char (Li and Witty, 2009). These results, indeed confirmed this assertion. In Table 4.7, Duhva and Matla char samples with low proportions of organic matter (16% and 6%, respectively) resulted in a higher proportion of melted minerals covering the char surface (16 and 19%, respectively), while Grootegeluk char with 64% of organic matter resulted in 4% of melted minerals covering the char surface**.**

4.3.3.6 Surface area analysis (BET results)

The surface area is one of the most important features for characterising the microscopic features of char. The surface area of the different coal samples and the chars generated after gasification was determined using N_2 adsorption. The results are presented in Table 4.11. There was an increase in the surface areas of Duhva and Grootegeluk char, but there was a decrease in the surface area for Matla char after gasification. Similar results were obtained in recent studies by Li and Witty (2009), where the evolution of surface area was used to study the effect of melted minerals on char structural change. They observed that melted minerals have a high tendency to close the micro- and mesopores in carbon, which create the surface area in the char. The surface area of particles prepared at 1400 ^{o}C dropped sharply at 88% conversion. Similarly, in this study the surface area dropped at 82% conversion for Matla coal. Additional tests carried out on Grootegeluk coal showed a drop in surface area at 87%, as shown in Table 4.12.

This may suggest that, at high conversion, more residual carbon in the char was consumed and there was not sufficient residual carbon to encapsulate the minerals. Thus, more mineral matter tends to cover external surface of the char in the form of melted ash minerals.

Table 4.11 Surface area of the different coal and char samples

Coal	Malta coal	Matla Bed Char	Duhva Coal	Duhva Bed Char	Grootegeluk Coal	Grootegeluk Bed Char
Surface area (m^2/g)	12.1	10.7	7.5	15.1	5.9	141.3

Table 4.12 Evolution of surface area for Grootegeluk char samples

Properties	Char 910R30	Char 1000R30	Char 960 R55	Char 1000R55
Carbon conversion	**57.15**	**75.19**	**78.15**	**87.10**
Surface area (m^2/g)	21.70	367.46	158.74	110.25

4.4 Conclusions

In terms of char development, the characterisation of carbon based on petrographic analysis showed that the reactive macerals have been transformed from normal coal forms into very different mixtures of partially reacted coal, highly reflecting char, coke and inorganic matter. The relative proportions of the various types of chars can be related to the properties of the parent coal. Higher proportions of porous chars are found in coals that have higher reactive macerals (vitrinite) such as Grootegeluk coal whereas much higher proportions of inertinitic chars are found in Matla and Duhva (High inert coal macerals). The inertnitic–coally materials had increased in reflectance but not in porosity. It was also observed that inertinite-rich coals experienced a greater degree of structural transformation into the disordered forms of char, whilst the vitrinite-rich coal indicated that the vitrinite became more graphitised during gasification.

In addition, the structural transformation of the crystalline form of the clay mineral, i.e, kaolinite, into an amorphous form as well as the disappearance of the carbonate minerals in all three coals after gasification correlated to the amount of inertinite present in the coals. Thus, the higher the proportion of inertinite in the parent coal, the higher the proportion of melted minerals in the char. Char samples with low proportions of organic matter showed in higher proportion of melted minerals covering the char surface**.**

CHAPTER 5 TEXTURAL PROPERTIES OF CHARS AS DETERMINED BY PETROGRAPHIC ANALYSIS: COMPARISON BETWEEN AIR-BLOWN, OXYGEN-BLOWN AND OXYGEN-ENRICHED GASIFICATION.

5.1 Introduction

A viable solution for the gasification of high ash and other low quality coals is the use of oxygen-enriched air as a gasification agent (Belyaev *et al*. 2003; Belyaev, 2008). The use of oxygen-enriched air can lead to the higher reactivity of coal particles (Rathnam *et al.* 2009). This is because, in an oxygen-enriched environment, devolatilization and combustion of coal particles are likely to occur faster than with air (Borah *et al*. 2008). In addition, enhanced tar decomposition and char gasification occur, which will contribute to higher gasification efficiency. The use of enriched oxygen is also an effective method to capture CO_2 (Valero *et al.* 2006).

The use of enriched oxygen increases the bulk gasification temperature in the absence of any additional coolant/heat sink. An increase in enriched air means that the same amount of combustible matter is burned whilst the nitrogen flow that had to be heated decreased, leading to higher bed temperature. This allows for the addition of quality steam while maintaining the thermal level in the gasifier (Campoy *et al.* 2009). The appropriate combination of temperature and steam leads to higher CO and H_2 yields, heating value, carbon conversion and gasification efficiency, while maintaining bed stability and reducing ash melting. However, a detailed characterisation of bed char generated under oxygen enriched gasification has not been reported in the literature.

In this chapter, textural properties of chars generated in a fluidised bed gasifier under air-blown, oxygen-blown and oxygen-enriched conditions were determined by detailed petrographic analysis. The char samples were assessed in terms of their microscopic characteristics (reflectance properties, carbon rich forms and basic forms of visible minerals). The objective was to study the impact of different gaseous environments during the transformation of coal to char under similar fluidised bed conditions.

5. 2 Experimental

5.2.1 Parent coal sample and gasification

A South African low grade coal from Grootegeluk Colliery with a particle size range of 1-2.5 mm was used in all experiments. This is currently used as feed in a local power station. The properties of the coal are presented in Table 4.1. The coal may be described as Bituminous, Medium Rank C, with a mean random reflectance value of 0.67% Rr. It was characterised by a low calorific value (19.8 MJ/kg) and a high ash content (35.7% ad), and is therefore categorised as a low grade product, Grade D.

The gasification tests were carried out under air-blown condition, oxygen-blown and oxygen-enriched conditions. The flow rate of air and oxygen determine the oxygen content in the enriched inlet. For air-blown gasification air was used as oxygen supplier, so the oxygen percentage of the enriched air (OP) was 21% v/v for all the tests and the additional oxygen flow rate was nil. For oxygen-enriched gasification the OP of the enriched air was 34%. For oxygen-blown gasification, the air flow rate was nil and only oxygen and steam were used as gasification agents. Full details of the test programme are given in Table 5.1. After each test, char samples were taken from the bed inventory and analysed.

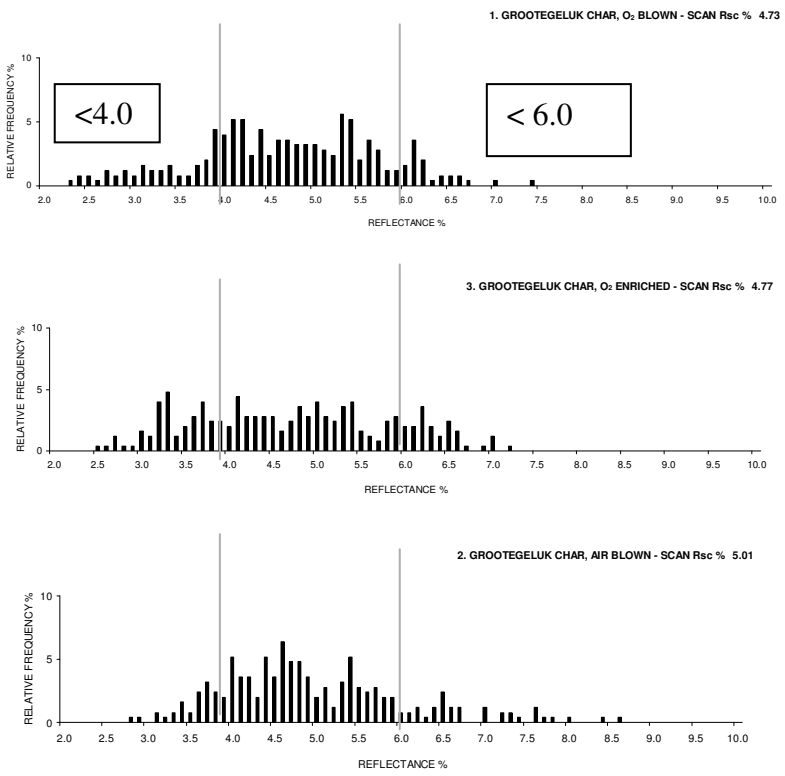
Table 5.1 Details of gasification tests carried out under air-blown, oxygen-blown and oxygen-enriched conditions

	Air Steam	**Air +Oxygen + Steam**	**Oxygen+ Steam**
Coal feed rate (kg/h)	23.0	23.0	22.8
Air flow rate(kg/h)	47.8	22.7	0
Oxygen flow rate(kg/h)	0	6.6	315
Steam flow rate(kg/h)	10	20	36.3
Oxygen in “air” (%)	21	34.40	100

5.3 Results and discussion

5.3.1 Reflectance properties and carbon forms

In order to assess the reactivity and relative molecular of the organic constituents during the char forming process, reflectance measurements were taken on all char forms. The results for the various gasification conditions are presented in Figure 5.1. The char scan reflectance histograms revealed that the carbon-rich particles had attained greatly varying levels of reflectance as a result of the coal-to-char transformation process. A reflectance value of the carbon of above 4% Rv_{rand} (random reflectance) represented highly reflecting chars with relatively high levels of molecular ordering while reflectance levels in the range of between 2% and 4 % Rv_{rand} represented partially consumed char**.** Organic forms below 2 % were considered to be heat-affected coally particles. The results indicate that the overall mean scan reflectance values shifted dramatically towards substantially higher ranges of the order of 5% Rv_{rand} and above when temperatures of 925-950 ^{o}C were applied. The air-blown char was highest in overall reflectance with a mean value of 5.01%.Rv_{rand} This char also displayed the highest proportion of values above 4% of reflectance (84.8%), indicating that these char forms were of a relatively higher degree of molecular ordering in this case. The oxygen-blown char was lowest in overall reflectance (4.73% Rv_{rand}), with a lower proportion of well-ordered carbon forms above 4% (78.4%). A significant proportion of char forms exhibited reflectance values of below 4%. The oxygen-enriched char showed an overall reflectance of 4.77% similar to the oxygen-blown char, but moderate proportions of char forms extended into both lower and higher reflecting categories.



Mean values of Rr%
Full char scan analyses

O_2-blown char – 4.73

O_2-enriched – 4.77

Air-blown – 5.01

Figure 5.1: Char reflectance histogram for O_2-blown, O_2-enrinched and air blown gasification of Grotegeluk char

These results indicate a greater proportion of the well ordered carbon in the oxygen-blown sample and is likely to have already been consumed (burnt away). More highly reflecting unreacted carbon remained in the air-blown sample indicating possible delay in consumption of this material. This finding is confirmed by the carbon form analysis data shown in Table 5.2. Photomicrographs of the various carbon forms are presented in Figure 5.2. The oxygen-blown char had the lowest concentration of well-developed highly porous isotropic coke forms and the lowest mean reflectance value, while the air-blown char had the highest percentage of highly porous coke forms and the highest mean reflectance value. In oxygen-blown gasification such thin-walled structures had presumably been consumed to a greater extent. Thin-walled coke represented 17% in the case of oxygen-blown gasification, and 23% and 26% for oxygen-enriched and air-blown gasification.

Table 5.2: Carbon form analysis

Organic/inorganic constituents	Air + Steam	Air+ Oxygen + Steam	Oxygen+ Steam
Isotropic coke-thin walled, very porous %	26	23	17
Isotropic coke-thick walled, porous %	18	25	25
Mixed porous %	11	8	10
Relatively unchanged inertinite %	19	16	11
Partially consumed carbon %	19	23	30
Organic/inorganic associations % (minerals 25%-50%)	7	5	7
Mean reflectance value Rr %	5.01	4.77	4.73

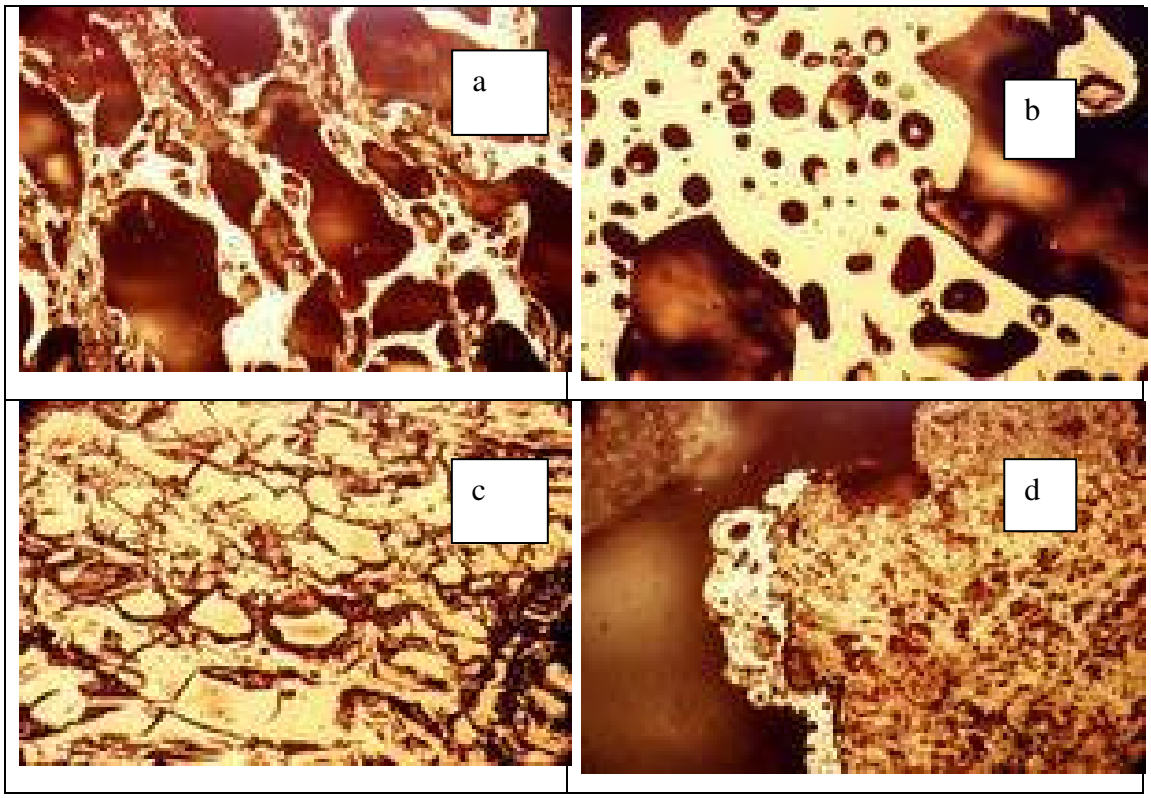


Figure 5.2: (a) Thin-walled isotropic coke; (b) Thick-walled isotropic coke; (c) Relatively unchanged inertinite; (d) partially consumed carbon (Magnification $=2x10^5$)

In addition, due to the enhanced reactive environment in oxygen-enriched and oxygen-blown conditions, there was a decrease in the proportion of relatively unchanged inertinites and a consequent increase under air-blown conditions. Relatively unchanged inertinites transform to dense chars and are derived from inert or relatively inert coal macerals in the parent coals which had not softened or expanded to an appreciable extent on gasification. These forms appear to have largely retained their original coal maceral forms and shapes in higher proportions in the air-blown conditions, i.e. 19% of both relatively unchanged inertinites and partially consumed carbon were present in the air-blown sample whereas relatively unchanged inertinites represented 11% and 16% respectively in the oxygen-blown and oxygen-enriched samples with higher proportions of partially consumed carbon (30% and 23% respectively). These results indicate that a higher proportion of transformation and potential consumption has taken place in oxygen enriched and concentrated conditions whilst, on the other hand, air-blown conditions tend to limit such reactivity

Previous workers Borrego and Martin (2010) working on anthracites have reported an increase in mean reflectance values for low to moderate oxygen concentrations in the reacting atmosphere and then an apparent decrease in mean reflectance values at higher oxygen concentrations. In a second study, two anthracite samples were studied under oxy-fuel conditions at 1300 ^{o}C, one vitrinite-rich (VAN) sample and the other an inertinite sample (DAN). In the case of VAN, the maximum reflectance increased with an oxygen concentration of up to 21%. Further increases in the oxygen content led to a reduction in the maximum reflectance. In the case of DAN, there was a reduction at 10%.

Pusz *et al*. (2002) obtained similar results for six different anthracites carbonized under inert conditions in the temperature range of 400 to 1800 ^{o}C. It was found that the mean reflectance value increased up to 1200-1400 ^{o}C and then decreased at higher temperatures. The authors suggested that the textural transformation process is a two stage process, with chemical alteration (devolatilisation, increased aromaticity) occurring in stage 1 when the mean reflectance value increases, and then physical alteration (decreased porosity) occurring in stage 2 when there is a decrease in the mean reflectance value. These results may, however, have also been due to the greater consumption of the high reflecting highly reactive char forms at the higher

temperatures and/or higher oxygen concentrations thereby leaving only lower reflecting forms which would explain the apparent reduction in reflectance at high oxygen concentrations. Alternatively, such reductions in reflectance may, under some conditions (neutralizing atmospheres), be due to advanced re-"crystallisation" of the molecular structure at these higher temperatures.

In this study, gasification was carried out under air-blown, oxygen-blown and oxygen-enriched conditions at temperature range of 925 to 950 ^{o}C. The temperature was lower than those applied by Pusz *et al* (2002) (1200-1800 ^{o}C) and Borrego and Martin (2010) (1300 ^{o}C) but similar results were obtained, i.e. lower mean reflectance values were found in chars exposed to oxygen-enriched atmospheres. However, other factors have emerged in parallel with increasing oxygen atmospheres. These are discussed further below.

5.3 2 Inorganic mineral and organic maceral associations

Carbon char forms and the organic and inorganic constituents of the char samples are described in Tables 5.2 and 5.3. The presence and proportions of minerals/ash in association with organic matter is shown in the microlithotype analysis in Table 4.1. The char-to-mineral matter proportions (organic constituents versus visible mineral matter as determined by volume in percentage terms) indicate that the oxygen-blown sample was lowest in total carbon-rich char forms (53%). This once again suggests a higher rate of consumption of carbon in this case, with a higher proportion of melted minerals (31%) left remaining. The other two samples, oxygen-enriched and air-blown, have higher proportions of organic matter (58% and 60% respectively), with lower melted mineral matter (24% in both cases)

From the carbon form data in Table 5.2 and the mineral analysis data in Table 5.3, an attempt was made to correlate char porosity and melted mineral content. This is graphically presented in Figure 5.3. The results indicate a trend between the proportion of highly porous thin-walled coke forms and the proportion of melted 'slag' minerals that have surrounded/penetrated into the carbon. The ratio of the percentages of engulfing melted minerals to thin-walled coke was highest in the oxygen-blow char (11:17). This suggests that the temperatures in those gaseous environments were highest and especially in the region of the highly porous chars

where the minerals melted thereby contributing to the blockage of some of the highly porous surfaces of those chars. Photomicrographs of the melted "slag" minerals (penetrating or surrounding carbon and occurring as separate bodies) are presented in Figure 5.4.

In addition to the effect of a higher particle temperature as a result of the bulk gas shifting from air to oxygen, the local reducing gases such as CO and CO_2 have an effect on the melting of minerals within the char matrix. (Shannon *et al*. 2009; Zhang *et al.* 2011). Zhang *et al*. (2011) studied the transformation of minerals in air and O_2/CO mixtures in a lab-scale drop tube furnace. They reported that the existence of a fairly strong reducing condition on the char surface in O_2/CO_2 mixtures had a higher effect on the melting of included minerals in the char than a reduction in char particle temperature.

In this study, we could not distinguish the effect of char particle temperature and local reducing temperature on the proportion of melted minerals formed in the different gasification temperature because we could not measure the particle temperature. However results obtained showed that the percentage of CO formed increased from 10.2% in air-blown gasification to 21.7% in oxygen blown gasification .This indicates that oxygen blown gasification has a more reducing environment. Also, XRD analysis of the char particles showed the formation of magnetite in chars obtained from oxygen blown gasification and this was not present in the air–blown chars. The formation of magnetite from the oxidation of pyrite and/ or siderite occurs at more reducing conditions (Srinivasachar *et al*. 2000). This suggests that a more reducing environment is prevalent at higher gasification rate and in this case it was in the oxygen blown gasification.

Table 5.3: Organic/ Inorganic constituents

Organic/inorganic constituents	Air + Steam	Air +Oxygen + Steam	Oxygen+ Steam
Total organic material %	60	58	53
Relatively unchanged visible minerals %	16	18	16
Melted "slag" minerals penetrating/ surrounding carbon %	8	10	11
Melted "slag" minerals - separate bodies %	16	14	20
Total	100	100	100

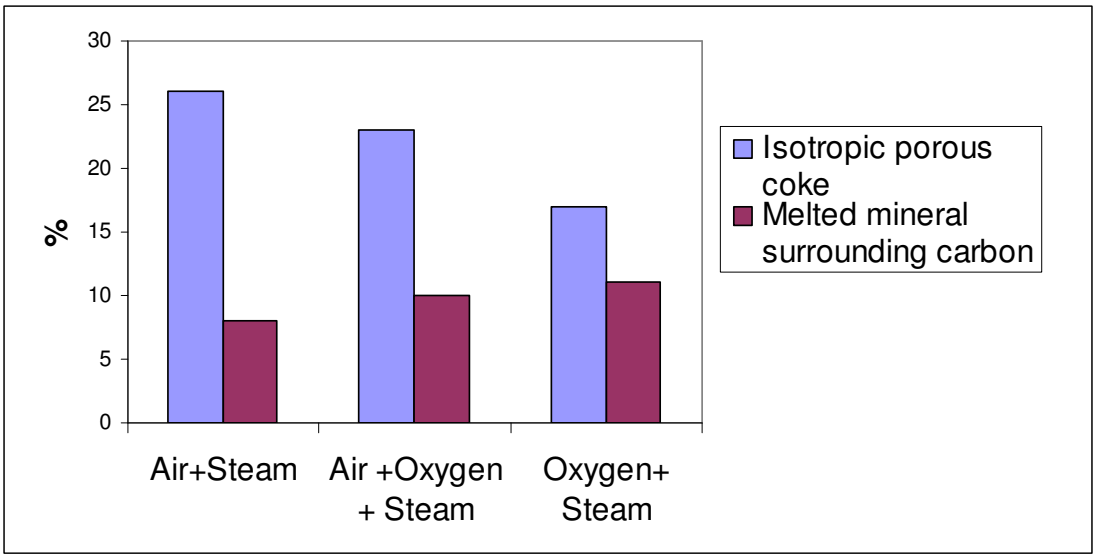


Figure 5.3: Correlation between thin-walled highly porous isotropic coke and melted minerals surrounding/penetrating carbon. This trend indicates that the greater consumption of these char forms is linked to increasing melting of minerals, all of which indicates increasing particle temperature passing from air to O_2 enrich to O_2 gaseous environments.

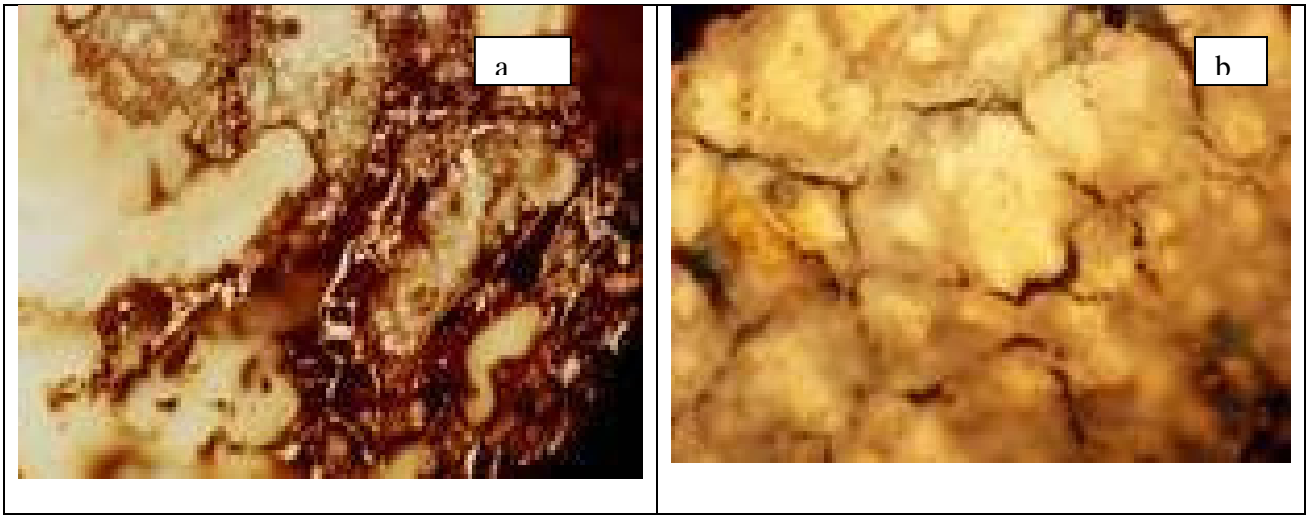


Figure 5.4: (a) Melted "slag" minerals - penetrating/ surrounding carbon (b) Melted "slag" minerals as a separate body

5.4. Correlation to previous workers' concepts

The reduction in mean reflectance values in the oxygen-blown and oxygen-enriched samples in this research may indicate that, on the basis of Pusz et al (2002) and Borrego and Martin's work (2010), that stage 1 alterations (chemical) in the chars quickly transformed to stage 2, the physical alterations, while the chemical alterations in the air-blown gasification progressed much more slowly from one stage to the next due to possibly lower particle combustion temperatures. However, at this stage, apart from a reduction in mean reflectance values in one sample, there is little else in the way of evidence to encourage the adoption of this approach as being the only reason for such variations in reflectance

5.5 Conclusions

The oxygen-blown sample possessed the lowest proportion of total carbon forms of all three samples (53% by volume, mineral matter basis relative to 58 and 60% in the other two samples), the lowest proportion of thin-walled highly porous and reactive char forms (17% relative to 23 and 26%) and the highest proportion of partially consumed carbon/char forms (30% relative to 19 and 23%). This sample also exhibited the lowest mean reflectance value (4.73% RoVr) with the lowest proportion of chars with reflectance values above 4% RR. These results suggest that a greater degree of consumption of carbon took place under the oxygen-blown conditions, possibly with higher temperatures, and that under these conditions, the highly

reflecting porous thin-walled chars would have been consumed first and fastest thereby leaving the higher proportion of partially consumed chars and inertinites behind which, in turn, would have lead to the occurrence of lower reflectance readings.

These conditions also resulted in the presence of higher proportions of melted "slag" minerals in the oxygen-blown sample which totalled 31% compared to 24% in the other two samples. The coating and penetration of the carbon particles by these molten minerals relative to the proportion of thin-walled very porous isotropic coke present was most pronounced

The oxygen-enriched and air-blown chars displayed higher proportions of organic matter relative to the oxygen-blown sample, and higher proportions of the high reflecting thin-walled porous chars with higher mean reflectance values and reduced proportions of melted mineral matter. These results indicate that both of these samples underwent reduced levels of carbon consumption and at lower temperatures relative to the oxygen-blown sample.

Of these two samples, the air-blown sample possessed the greater proportion of unburnt carbon material, the lowest proportion of melted slag minerals, the highest proportion of thin-walled reactive chars and the highest reflectance values relative to the oxygen-enriched sample. These results thereby indicate that the air-blown sample had the lowest degree of consumption of all three sets of conditions. This, in turn, implies that the temperatures operating under these conditions were the lowest of all the sets of conditions.

In summary, it would appear that the conditions under which the most rapid rates of consumption would occur, in decreasing order of reactivity, particle temperature and local reducing conditions would be (i) oxygen-blown, (ii) oxygen-enriched and (iii) air-blown. Of moderate concern is the fact that the proportion of molten mineral matter would increase at the highest levels of reactivity and temperature which, in turn, may contribute to the blockage of some of the surface areas in the high porosity chars and could lead to slagging in operating gasifiers.

These results have important implications for the future, namely to ensure the highest optimum efficiencies in future gasification processes by selecting the most appropriate gaseous environments and by preventing or minimising the occurrence of slagging. This is specifically applicable to operations involving fluidised bed technologies and would be of value in countries in which high ash coals will be used in such technologies.

CHAPTER 6 MINERAL-CHAR INTERACTION DURING GASIFICATION OF HIGH ASH COALS IN FLUIDISED BED GASIFICATION

6.1 Introduction

The main aim of this chapter is to understand the impact of interaction that occurs between char and mineral during the gasification of high ash coals, both inertinite-rich and vitrinite coals. The decomposition of clay minerals during fluidised bed gasification results in the formation of amorphous aluminosilicates (Oboirien *et al.* 2011). In section 4.3.3.4 and 4.3.3.5, it was shown, through combined petrographic and FTIR analyses, that some of the molten matter penetrated into cracks and pores in the chars. Such inert mineral boundaries may be expected to severely reduce the ability of the carbon to react further by preventing the reaction gas from coming in contact with the carbon (Sekine *et al*. 2006). In addition to the physical effects on char reactivity, the molten ash can also participate in a chemical reaction at the char-mineral interface that involves the modification of the carbon properties. Wang *et al.* (1995) have shown that coke in the vicinity of iron possessed a much more ordered graphitic structure than coke far away from iron. For high ash coals**,** a significant proportion of inorganic elements occur in association with the char matrix. The inorganic elements are mainly aluminium and silicon (Lunden *et al.* 1998; Sekine *et al.* 2006). These elements indicate the formation of a range of silicates and alumina-silicates minerals (Falcone, 1986). There are limited numbers of investigations that directly cite the influence of mineral phase of silicates or associated elements on char structural evolution. This study aims to determine the impact of Al silicates clays on the modification of local carbon in a char matrix. Furthermore, an attempt has been made to model the impact of the interactions on char reactivity during gasification. The char samples were generated from two high ash South African coals. The two coals are typical South African coals used as feeds in power generation stations. The coals are New Vaal, which has high ash with high inertinite content and Grootegeluk, which has high ash and high vitrinite content.

6.2 Experimental

Several gasified char samples were prepared from the two coal samples, using the in-house pilot-scale fluidized gasifier at the CSIR (Engelbrecht *et al.* 2010). The gasifier was operated under oxygen enriched conditions at 34% oxygen (13% enrichment) and at different temperatures and residence times. Table 6.1 a-c shows Proximate analysis,

ash chemistry, coal petrology and mineralogy data of the coal samples prior to gasification. In addition, Table 6.2a and 6.2b show full details of the test programme.

Table 6.1a: Proximate, ultimate and as chemistry data for New Vaal coal and Grootegeluk coal samples

Sample	New Vaal	Grootegeluk
Proximate analyses		
*Calorific value (**MJ/Kg)ad***	18.11	21.40
*Ash **(wt%)ad***	37.15	37.50
*Moisture **(wt%)ad***	5.84	1.90
*Volatile matter **(wt %)ad***	22.24	28.30
*Fixed Carbon **(wt%)ad***	34.77	34.77
(Calculation)		
Ultimate analyses (wt% ad)		
C	42.58	49.20
H	2.19	3.87
N	0.89	0.97
O (Calculation)	7.54	6.79
S	0.69	1.47
Ash analysis		
SiO_2	56.70	68.60
Al_2O_3	31.70	20.05
Fe_2O_3	2.61	5.59
TiO_2	1.55	0.72
CaO	2.50	0.71
Na_2O	0.19	0.12
K_2O	0.44	1.25
P_2O_5	0.25	0.08
Ash melting temperature		
DT(^oC)	1600	1350
ST(^oC)	1600	1410
HT(^oC)	1600	1480
FT(^oC)	1600	1500

Table 6.1 b: Coal petrology data for New Vaal coal and Grootegeluk coal samples

Sample	New Vaal	Grootegeluk
Macerals analysis (mmf)		
Vitrinite content %		
Liptinite content %	26	83
Inertinite content %	5	5
Mean random reflectance %	69	12
Total reactive macerals %	0.56	0.67
	51	91
Microlithotype (mmb)		
Vitrite %		
Liptite %	7	24
Inertite %	0	0
Intermediates %	26	8
Carbominerite %	27	22
Minerite %	19	29
	21	17

Table 6.1 C: Coal mineralogy data for New Vaal coal and Grootegeluk coal samples

Sample	New Vaal	Grootegeluk
Kaolinite	80.78	38.66
Quartz	13.70	49.73
Mica	0.0	8.05
Pyrite	2.20	2.58
Rutile	3.32	0.44
Siderite	0.0	0.54

Table 6.2 a: Grootegeluk Coal

Test number	Temperature (^{o}C)	Residence time (Mins)
1	910	35
2	960	35
3	960	55
4	1000	35
5	1000	45
6	1000	55

Table 6.2 b: New Vaal Coal

Test number	Temperature (^{o}C)	Residence time (Mins)
1	910	20
2	910	30
3	960	20
4	960	30
5	1000	20

6.3 Results and discussion

6.3.1 Carbon and ash analyses of char samples

The results of carbon and ash analyses conducted on the chars generated for both coals at different conditions are presented in Tables 6.3 and 6.4. The results indicate that an increase in both temperature and residence time led to an increase in carbon conversion (i.e. lower organic carbon content and higher ash content in the char particles) for both coals. At a constant temperature and residence time, New Vaal char particles had a higher carbon conversion than Grootegeluk char particles. New Vaal char particles had a low content of organic matter and high proportion of transformed minerals, while Grootegeluk char particles had a higher proportion of organic matter and lower proportion of transformed minerals. Based on the work of Sharonova *et al*. (2008), it appears that the char with a lower organic matter content could possibly have a lower degree of structural transformation (carbon reordering). Sharonova et *al*. (2008) reported that char particles of a high reactivity Russian coal with a low organic content had a lower degree of carbonisation. On the contrary char particles of lower reactivity from another Russian coal had a higher organic content and a higher degree of carbonisation. This was attributed to the difference in maceral composition and rank. The high reactivity coal is a lower rank coal and is vitrinite–rich while the lower reactivity coal is more metamorphized, and contains considerable quantity of inertinite. In this study, the degree of structural transformation of organic matter in the char was determined by Raman analysis. The degree of mineral matter transformation in the char was determined by XRD and SEM/EDX analysis. A combination of

petrographic and Raman studies as well as SEM and EDX analyses, were used to study the interaction between the transformed silicates minerals and the carbon in the char.

Table 6.3: Organic/ Inorganic constituents of Grootegeluk chars

Temperature (^{o}C)	Residence time(Mins)	Carbon in the bed char (%)	Ash in the bed char (%)	Fixed carbon conversion (%)
910	35	38.64	61.56	40.32
960	35	28.24	71.76	57.44
960	55	16.4	83.60	69.55
1000	35	21.71	78.39	65.42
1000	45	10.80	89.90	74.96
1000	55	4.50	95.50	82.16

Table 6.4: Organic/ Inorganic constituents of New Vaal chars

Temperature (^{o}C)	Residence time(Mins)	Carbon in the bed char (%)	Ash in the bed char (%)	Fixed carbon conversion (%)
910	20	13.70	86.3	75.94
910	30	5.49	94.51	80.45
960	20	4.40	95.6	84.55
960	30	3.29	96.71	85.57
1000	20	2.50	97.50	87.57

6.3.2 Carbon structure of the chars samples

Figure 6.1 shows the change in the Raman spectrum of Grootegeluk char at 910 ^{o}C and 1000 ^{o}C. At 1000 ^{o}C both the D and G band peaks became sharper. This observation is consistent with the finding of Kawakami *et al.* (2006) who noted that the D-band width decreased with heat treatment for two disordered char samples that are derived from bamboo and wood charcoals. In this study, the D band width decreased from 128 cm^{-1} at 910 ^{o}C to 107 cm^{-1} at 1000 ^{o}C .The narrowing of the D band suggests a more uniformed carbon structure, resulting from a decrease in both the concentration and distribution of amorphous carbon structures. The G-band width, which is related to the crystalline component in the coal, decreased from 62 cm^{-1} at 910 ^{o}C to 56 cm^{-1}at 1000 ^{o}C. This indicates a lower growth in the crystalline component of the coal sample.

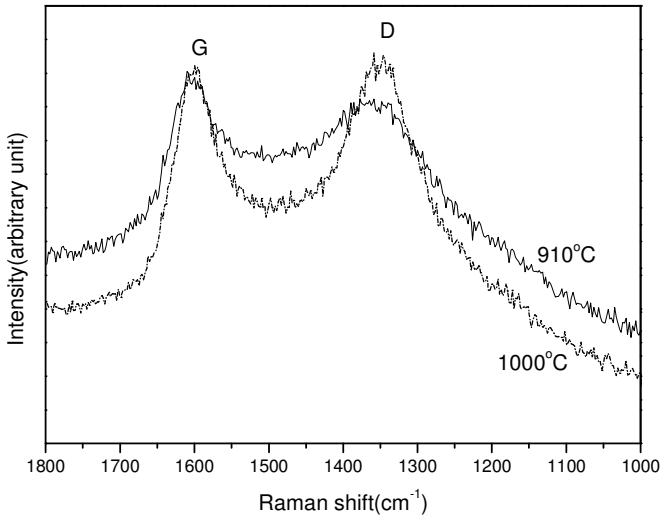


Figure 6.1 Raman spectra of Grootegeluk chars at 910 ^{o}C and at 1000 ^{o}C

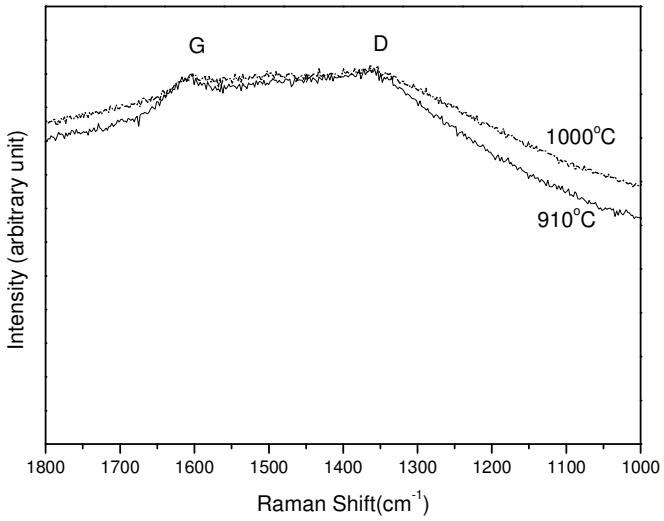


Figure 6.2 Raman spectra of New Vaal char 910 ^{o}C and at 1000 ^{o}C

Figure 6.2 shows the Raman spectra for the New Vaal char particles at 910 ^{o}C and 1000 ^{o}C. There was a negligible change in both the D and G band peak when the temperature was increased from 910 ^{o}C to 1000 ^{o}C. The D-band width decreased from 151 cm^{-1} at 910 ^{o}C to 141 cm^{-1} at 1000 ^{o}C, and there was no change in G-bandwidth.

These results indicate that increased ordering of the amorphous region can be correlated to the proportions of inertinite and vitrinite macerals in the coals. The Grootegeluk coal sample with high vitrinite content had the highest degree of ordering while the New Vaal coals with high inertinite contents had low degrees of ordering. It also indicates that there was no growth in the crystalline component for New Vaal chars however there was an increase in the crystalline component for the Grootegeluk coal. This result is in agreement with the suggestion of Sharonova *et al*. (2008), that char particles with a high reactivity coal had lower content of organic substance and lower degree of carbonisation organic matter. In this study, New Vaal char particles with a higher carbon conversion had lower degree of structural transformation and Grootegeluk with a lower carbon conversion had a higher degree of carbon conversion/structural transformation

6.3.3 Characterisation of minerals phases in the char samples

The XRD diffrcatogram of the Grootegeluk char generated at 1000 ^{o}C and 35 mins, is presented in Figure 6.3. Similar diffrcatograms were obtained from the other test conditions. The major minerals in the char particles are anatase, fayalite, mullite, wustite and quartz. The presence of the minerals may be explained as follows: in the parent coal sample, Quartz and kaolinite (80%) are the major mineral matter present. However, kaolinite decomposes to metakaolin (Al_2O_3. SiO_2) between 550 and 600 ^{o}C and remains stable up to 1000 ^{o}C. With an increase in temperature (up to ~1200 ^{o}C), mullite, an alumina-rich aluminosilicate (Gupta *et al*. 2008), is formed due to the decomposition of metakaolinite (Van Dyk, 2008). Wustite is formed at around 900 ^{o}C mainly due to the decomposition of hematite and siderite (Zhang *et al.* 2009). With a further increase in temperature, wustite starts to react with mullite and quartz to form fayalite (Wu *et al*. 2010). Fayalite is a layer-silicate mineral rich in iron and silicate (Bai *et al*. 2009).

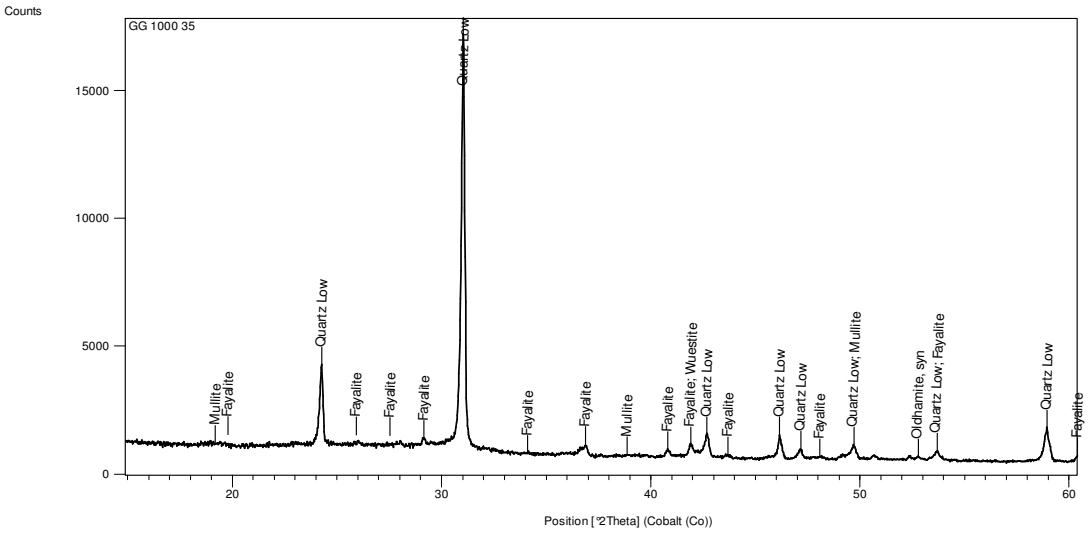


Figure 6.3 XRD spectrum of Grootegeluk char obtained at 1000^{o}C and 35 mins

The content of mineral matters in the various Grootegeluk chars generated at different temperatures was determined with the RIR method (Schreiner, 1995) and the result is presented in Figure 6.4. In this study, the concentration of mullite increased from 0.3% at 910 ^{o}C to 13.33% at 1000 ^{o}C. It further increased to 14.33% when the

residence time increased from 35 mins to 45 mins. However, it decreased slightly to 11.26 % when the residence time was increased to 55mins. Similar trends were observed for fayalite but the decrease in concentration started at 45 mins. The decrease in the concentration of both mullite and fayalite could be due to the partial melting of these minerals (Wu *et al*. 2010; Bai *et al*. 2011). Fayalite starts to melt at relatively lower temperature than mullite (Zhang *et al.* 2011). In this study, the melting temperature was the same (1000 ^{o}C) but fayalite starts melting at 45 mins while mullite starts melting at 55mins.

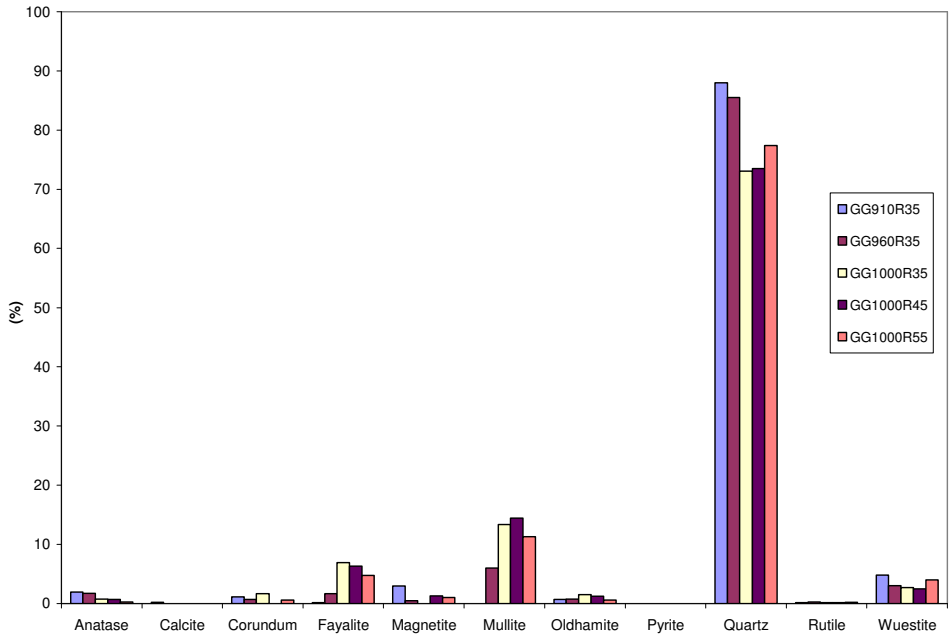


Figure 6.4 Mineral matter in Grootegeluk char at different temperatures and residence time

For New Vaal char particles, there was no formation of fayalite, but mullite was formed. The result of the mineral transformation of New Vaal chars under gasification from 910 ^{o}C to 960 ^{o}C is presented in Figure 6.5. Mullite was formed at 960 ^{o}C and the concentration increased from 11% to 24% when the residence time was increased from 20 mins to 30 mins. On this basis it appears that there are two main phases of silicates in the char particles, namely, high melting point silicates such as mullite and low melting point silicates such as fayalite.

These silicates can further be grouped based on their reactivity. Gupta *et al.* (2008) reported that on the basis of the chemical nature of silicates, they can be characterised as least reactive, moderately reactive and reactive. High melting point silicates such as mullite are the least reactive silicates and low melting point silicates such as fayalite are the moderate reactive silicates.

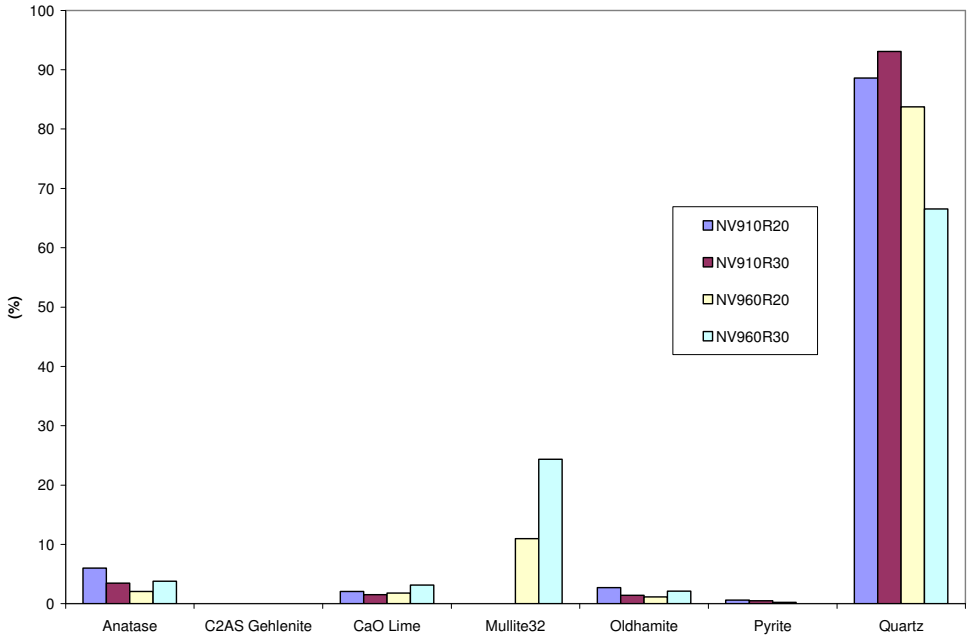


Figure 6.5 Mineral matter in New Vaal Char at different temperatures and residence time

Zhang *et al.* (2011) studied the reaction activity and thermal stability of mullite and fayalite at molecular level using quantum chemical calculation. The chemical activity of the highest occupied molecular orbits (HOMO) in mullite cluster is stronger than that of the lowest unoccupied molecular orbit (LUMO) in the mullite cluster. Based on the frontier orbital theory (Fujimoto, 1977), the frontier orbitals in the HOMO or LUMO have more chemical reactivity and less thermal stability than any other orbits and play a key role in the reaction activity and thermal activity of minerals at the molecular level. Hence the energy which the electron in the external shell of the molecule needs to transfer from the HOMO to LUMO (ΔE) in the mineral molecule can be used to calculate the thermal reaction activity and thermal stability of minerals. A smaller value of ΔE means higher reaction activity and lower thermal stability.

The ΔE value of fayalite is 1.659 eV, and is lower than that of mullite which is 6.8 eV (Zhang *et al.* 2011; Li *et al*. 2009). This indicates that the different phases and proportion of the melted silicates minerals would have a different impact on the modification of local carbon matrix, and hence on char reactivity. The interaction between the transformed silicates minerals and the carbon in the char will be studied in the next section.

6.3.4 Char-mineral interaction

In this section, the impact of the different phases of silicate minerals in the char particles on the modification of the local carbon was investigated. In order to do this it is necessary to determine the distribution of the melted minerals on the char matrix. Limited contact of the melted mineral with the local carbon in the char matrix will indicate non- or low interaction/ modification of the carbon (Wang *et al.* 1995).

SEM analysis can be used to examine the physical and chemical distribution of minerals in the carbon matrix. On the physical basis, minerals distribution can be classified into three groups, namely, *discrete agglomerate*, i.e. coarse minerals in limited contact with the carbon in the char matrix; *disseminated*, i.e., minerals in close contact with carbon, and *pore inclusions*, i.e., the presence of fine materials in the char (Gupta *et al*. 2008). In this study, both Grootegeluk char particles and New Vaal char particles were characterised on the basis of the presence of fine disseminated phases and discrete agglomerates. This is illustrated in Figures 6.6 and 6.7. The proportion of fine disseminated phases and discrete agglomerates could not be estimated by this technique.

The proportion of melted minerals making contact with the carbon phase was estimated from petrographic analysis. Results obtained for chars generated at 960 ^{o}C and 30 mins in oxygen-enriched conditions for both coals showed that melted minerals predominated in the New Vaal char in nearly 80% of the whole sample, compared to about 24% in the Grootegeluk char. Melted minerals which had bordered, penetrated or engulfed carbon fragments accounted for approximately 4% in the New Vaal char while for Grootegeluk char about 14% penetration into the carbon matrix was observed. The ratio of melted minerals penetrating/surrounding the carbon to melted minerals in separate bodies in the New Vaal char was 1 to 20 and 1 to 2.4 in Grootegeluk char. This indicates that a lower proportion of disseminated phases and a

high proportion of discrete agglomerates in the New Vaal char and approximately equal amounts of both types of mineral distribution ARE present in the Grooteguluk char.

XRD analysis tends to support this form of mineral distribution of the melted minerals. The results showed the presence of fayalite, a low melting point mineral in the Grooteguluk char. Mineral phases with a higher proportion of low melting minerals such as fayalite result in the formation of more slag (liquid) and a less viscous melt leads to more melted mineral covering the pores and the surface of the char. Fayalite was not found in New Vaal char.

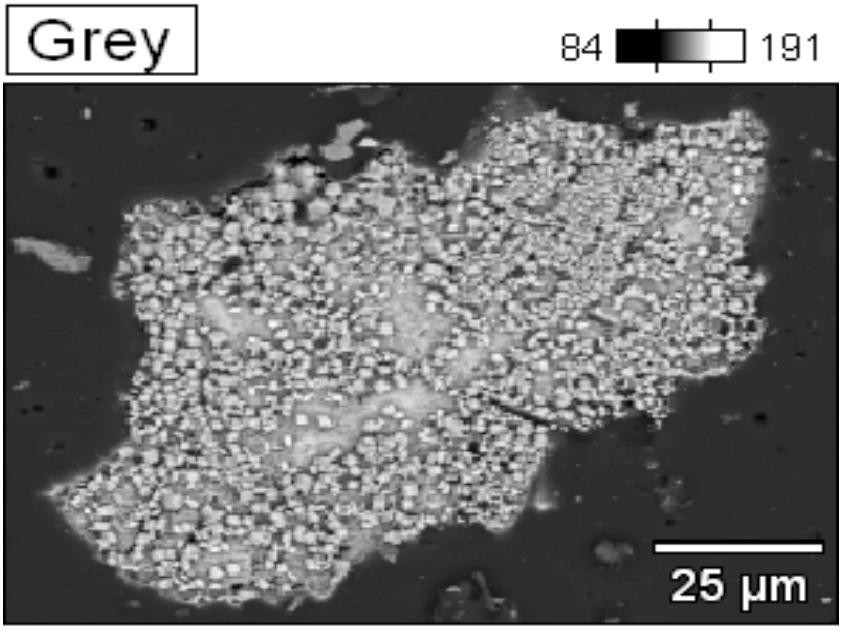


Figure 6.6 SEM images illustrating discrete agglomerate mineral distribution in a Grootegeluk char.

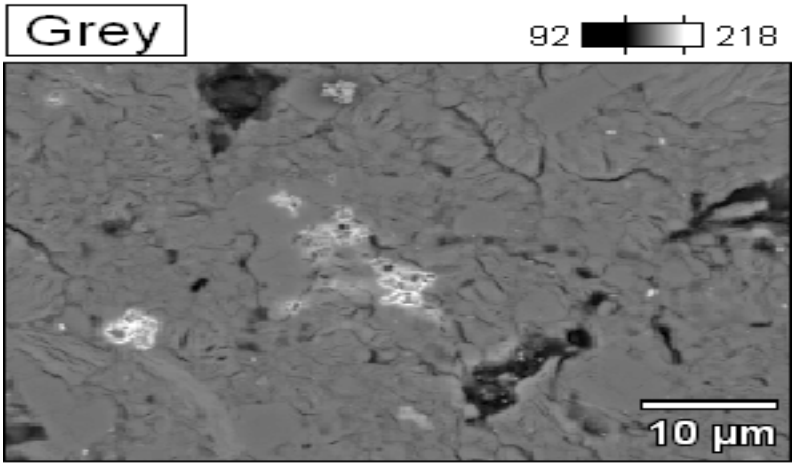


Figure 6.7 SEM images illustrating disseminated mineral distribution in a Grootegeluk char

The distribution of associated elements of silicate minerals in the fine disseminated phases and discrete agglomerates for both Grootegeluk char and New Vaal char generated at 960 ^{o}C and 30 mins was determined using the X-ray elemental maps. Figures 6.8 and 6.9 shows the proportion and distribution of various elements for both discrete agglomerates and disseminated phases respectively for Grooteguluk char. In Figure 6.8 the X-ray mapping of discrete agglomerates showed the presence of C (88 %), Ca (46%), Si (15%), Al (7.98%), Fe (2.61), and Mg (0.78) on the scale. EDS analysis also confirmed the proportion of elements in this order. Figure 6.8 also showed that the distribution of the elements was not uniform and was also not in accordance to the proportion of the elements. Both C and Ca had a uniform distribution while the others were discrete. Si and Al were more concentrated at the edges or surface

In Figure 6.9 the X-ray mapping of disseminated phase distribution showed the presence of C (68%), Si (33%), Al (18%), K (4.54), Fe (2.75), and Na (0.74) on the scale. EDS analysis also confirmed the proportion of elements in this order. With regards to the mineral distribution C, Si and Al had a uniform distribution while Fe, K and Na had a discrete distribution. This indicates that the distribution of Si and Al

elements with respects to carbon are different for the discrete agglomerates and the disseminated phase.

Sekine *et al.* (2006) also observed a uniform distribution or location of Si and Al to carbon, using X-ray mapping and Raman mapping. However, they did not report on the location of other elements such as Ca, Mg and Fe. The mapping of the carbon that was in good accordance with the Si and Al distributions showed a non-graphitic carbon. However, the carbon might be non-graphitic since its native or original structure might have changed.

The method used in the evaluation of FT-Raman spectra is not well suited for studying the carbon structure of disordered carbon such as coal chars. The method involved the calculation of the ratio of the half-width of G-band to D-band (I_D/I_G). This does not account for the valley between the G and D bands which reflect the amorphous region in coal char (Dong *et al.* 2009). The increased reordering of the amorphous regions would lead to an intensity of the valley (I_V/I_G). In this study, a combination of both ratios I_D/I_G vs. I_V/I_G mapping was used to evaluate the carbon structure of the chars.

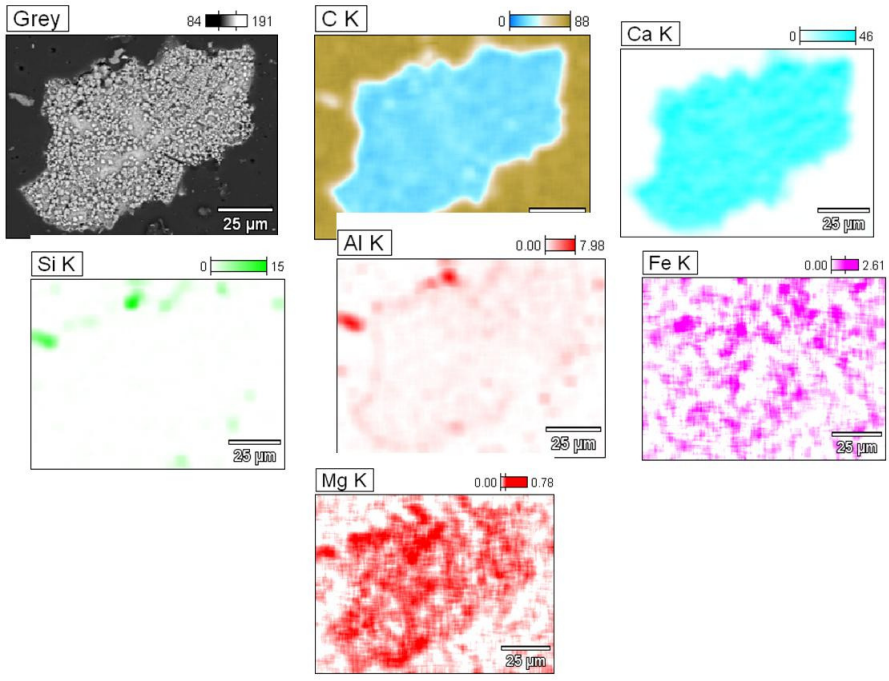


Figure 6.8 X-ray mapping for discrete agglomerates for Grootegeluk char generated at 960 ^{o}C and 30 mins under oxygen-enriched gasification conditions.

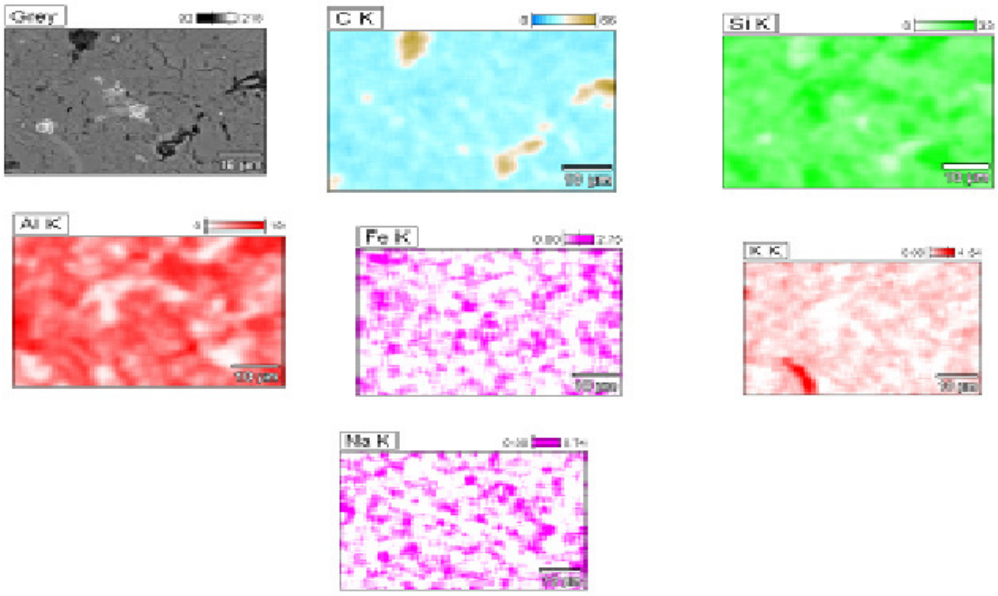


Figure 6.9 X-ray mapping for discrete agglomerates for Grootegeluk char generated at 960 ^{o}C and 30 mins under oxygen-enriched gasification conditions.

Figures 6.10 and 6.11 show the surface contour plots of Grootegeluk char generated at 960 ^{o}C and 30 minutes under oxygen-enriched gasification conditions. The legend on each map gives the range of values of the relevant ratio of I_D/I_G and I_V/I_G ratios. These parameters were evaluated from across the surface of the particle on the 7x7 grid (See Appendix B). The I_D/I_G ratio is a parameter indicating the dimension of the graphitic microcrystalline: a higher I_D/I_G ratio will indicate a more ordered graphitic structure. The I_V/I_G ratio represents the degree of disorderness in the char structure, therefore a decrease in I_V/I_G ratio leads to a more ordered and uniformed carbon while an increase in the ratio suggests an amorphous structure. In Figure 6.10, the average I_D/I_G ratio for the carbon structure in Grootegeluk char with minerals in the disseminated phases was 0.832, although the values were different at the different points or surface on the map. This indicates that the carbon structure in the char is not homogenous. This might be due to the interaction of the decomposed minerals and the carbon in the char. According to Zhang *et al.* (2009) when the carbon in the char is not homogenous, their carbon structure is not determined only by the parent coal properties such as maceral and rank, rather it is also a function of the interaction of the decomposed mineral matter and the metastable liquid phase during char formation (fluidity).

Hence a structurally more ordered part will thus be formed in the interaction part and less from the unaffected part. (Zhang *et al* 2009). In this study, I_D/I_G values less than or equal to the average value of 0.832 (with a legend colour of green in Fig. 6.10) represents the unaffected part and I_D/I_G values higher than 0.832 represents structured and more ordered carbon due to interaction. The number of points involved in interactions for Grootegeluk char was 14**.**

In Figure 6.11, the average I_D/I_G ratio for the carbon structure in New Vaal char with minerals in the disseminated phases was 1.237, and is much higher than that of Grootegeluk char 0.832. However the number of interactions in New Vaal chars, i.e., 7, is much lower than for the Grootegeluk char (14). This result supports earlier (as reported in this work) petrographic results of melted minerals which show a higher proportion of melted minerals penetrating or surrounding carbon in Grootegeluk char than in New Vaal char. A higher proportion of melted minerals penetrating or surrounding carbon suggests a higher degree of interaction and modification of the local carbon.

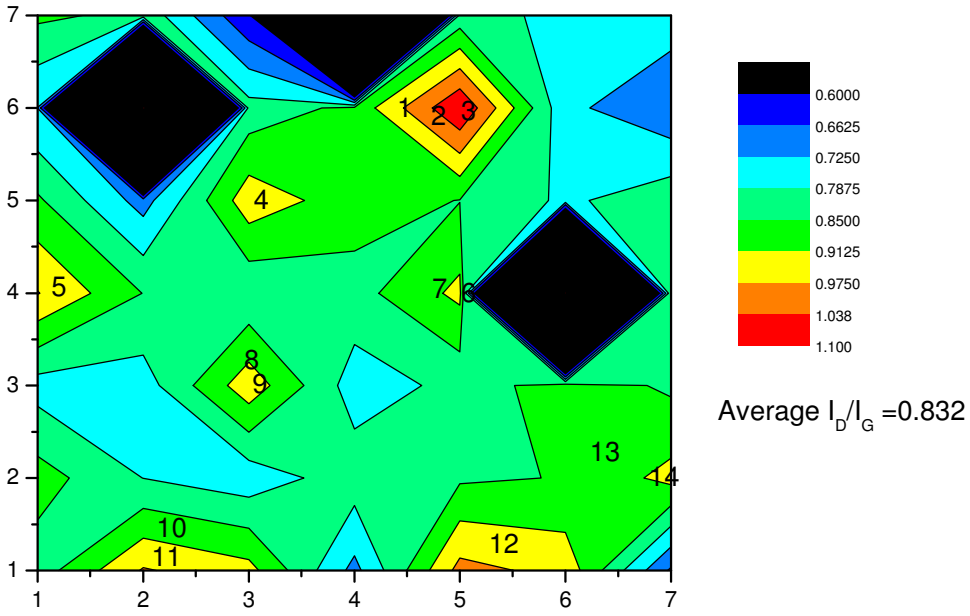


Figure 6.10 I_D/I_G mapping of Grootegeluk char with minerals in disseminated phases

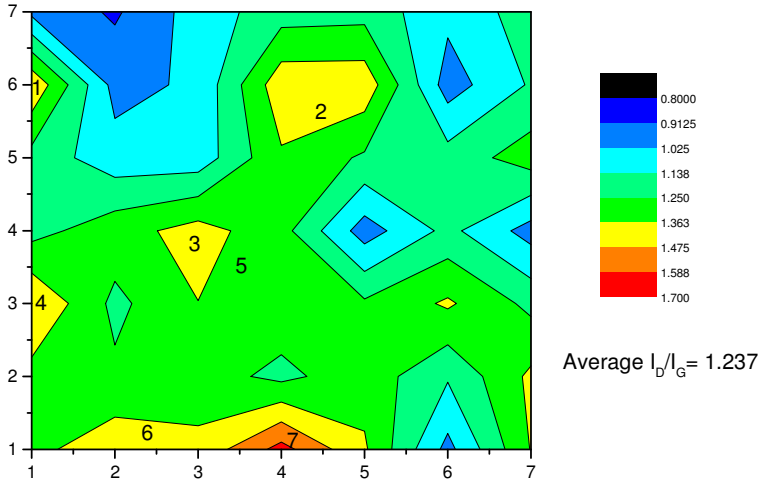


Figure 6.11 I_D/I_G mapping of New Vaal char with minerals in disseminated phases dispersed

In figures 6.12 and 6.13, the average I_v/I_G ratio for amorphous carbon in Grootegeluk and New Vaal char particles were 0.9169 and 0.778 respectively. The number of points involved in interactions was 13 for Grootegeluk char and 10 for New Vaal char. The degree of interactions was higher in the Grootegeluk char, for both types of carbon; the ordered carbon (14) and amorphous carbon (13) while it was ordered carbon (7) and amorphous carbon (10) for the New Vaal char. This suggests that a higher change in the reactivity of Grootegeluk char is expected than in the New Vaal. This will be addressed in the next section.

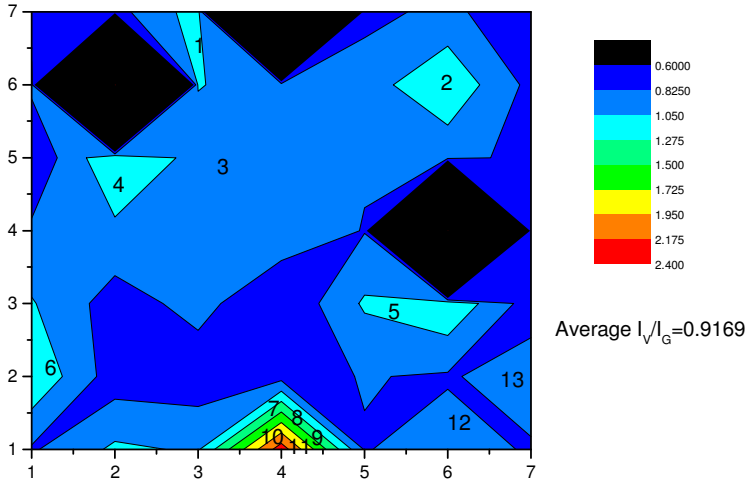


Figure 6.12 I_V/I_G mapping of Grootegeluk char with minerals in disseminated phases

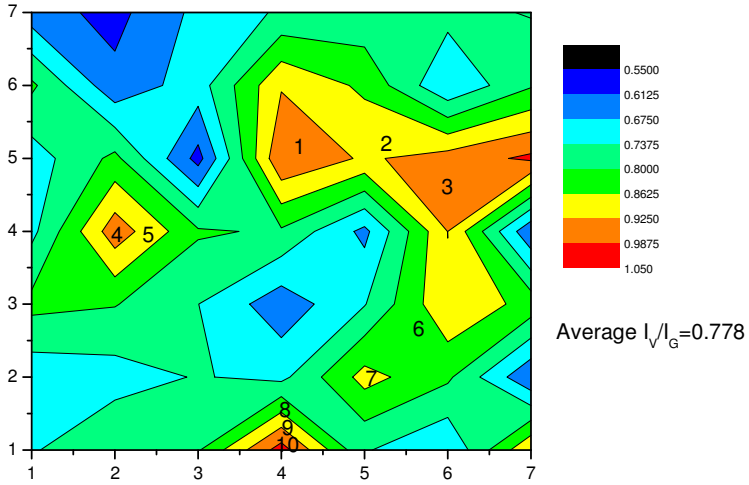


Figure 6.13 I_V/I_G mapping of New Vaal char with minerals in disseminated phases dispersed

6.3.5 Modelling of char-mineral interaction of high ash coals during fluidised bed gasification

The impact of mineral-char interaction in char matrix has been modelled by Lunden *et al*. (1998). This model was used to evaluate the effect of mineral matter on char reactivity and burnout that occurs during mineral-char interactions in the combustion

of a high volatile bituminous coal. The melted mineral matter can decrease the amount of carbon per surface area in the char or by increasing the carbon crystallite growth and thereby reducing its reactivity. The total surface area available for reaction can be related to the intrinsic reactivity and global reactivity by the following equation (Lunden *et al.* 1998):

$$q_g \approx q_i \left[(1 - F_m) S \rho_c V_p\right]^{1/2}, \qquad (6.1)$$

where the surface area is described by the specific surface area of the particle, S (m^2/g), the apparent density of the particle, ρ_c, the volume of the particle V_p, the fraction of surface occupied by the mineral matter F_m, qi is the intrinsic rate and q_g is the global rate.

This model does not account for the proportion of the exposed mineral matter that diffuses back into the char matrix. The proportion of melted mineral penetrating or diffusing into the char matrix is a function of the char morphology and the mineral phase. The proportion of melted mineral that penetrates into a dense char will be lower than into a porous char *(x)*. In the dense char there are essentially no large voids inside the particle but there are large voids in the porous char. Furthermore the presence of low melting point silicate minerals such as fayalite will lead to more melted mineral covering and penetrating into the char matrix. At this point, we should recall that petrographic analysis was used to evaluate the proportion of dense char and porous char in percentage volume, and also the proportion of melted mineral penetrating or surrounding the carbon matrix. Furthermore, XRD analysis was used to determine the mineral phase in the char particles, and to subsequently estimate their proportion.

The model also did not account for the effect of mineral carbon ordering. It assumed that the global rate (q_g) is equal to intrinsic rate (q_i), that is, $q_g=q_i$. This is because the original experimental technique could not distinguish between the potential effects of mineral matter on carbon ordering and molecular-level reactivity. If this is taken into account, then $q_g \neq q_i$, the reduced reaction rate will be q_g/q_i and the reaction order will vary and will not be constant (Murphy, 2010). That means the reaction order of 0.5 in Equation 6.1 will be not be constant.

The reduced reaction rate or the relative reactivity, R, can be estimated from reactivity index (Ye *et al.* 1997)

$$R = 0.5 / t_{50} \qquad (6.2)$$

where t_{50} is the time at carbon conversion rate of 50%. So $q_{0.5}$ will be the gasification rate for 50% carbon conversion.

The global or overall reaction of chars can also be related to the fractional carbon conversion (Xu *et al*. 2009). i.e.

$$q_g = k(1-x)^n \qquad (6.3)$$

where k is the reaction constant, and n is defined as reaction order. In order to determine the reaction order, the reduced gasification rate or relative reactivity qg/q_{50} was used, i.e.

$$\frac{q_g}{q_{0.5}} = \frac{(1-x)^n}{0.5^n} \qquad (6.4)$$

The gasification reactivity of Grootegeluk chars and New Vaal chars were determined using a TGA. The full details of the procedure have been given in Section 3.4.1 in Chapter 3 (Methodology).

Figures 6.14 and 6.15 present the overall or global gasification rate with carbon conversion for both coals and their chars. The gasification rate of Grootegeluk char was higher than the New Vaal char. This might be due to high content of residual carbon in the Grootegeluk char particles. The carbon content for the Grootegeluk char particles is 39% (GG Char 910 ^oC) and 28% (GG Char 960 ^oC) and for the New Vaal char particles are 14% (NV 910 ^oC) and 4% (NV 960 ^oC). The results also indicate that there was high variation in reactivity in the Grootegeluk chars.

According to Xu *et al*. (2009), reaction order can be used to estimate the extent of variation of gasification rate with carbon conversion. Thus Equation 6.4 was used to fit experimental data of $qg/g_{0.5}$ vs carbon conversion (x) and the reaction order was determined.

Figure 6.16 shows the fitted data for New Vaal char and the reaction order of 0.98 was obtained. The reaction orders of the other conditions were also evaluated and are presented in Table 6.5. The reaction order ranges from 0.66 to 0.87 for Grootegeluk char while for New Vaal char it ranged from 0.90 to 0.98 for New Vaal char. This result supports the earlier suggestion that a higher change in the reactivity of the Grootegeluk sample is expected and this may be due to higher degree of interaction between melted minerals and carbon in the char. The degree of interactions was higher in the Grootegeluk char, for both types of carbon; the ordered carbon (14) and amorphous carbon (13) while it was ordered carbon (7) and amorphous carbon (10) for the New Vaal char.

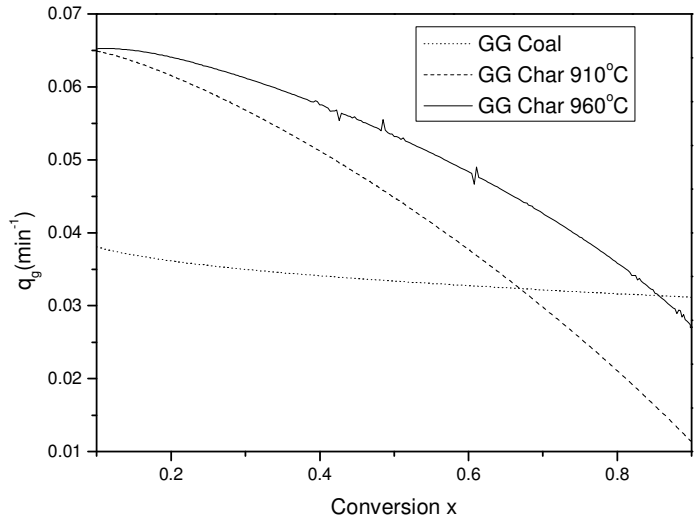


Figure 6.14 Gasification rate vs. carbon conversion of Grootegeluk coal and chars

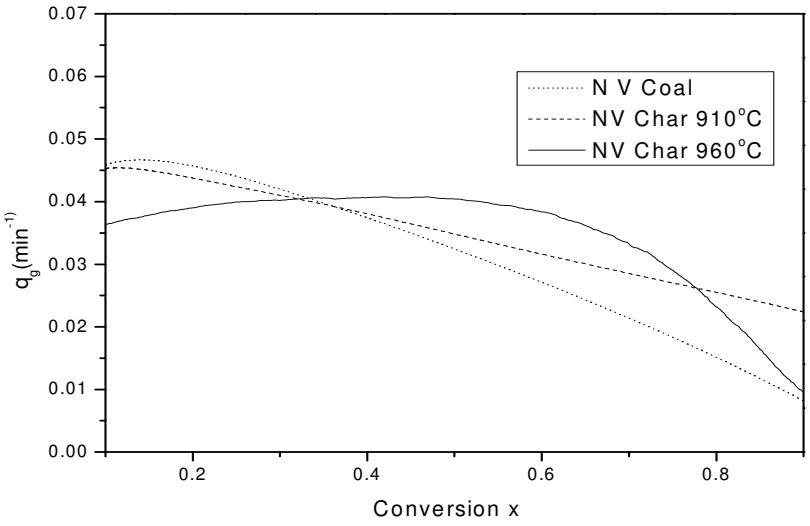


Figure 6.15 Gasification rate vs. carbon conversion of New Vaal coal and chars

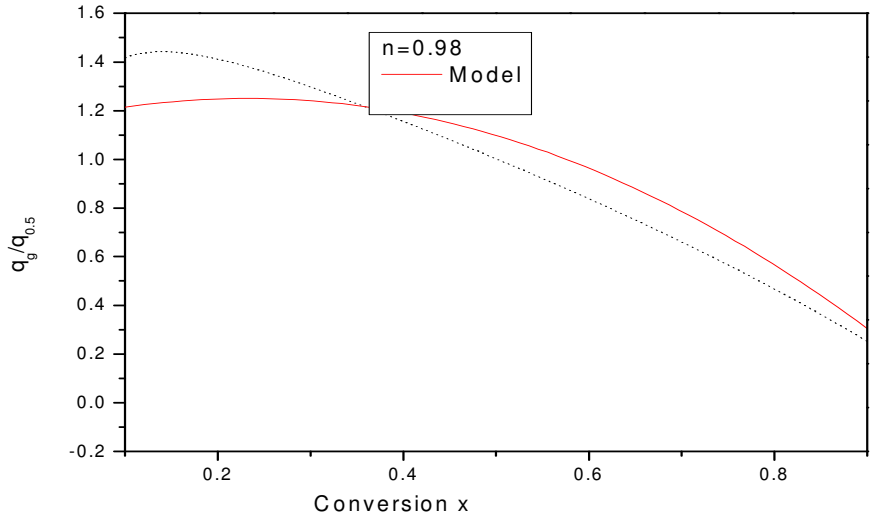


Figure 6.16 Estimation of reaction order of New Vaal Coal

Table 6.5 Comparison of intrinsic reaction rate of Grootegeluk coal chars and New Vaal coal chars

Samples	Reaction order (n)
GG Coal	0.85
GG Char 910	0.65
GG Char 960	0.66
NV Coal	0.98
NV Char 910	0.97
NV Char 960	0.90

6.4 Conclusions

This chapter aims to determine and quantify the effects of the different forms of interactions that could occur between transformed minerals and carbon in the char matrix of different char particles generated from two different high ash South African coals in a fluidised bed. The decomposition of clay minerals during fluidised bed gasification of both high ash inertinite–rich coals and vitrinite-rich coals resulted in the formation of amorphous aluminosilicates. Petrographic analysis showed some of the molten matter penetrated into cracks and pores in the chars. Such inert mineral boundaries may be expected to severely reduce the ability of the carbon to react further by preventing the reaction gas from coming in contact with the carbon.

Results obtained for chars generated at 960 ^{o}C and at 30 mins in oxygen-enriched conditions for both coals showed that melted minerals predominated in the New Vaal char and accounted for nearly 80% of the whole sample, compared to about 24% in the Grootegeluk char. Melted minerals which had bordered, penetrated or engulfed carbon fragments accounted for approximately 10% in the Grootegeluk char, while for New Vaal char, about 4% penetration into the carbon matrix was observed. The ratio of melted minerals penetrating OR surrounding the carbon to melted minerals in

separate bodies was 1:20 in the New Vaal char and 1:2.4 in Grootegeluk char respectively.

This indicates that a lower proportion of disseminated phases and a high proportion of discrete agglomerates occurred in the New Vaal char whilst approximately equal amounts of both types of mineral distribution was present in the Grooteguluk char.

XRD analysis tends to support this form of mineral distribution of the melted minerals. The results showed the presence of fayalite, a low melting point mineral in the Grooteguluk char. Mineral phases with a higher proportion of low melting minerals such as fayalite result in the formation of more slag (liquid) and a less viscous melt leads to more melted mineral covering the pores and the surface of the char. Fayalite was not found in New Vaal char.

In addition to the physical effects on char reactivity, the molten ash can also participate in a chemical reaction at the char-mineral interface that involves the modification of the carbon properties. A structurally more ordered carbon will be formed in the interaction part and a less ordered carbon is formed from the unaffected part**.** In this study, a combination of both ratios I_D/I_G vs. I_V/I_G mapping was used to evaluate carbon structure of chars, while X-ray mapping and EDS mapping was used to determine the distribution of elements such as Si, Al, Fe, Mg, Ca and K.

The average I_D/I_G ratio for the carbon structure in New Vaal char with minerals in the disseminated phases was 1.237, higher than that of Grootegeluk char, which is of 0.832. However the numbers of interactions in New Vaal char (7) was lower than for the Grootegeluk char (14). These results support earlier petrographic results on melted minerals which show a higher proportion of melted minerals penetrating or surrounding carbon in Grooteguluk char than in New Vaal char. Higher proportion of melted minerals penetrating or surrounding carbon suggest a higher degree of higher interaction and modification of the local carbon.

CHAPTER 7 CONCLUSIONS AND RECOMMENDATIONS

The aim of this research was to investigate the fluidised bed gasification of fine, high ash-content by studying the transformation of macerals and minerals and their interactions under various conditions. It is anticipated that this would provide new insights into the evolution of the typically high-ash inertinite-rich coals currently available on the South African domestic market.

In Chapter 4, the gasification performance of selected South African coals and their derived chars were correlated against a range of chemical, physical and optical characteristics including mineral and maceral (and specifically inertinite) contents. Changes in chemical microstructures following gasification under constant conditions in a fluidised bed gasifier was also observed and reported. In Chapter 5, the textural properties of chars generated under air-blown, oxygen-blown and oxygen-enriched conditions in a fluidised bed gasifier were determined by detailed petrographic analysis. In Chapter 6, the different forms of mineral-char interactions during the gasification of high ash coals in fluidised bed were described. The main conclusions of this thesis are summarised as follows:

7.1 Conclusions

Characterisation of South African coal and chars in fluidised bed gasification

- The Petrographic-based carbon form characterisation of chars showed that the reactive macerals had been transformed from normal coal forms into very different mixtures of partially reacted coal, highly reflecting char forms, coke and inorganic matter (ash). Higher proportions of porous chars were found in coals that have higher reactive macerals (vitrinite) such as Grootegeluk coal whereas much higher proportions of dense inertinitic chars were found in Matla and Duhva (High inert coal macerals).
- High vitrinite contents resulted in an increase in the order of the disordered carbon structure after gasification which lead to a greater degree of graphitised ordered

carbon structures. High inertinite contents resulted in low or no structural transformation of the chemical structure.

- The degree of transformation of the inorganic mineral constituents in the coals correlated to the proportion of inertinite present in the selected coals. Higher proportions of inertinite macerals and inertinitic chars resulted in higher proportions of melted minerals.
- FITR analysis indicated that some of the molten matter penetrated into cracks and pores in the chars. This was confirmed by petrographic analysis. The presence of such mineral matter or "slag" which bordered, penetrated or engulfed carbon fragments accounted for 15 % to 20 % in the Matla and Duhva respectively, whereas only 5 % was observed in the Grootegeluk char.

Textural properties of chars as determined by petrographic analysis: Comparison between air-blown, oxygen-blown and oxygen-enriched gasification.

- The oxygen-blown sample possessed the lowest proportion of total carbon forms of all three samples (53% by volume, mineral matter basis relative to 58 and 60% in the other two samples), the lowest proportion of thin-walled highly porous and reactive char forms (17% relative to 23 and 26%) and the highest proportion of partially consumed carbon/char forms (30% relative to 19 and 23 %).

- This sample also exhibited the lowest mean reflectance value (4.73% R_{vrand}) with the lowest proportion of chars with reflectance values above 4% R_{vrand}. These results suggest that a greater degree of consumption of carbon took place under the oxygen-blown conditions, possibly with higher temperatures, and that under these conditions, the highly reflecting porous thin-walled chars would have been consumed first and fastest thereby leaving the higher proportion of partially consumed chars and inertinites behind which, in turn, would have lead to the occurrence of lower reflectance readings.

- These conditions also resulted in the presence of higher proportions of melted "slag" minerals in the oxygen-blown sample which totalled 31% compared to 24% in the other two samples. The coating and penetration of the carbon

particles by these molten minerals relative to the proportion of thin-walled very porous isotropic coke present was most pronounced

- The oxygen-enriched and air-blown chars displayed higher proportions of organic matter relative to the oxygen-blown sample, and higher proportions of the high reflecting thin-walled porous chars with higher mean reflectance values and reduced proportions of melted mineral matter. These results indicate that both of these samples underwent reduced levels of carbon consumption and at lower temperatures relative to the oxygen-blown sample.

Mineral-char interaction during gasification of high ash coals in fluidised bed gasification

- The mapping of two Raman parameters I_D/I_G vs. I_V/I_G can be used to evaluate the impact of melted mineral on the local carbon

- X-ray mapping can be used to study the distribution of elements in relation to the local carbon

- X-ray mapping of discrete agglomerates showed the presence of C (88%), Ca (46%), Si (15%), Al (7.98%), Fe (2.61), and Mg (0.78). in relative order of proportion on the surface of the chars as indicated by EDS analysis. The distribution of elements was not uniform and also not in accordance with the proportions of the elements reported above. Both C and Ca had a uniform distribution across the surface of the analysed particles while other elements including Al, Si, Fe and Mg were limited to specific areas. Si and Al were more concentrated at the edges of the particles.

- The distribution of elements was not uniform and also not in accordance to the proportion of the elements. Both C and Ca had a uniform distribution while the other elements were discrete. Si and Al were more concentrated at the edges or surface.

- X-ray mapping of disseminated phase distribution showed the presence of C (68 %), Si (33 %), Al (18 %), K (4.54), Fe (2.75), and Na (0.74) in relative order of proportion on the surface of the chars as indicated by EDS analysis.

With regards to the mineral distribution C, Si and Al had a uniform distribution while Fe, K and Na had a discrete distribution.

- The results indicate that the distribution of Si and Al elements with respects to carbon are different for the discrete agglomerates and the disseminated phase.

- The average I_D/I_G ratio for the carbon structure in New Vaal char with minerals in the disseminated phases was 1.237, higher than that of Grootegeluk char, which is of 0.832. However the number of interactions in New Vaal char, that is, 7 was lower than 14 for the Grootegeluk char.

- The average I_v/I_G ratio for amorphous carbon in Grootegeluk and New Vaal char particles were 0.9169 and 0.778 respectively. The number of points involved in interactions was 13 for Grootegeluk char and 10 for New Vaal char.

- The degree of interactions was higher in the Grootegeluk char, for both types of carbon; the ordered carbon (14) and amorphous carbon (13) while it was ordered carbon (7) and amorphous carbon (10).

- The results indicate that a higher change in the reactivity of Grootegeluk char is expected than in the New Vaal char in the Grootegeluk coal due to higher degree of interaction and modification of the local carbon.

In summary, spectrographic analysis can be used to evaluate the types of coal suitable for fluidised bed gasification. This can be achieved by studying the relationship between the organic (maceral-to-char) and inorganic (mineral-to-ash) components in coal including their structure and behaviour. This can be used to predict the behaviour of a particular coal/char submitted for fluidised bed gasification. A higher loss of coal reactivity was obtained from vitrinites-rich coals due to a higher degree of structural transformation of carbon in the coal. Inertinite-rich coals experienced a lower loss of coal reactivity and lower degree

of structural transformation even at a longer residence time. The structural transformation of the macerals is due to substantial swelling (enhanced plasticity) and the modification of the local carbon by the melted minerals.

Furthermore, the gasification performance of low grade coals can be optimised by varying the oxygen content used for coal gasification.

7.2 Recommendations

- This study has shown that the decomposition of silicates clays in the vitrinite rich coals and inertinite coals are different .Higher decomposition of the clays was observed for the inertinite coals. Further studies should be carried out to investigate the roles of different macerals on the decomposition of clays during gasification. The nature and distribution of the clays and other minerals within the coals should also be included.

- The factors that determine the proportion of melted minerals covering the char surface are carbon conversion, temperature, and properties of the mineral matter (melting point and viscosity). Further studies should be carried out to determine the exact mechanism of redistribution.

- The mapping techniques developed in the study were tested for chars generated from Grootegeluk and New Vaal coals under oxygen-enriched conditions. It should be extended to chars generated from other conditions and also chars from different coals for validation**.**

- Techno-economic studies of the benefit of O_2 enrichment in the gasification of South African coals should be carried out.

References

Alvarez D, Borrego AG and Menéndez R (1997). Unbiased methods for the morphological description of char structures. *Fuel*, *76*, 1241-1248.

Alvarez D, Borrego AG and Menendez R (2003). *Procceedings of the 12th International Conference on Coal Science*; The Australian Institute of Energy: Toukley, New South Wales, Australia, 2003; p CD-6.

Alvarez D and Borrego AG (2007). The evolution of char surface area along pulverised coal combustion. *Energy & Fuels, 21*, 1085-1091.

Alonso MJG, Borrego AG, Alvarez D, Parra JB, and Menendez R (2001) Influence of pyrolysis temperature on char optical texture and reactivity. *Journal of Analytical and Applied Pyrolysis*, 58-59, 887-909.

Androutsopoulos GP and Hartzilyberis KS (2001). Electricity generation and atmospheric pollution: The role of solid fuels gasification. *Global Nest: the International Journal,* 3,171-178

Bai J, Wen L, Chun-zhu L, Zong-qing B and Bao-qing L (2009). Influences of mineral matter on high temperature gasification of coal char. *Journal of Fuel Chemistry and Technology*, 37, 134-138.

Bai J, Li W and Bai Z (2011). Effects of mineral matter and coal blending on gasification. *Energy & Fuels*, 25, 1127-1131.

Bar-Ziv E, Zaida A, Salatino P and Senneca O (2000). Diagnostics of carbon gasification by raman microprobe spectroscopy. *Proceedings of the Combustion Institute*, *28*, 2369-2374

Basu P (2006). Combustion and Gasification in Fluidised Beds. Taylor & Francis, Boca Raton.

Bhattacharya SP (2006). Gasification performance of Australian lignite's in a pressurised fluidised bed gasifier process development unit under air and oxygen-enriched air blown conditions. *Process Safety and Environmental Protection*, 84, 453-460.

Bayarsaikhan B, Sonoyama N, Hosokai S, Shimada T, Hayashi J, Li C and Chiba T (2006). Inhibition of steam gasification of char volatise in a fluidised bed under cpntinous feeding of brown coal. *Fuel,* 85, 340-349.

Beeley T, Crelling J, Gibbins, Hurt R, Lunden M, Man C, Williamson J and Yang (1996).Transient high-temperature thermal deactivation of monomaceral-rich coals chars. *Symposium (International) on Combustion*, *26, 3103-3110.*

Bend SL Edwards IA and Marsh H (1991) Coal provincialism, coal characterization and char formation. *Fuel ,* 70, 1147-1150.

Belyaev AA, Yampolskii YP, Starannikova LE, Polyakov AM, Clarizia G, Drioli E, Marigliano G and Barbieri G (2003). Membrane air separation for intensification of coal gasification process. *Fuel Processing Technology,* 80, 119-141.

Belyaev AA (2008). Gasification of low-grade fuels in a spouted bed for power generation. *Solid Fuel Chemistry,* 42, 14-21.

Borah RC, Ghosh P, and Rao PG (2008). Devolatiisation of coals of north-eastern India under fluidised bed conditions in oxygen enriched air. *Fuel Processing Technology,* 89, 1470-1478.

Borrrego AG, Alvarez D and Menendez R (1997). Effects of inertinite in coal on char structure and combustion. *Energy & Fuels,* 11, 702-708.

Borrego AG, and Martin AJ (2010). Variation in the structure of anthracite at a fast heating rate as determined by its optical properties: An example of oxy-combustion conditions in a drop tube reactor. *International Journal of Coal Geology,* 81, 301-308.

Bryers RW (1996). Fireside slagging, fouling, and high-temperature corrosion of heat-transfer surface due to impurities in steam-raising fuels**.** *Progress in Energy and Combustion Science*, 22, 129-120.

Cai HY, Guell AJ, Chatzakis IN, Lim JY, Dugwell DR and Kandiyoti R (1996). Combustion reactivity and morphological change in coal chars: Effect of pyrolysis temperature, heating rate and pressure. *Fuel*, 75, 15-24.

Cai HY, Megaritis A, Messnbock R, Dix M, Dugwell DR and Kandiyoti (1998). Pyrolysis of coal maceral concentrates under pf-combustion conditions (I): changes in volatile release and char combustibility as a function of rank .*Fuel*, 77, 1273-1282.

Cairncross B (2001). An overview of the Permain (Karoo) coal deposits of Southern Africa. *African Earth Sciences,* 33, 529-562.

Campoy M, Gomez-Barea A, Vidali FB and Ollero P (2009). Air-steam gasification of biomass in a fluidised bed: Process optimisation by enriched air. *Fuel Processing Technology,* 90, 677-685.

Chen H, Luo Z, Yang H, Ju F and Zhang S (2008). Pressurised pyrolysis and gasification of Chinese typical coal samples. *Energy & Fuels*, 22, 1136-1141.

Choudhury N, Biswas S, Sarkar P, Kumar M, Ghosal S, Mitra T, Mukherjee A and Choundhury A (2008). Influence of rank and macerals on the burnout behaviour of pulverised Indian coal. 74, *Coal Geology,* 145-153.

Craver RE (1971) Procedures in Sedimentary Petrology, Wiley

Crelling JC, Hippo EJ, Woerner BA and West DP (1992). Combustion characterises of selected whole coals and macerals. Fuel, 71, 151-158.

Collot AG (2006). Matching gasification technologies to coal properties. *Coal Geology,* 65, 191-212.

Cousins A, Paterson N, Dugwell DR, and Kandiyoti R (2006). An investigation of the reactivity of chars formed in fluidised bed gasifiers: The effect of reaction conditions and particle size on coal char reactivity. *Energy & Fuels*, 20, 2489-2497.

Dong S, Alvarez P, Paterson N, Dugwell DR and Kandiyoti R (2009). Study of the effect of heat treatment and gasification on the carbon structure of coal chars and metallurgical cokes using Fourier Transform Raman Spectroscopy. *Energy & Fuels,* 23, 1651-1661.

Everson RC, Neomagus WJP, Kaitano R, Falcon R, Van Alphen C and du Cann VM (2008). Properties of high ash char particles derived from inertinite-rich coal: 1. chemical,structural and petrographic characteristics. *Fuel*, 87, 3082, 3090.

Engelbrecht AD, North BC and Hadley TD (2008). Clean coal technology: Gasification of South African coals. IFSA 2008.

Engelbrecht AD, North BC and Oboirien BO (2010). Making the most of South Africa's low-quality coal: Converting high-ash coal to fuel gas using bubbling fluidised bed gasifiers. Science Real and Relevant: 3rd CSIR Biennial Conference

Falcon R(2011) Personal communication.

Falcone K and Schobert HH (1986) Mineral matter and ash in coal; Vorres KS ed; ACS Symposium Series, 301, 114-126.

Fermoso J, Gil MV, Borrego AG, Pevida C, Pis JJ and Rubiera F (2010). Effect of the pressure and temperature of devolatisation on the morphology and steam gasification reactivity of coal chars. *Energy & Fuels.* 24, 5586-5595.

Fujimoto H and Inagaki S (1977). Orbital interaction and chemical bonds polarisation in chemical reactions. *J Am. Chem. Soc*. 7424-7432.

Gaigher, G.L. (1980), Mineral matter in some South African coals, MSc, University of Pretoria, South Africa.

Grigore M, Sakurovs R, French D and Sahajwalla (2008). Mineral matter in coals and their reactions during coking. *Fuel,* 301-308.

Gupta S, Sahajwalla V, Burgo J, Chaubal and Youmans T (2006). Carbon structure of coke at high temperatures and its influence on coke fines in blast furnace dust. *Metallurgical and Material Transactions* B, 36B, 385-394.

Gupta S, French D, Sakurovs R, Grigore M, Sun H, Cham T, Hilding T, Hallin M, Lindblom B and Sahajwalla V(2008). Minerals and iron-making reactions in blast furnaces. *Progress in Energy and Combustion Science,* 34, 155-197.

Guo X, Tay HL, Zhang S and Li C (2008). Changes in char structure during the gasification of a Victorian brown coal in steam and oxygen at 800^{o}C. *Energy & Fuels,* 22, 4034-4038.

Harris DJ, Roberts DG and Henderson DG (2003). *Gasification Behaviour of Australian Coals,* Final Report for ACARP Project C9066.

Henderson C (2003). "Clean Coal Technologies." *CCC/74*, IEA Clean Coal Centre
Holt N (2004). Coal based IGCC plants- recent operating experience and lessons learned. *Pro. Gasification Technologies conference*, San Francisco.

Hurt R, Sun JK and Lunden M (1998). A kinetic model of carbon burnout in pulverized coal combustion. *Combustion and Flame,* 113, 181-197.

Ibarra JV, Munoz E and Moliner R (1996). FT-IR study of the evolution of coal structure during the coalification process. *Org. Geochem.*, *24* ,725-735.

Inglesi R and Pouris A (2010). Forecasting electricity demand in South Africa: A critique of Eskom's projections. *South Africa Journal of Science*, 106.

IRP(2010)http://www.doirp.co.za/content/INTEGRATED_RESOURCE_PLAN_ELECTRICITY_2010_v8.pdf (Acesssed, October, 2010).

Iyengar RK and Haque R (1991) Gasification of high-ash Indian coals for power generation. *Fuel Processing Technology,* 22,247-262.

Jasienko S, Matuszewska A and John A (1995). Properties and structure of hard coals from the borehole Niedobczyce IG-1 in the Rybnik Coal District, Upper Silesian Coal Basin, their petrographic and group constituents. 2. Variations in petrographic composition of the coals along the depth of borehole and alterations in structure of the

coals characterised by vitrinites spectroscopic analyses (X-ray, IR) *Fuel Processing Technology*, *41, 221-232.*

Jones RB, McCourt CB, Morley C and King K (1985). Maceral and rank influence on the morphology of coal char. *Fuel*, 64, 1460.

Kalkreuth W, Borrego, AG Alvarez, D, Menendez R, Osório E, RibaVilela A, Cardozo Alves T (2005). Exploring the possibilities of using Brazilian subbituminous coals for blast furnace pulverized coal injection. *Fuel*, *84*, 763-772.

Kawakami M, Karato T, Takenaka T, Yokoyama S (2005). Structure Analysis of coke, wood charcoal and Bamboo Charcoal by Raman spectroscopy and their reaction rate with CO_2. *ISIJ International*, 45 1027-1034

Keown DM, Hayashi JI, and Li CZ (2008). Drastic changes in biomass char structure and reactivity upon contact with steam, *Fuel* 87, 1127–1132.

Kerkkonen O(1997). Influence of ash reactions on feed coke degradation in the blast furnace. *Coke Making International,* 9-34-41.

Kosminski A , Ross DP and Agnew JB (2006). Reactions between sodium and kaolin during gasification of a low rank coal . *Fuel Processing Technology*, 87, 1051-1062.

Kruszewska, KJ (2003). Fluorescing macerals in South Africa coals. *International Journal of Coal Geology,* 23, 79-94.

Li X, Hayashi J and Li CZ, (2006). FT-Raman spectroscopic study of the evolution of char structure during the pyrolysis of a Victorian brown coal. *Fuel***,** *85*, 1700-1707.

Li CZ (2007). Some recent advances in the understanding of the pyrolysis and gasification behaviour of Victorian brown coal, *Fuel,* 86, 1664–1683.

Li S and Whitty KJ (2009). Investigation of coal char-slag transition during oxidation: Effect of temperature and residual carbon. *Energy & Fuels,* 23, 1998-2005.

Li J, Du MF, Zhang ZH, Guan RQ, Chen YS, and Liu TY (2009) Selection of fluxing agent for coal ash and investigation of fusion mechanism: A first-principles study. *Energy & Fuels*, 23, 704-709.

Lin SY, Harito M, Horio M.(1994) Characteristics of coal char gasification at around ash melting melting temperature. *Energy & Fuels*, 8, 598-606.

Liu H, Luo C, Kato S, Uemiya S,Kaneko M and Toshinori Kojima (2006). Kinetics of CO_2/Char gasification at elevated temperatures: Part I Experimental results *Fuel Processing Technology*, *87, 775-781.*

Liu C (2007). Some recent advances in the understanding of pyrolsis and gasification behaviour of Victorian brown coal. *Fuel,* 86, 1664-1683.

Lu L, Sahajwalla D and Harris D (2000) Characteristics of chars prepared from various pulverised coals at different temperatures using drop tube furnace. *Energy & Fuels*, 14, 869-676.

Lu L, Sahajwalla D, Kong C and Harris D (2001) Quantitative X-ray diffraction analysis and its application to various coals. Fuel, 39, 1821-1833.

Lunden MM, Yang NYC, Headley J and Shaddix CR (1998). Mineral-char interactions during char combustion of a high volatile coal. *Proceedings of Combustion Institute,* 1695-1702.

Maity S and Choudhury A (2008). Influence of Nitric Acid Treatment in Different Media on X-ray Structural Parameters of Coal. *Energy and Fuels,* 22, 4087-4091.

Matije RH, French D, Ward CR, Pistorius PC and Zhonsheng L (2011). Behaviour of coal matter in sintering and slagging of ash during the gasification process. *Fuel Processing Technology*, 92, 1426-1433.

Matsuoka K, Suzuki Y, Eylands K, Benson S and Tomita A (2006). CCSEM study of ash forming reactions during lignite gasification. *Fuel,* 85, 2371-2376.

Mendez Lb, Borrego AG, Martinez-Tarazona MR and Menedez R (2003). Influence of petrograhic and mineral composition of coal particles on their combustion reactivity. *Fuel,* 1875- 1882.

Messenbock RC, Paterson NP, Dugwell DR, Kandiyoti RK (2000), Factors governing reactivity in low temperature coal gasification. Part I. An attempt to correlate results from a suite of coals with experiments on maceral concentrates *Fuel, 79*, 109-121.

Murphy JJ and Shaddix CR (2010). Effect of reactivity loss on apparent reaction order of burning char particles. *Combustion and Flame, 157*, 535-539.

Ninomiya Y and Sato A (1997). Ash melting behaviour under coal gasification conditions. *Energy Conversation and Management,* 38, 1405-1412.

Oboirien BO, Engelbrecht AD, North BC, Du Cann VM, Verryn S and Falcon R. (2011). Study on structure and gasification characteristics of selected South African bituminous coal in fluidised bed gasification *Fuel Processing Technology*, 92, 735-742.

Painter P, Sobkowiak M, Heidary S and Coleman M (1994). Current status of FT-IR the analysis of coal structure *Am. Chem. Soc. Div. Fuel Chem.39 (1)*,49-53.

Pinetown KL, Ward CR and van der Westhuizen WA (2007). Quantitative evaluation of minerals in coal deposits in the Witbank and Highveld Coalfields, and the potential impact on acid mine drainage. *International Journal of Coal Geology,* 77, 166-183.

Pusz S, Duber S and Kwiecinska BK (2002). The study of textural and structural transformations of carbonised anthracites. *Fuel Processing Technology*, 77-78, 173-180.

Pusz S, Krzesinka M, Smedoski L, Majewska J, Pilawa B and Kwiecinska B (2010). Changes in a coke structure due to reaction with carbon dioxide *International Journal of Coal Geology*, 81, 287-292.

Rathnam RK, Elliott L, Wall TF, Liu Y and Moghtaderi B (2009). Differences in reactivity of pulverised coal in air (O_2/N_2) and oxy-fuel (O_2/CO_2) conditions. *Fuel Processing Technology,* 90,797-802.

Rouzand JN and Oberlin A (1989). Structure, microtexture, and optical properties of anthracene and saccharose-based carbons. *Carbon*, *27, 517-529.*

Rusell NV, Beeley TJ , and Man CK (1998). Development of TG measurement of intrinsic char combustion reactivity for industrial and research purpose. *Fuel Processing Technology,* 57, 113-130.

Sadezky A, Muckenhuber H, Grothe- H, Niessner R and Pöschl U (2005). Raman microspectroscopy of soot and related carbonaceous materials: Spectral analysis and structural information. *Carbon,* 43, 1731-1742.

Salatino P and Senneca O (2007). Overlapping of purely thermally activated and heterogeneous processes in combustion and gasification of solid fuels. Third European Combustion Meeting ECM 2007.

Schimmoller BK (2005). Coal gasification: striking while the iron is hot. *Power Engineering*, 30-40.

Schreiner WN (1995). A standard test method for the determination of RIR values by X-ray diffraction. *Powder Diff*, 10, 25-33.

Sekine Y, Ishikawa K, Kikuchi E, Matsukata M and Akimoto A (2006). Reactivity and structural change of coal during steam gasification. *Fuel,* 85, 122-126.

Senneca O, Salatino P and Masi (1998). Microstructural changes and loss of gasification reactivity of chars upon reactivity of chars upon heat treatment. *Fuel*, 77, 1483-1493.

Senneca O and Salatino P (2002). Loss of gasification reactivity toward O_2 and CO_2 upon heat treatment of carbons. *Proceedings of the Combustion Institute*, 29, 485-493.

Senneca O, Salatino P and Menghini D (2007). The influence of thermal annealing on oxygen uptake and combustion rates of a bituminous coal char. *Proceedings of the Combustion Institute, 31,1889-1995*

Shannon GN, Matsuura H, Rozelle P, Fruehan RJ, Pisupati S and Sridhar S (2009). Effect of size and density on the thermodynamic predictions of coal particle phase formation during coal gasification. *Fuel Processing Technology*, 90, 1114-1121.

Sharma A, Kyotani T and Tomita A (2000). Direct Observation of Raw Coals in Lattice Fringe Mode Using High-Resolution Transmission Electron Microscopy. *Energy & Fuels,* 14, 1219-1225.

Sharma A, Kadooka H, Kyotani T and Tomita A (2002). Effect of microstructural changes on gasification reactivity of coal during low temperature gasification. *Energy & Fuels,* 16, 54-61.

Sharonova OM, Anshits NN, Yumashev VV, and Anshits AG (2008). Composition and morphology of char particles of fly ashes from industrial burning-ash coals with different reactivity. *Fuel,* 87, 1989-1997.

Sheng C (2007). Char structure characterised by Raman spectroscopy and correlations with combustion reactivity. *Fuel*, 86, 2316-2324.

Shirazi AR, Bortin O, Eklund L and Lindqvist O (1995). The impact of minerals matter in coal on its combustion and a new approach to the determination to the determination of the calorific value of coal. *Fuel*, 74, 247- 251.

Srinivasachar S Helble JJ and Boni AA (1990) Mineral behaviour during coal combustion 1. Pyrite transformations . *Progress in Energy and Combustion Science*, 6, 28-292.

Street PJ; Weight RP and Lightman P (1969). *Fuel , 48*, 343-365.

Sun Q, Li W, Chen H and Li B (2003). The variation of structural characteristics of macerals during pyrolysis, *Fuel*, 82, 669-676.

Taylor GH, Teichmuller M, Davis A, Diessel CFK, Littke R, and Roberts P (1998). Organic Petrology: a New Handbook Incorporating Some Revised Parts of Stach's Textbook of Coal Petrology. Gebrueder Borntrager, Berlin.

Tran KN, Berkovich AJ, Tomsett A and Bhatia SK (2008). Crystalline structure of carbon anodes during gasification. *Energy &Fuels*, 22, 1902-1910.

Tuinstra F and Koenig JL (1970). Raman spectrum of graphite. *J Chem Phys,* 53N, 1126-1130.

Valero A and Sergio U (2006). Oxy-co-gasification of coal and biomass in an integrated gasification combined cycle (IGCC) power plant. *Energy,* 31, 1643-1655.

Van Dyk JC, Melzer S, Sobiecki A (2006). Mineral matter transformation during Sasol fixed bed dry bottom gasification-utilisation of HT-XRD and Factsage modelling . *Mineral Engineering* 19, 1126-1135.

Van Niekerk D, Pugmire RJ, Solum MS, and Mathews JP (2008). Structural characterisation of vitrinite-rich and inertinite-rich Permian-aged South African bituminous coals. *International Journal of Coal Geology,* 76, 290-300.

Wang W, Thomas KM, Poultney RM and Willmers RR (1995). Iron catalysed graphitisation in the blast furnace. *Carbon,* 11, 1525-1535.

Wang J, Du J, Chang L and Xie K (2009). Study on the structure and pyrolysis characteristics of Chinese western coals. *Fuel Processing Technology*, 91 430–433.

Wu S, Gu J, Zhang X, Wu Y and Gao J (2008). Variation of carbon crystalline structures and CO_2 gasification reactivity of Shenfu coal chars at elevated temperatures. *Energy & Fuels*, 22, 199-206.

Wu X, Zhang Z, Chen Y, Zhou T, Fan J, Pao G, Kobayashi N, Mori S and Itaya Y (2010). Main mineral melting behwviour and mineral reaction mechanism at molecular level of blended ash under gasification condition. *Fuel Processing Technology*, 91, 1591-1600

Xu S, Zhou Z, Gao X, Yu G and Gong X (2009). The gasification reactivity of unburned carbon present in gasification slag from entrained–flow gasifier. *Fuel Processing Technology,* 90, 1062-1070.

Yan R, Liang DT, Laursen K, Li Y, L. Tsen Land Tay JH (2003) Formation of bed Agglomeration in a Fluidized Multi-Waste Incinerator. *Fuel,* 82, 843–851

Ye DP, Agnew JB and Zhang DK (1997). Gasification of South Australian low-rank coal with carbon dioxide and steam: Kinetics and reactivity studies. *Fuel,* 77, 1029-1219.

Yu J, Lucas J, Strezov V and Wall T (2003). Swelling and char structures from density fractions of pulverised coal. *Energy & Fuels*, 17, 1160-1174.

Zhang S, Lu J, Zhang J and Yue G (2008). Effect of pyrolysis intensity on the reactivity of coal char. *Energy & Fuels*, 22, 3213-3221.

Zhang H, Pu W, Ha S, Li Y and Sun M (2009). The influence of included mineral on the intrinsic reactivity of chars prepared at 900 ^{O}C in a drop tube furnace and muffle furnace. *Fuel,* 88, 2303-2310.

Zhang Z, Wu X, Zhou T, Chen Y, Hou N, Piao G, Kobayashi N, Itaya Y and Mori S (2011). The effect of iron-bearing mineral behaviour on ash deposition during coal combustion. *Proceedings of the Combustion Institute*, 33, 2853-2861.

Zhang L, Jiao F, Binner E, Battacharya S,Ninomiya Y and Li C (2011). Experimental investigation of the combustion of coal in air and O_2/CO_2 mixtures: 2. Variation of the transformation behaviour of mineral matter with bulk composition. *Fuel*, 90, 1361-1369.

Zhu W, Song W and Lin W (2008). Effect of particle size on pyrolysis and char reactivity for two types of coal and demineralised coal. *Energy & Fuels*, 22, 2482-2487.

Zhuo Y, Lemaignen L, Chatzakis IN, Reed GP, Dugwell DR and Kandiyoti R (2000). An attempt to correlate conversions in pyrolysis and gasification with FT-IR spectra of coals. *Energy & Fuels*, 14, 1049-1058.

Appendix A

TABLE 1: CHAR SCAN REFLECTANCE DATA

Rr %	1 GROOTEGELUK CHAR SCAN PSA 2009 48	2 MATLA CHAR SCAN PSA 2009 49	3 DUHVA CHAR SCAN PSA 2009 50
	MEAN Rsc % 4.96	MEAN Rsc % 4.77	MEAN Rsc % 5.08
	σ 1.001	σ 1.230	σ 0.993
	RANGE % 2.1 - 7.9	RANGE % 2.1 - 7.5	RANGE % 2.4 - 7.7
	RELATIVE FREQUENCY %	RELATIVE FREQUENCY %	RELATIVE FREQUENCY %
2.0			
2.1	0.8	1.0	
2.2		2.0	
2.3			
2.4	0.8	2.0	0.4
2.5		1.0	0.4
2.6	0.4	1.0	0.4

2.7		0.4								0.4		
2.8						1.0				0.4		
2.9	> 2 < 3%	0.4		2.8	> 2 < 3%			8.0	> 2 < 3%	0.4		2.4
3.0		1.6				1.0				0.4		
3.1						1.0				1.2		
3.2		0.4				1.0				0.4		
3.3		0.4				1.0				0.4		
3.4		0.8				1.0				0.8		
3.5		4.0				1.0				2.4		
3.6		1.2				3.0				2.0		
3.7		0.8				5.0				2.0		
3.8		3.6				1.0				1.6		
3.9	> 3 < 4%	2.4		15.2	> 3 < 4%	4.0		19.0	> 3 < 4%	1.2		12.4
4.0		3.2	12.8			3.0	12.0			1.6	6.4	
4.1		2.0	8.2			4.0	16.4			1.6	6.6	
4.2		4.4	18.5			2.0	8.4			2.8	11.8	
4.3		1.6	6.9			3.0	12.9			2.0	8.6	
4.4		3.2	14.1			5.0	22.0			3.2	14.1	
4.5		3.2	14.4			2.0	9.0			4.0	18.0	
4.6		3.2	14.7			2.0	9.2			2.0	9.2	
4.7		4.0	18.8			1.0	4.7			3.2	15.0	
4.8		2.8	13.4			3.0	14.4			5.2	25.0	
4.9	> 4 < 5%	3.6	17.6	31.2	> 4 < 5%	3.0	14.7	28.0	> 4 < 5%	4.8	23.5	30.4
5.0		3.6	18.0			4.0	20.0			4.0	20.0	
5.1		2.0	10.2			3.0	15.3			3.2	16.3	
5.2		3.2	16.6			4.0	20.8			6.0	31.2	
5.3		5.2	27.6			7.0	37.1			4.0	21.2	

5.4		2.0	10.8			1.0	5.4			3.2	17.3			
5.5		5.6	30.8			1.0	5.5			5.2	28.6			
5.6		7.6	42.6			3.0	16.8			6.4	35.8			
5.7		3.6	20.5			3.0	17.1			1.6	9.1			
5.8		1.2	7.0			2.0	11.6			3.2	18.6			
5.9	> 5 < 6%	5.2	30.7	39.2	> 5 < 6%	1.0	5.9	29.0	> 5 < 6%	2.8	16.5	39.6		
6.0			0.0			3.0	18.0			3.6	21.6			
6.1		1.6	9.8			2.0	12.2			2.4	14.6			
6.2		2.4	14.9				0.0			1.6	9.9			
6.3		1.2	7.6			2.0	12.6			0.4	2.5			
6.4		1.2	7.7			1.0	6.4			1.2	7.7			
6.5		2.0	13.0			1.0	6.5				0.0			
6.6		1.2	7.9				0.0			1.2	7.9			
6.7		0.4	2.7			1.0	6.7				0.0			
6.8			0.0			1.0	6.8			0.4	2.7			
6.9	> 6 < 7%	0.4	2.8	10.4	> 6 < 7%		0.0	11.0	> 6 < 7%	1.2	8.3	12.0		
7.0		0.4	2.8				0.0			0.4	2.8			
7.1			0.0			1.0	7.1			0.4	2.8			
7.2		0.4	2.9			1.0	7.2				0.0			
7.3			0.0			1.0	7.3			0.8	5.8			
7.4			0.0			1.0	7.4			0.4	3.0			
7.5	> 7%		0.0	1.2	> 7%	1.0	7.5	5.0	> 7%		0.0	3.2		
7.6			0.0				0.0				0.0			
7.7			0.0				0.0			1.2	9.2			
7.8			0.0				0.0				0.0			
7.9		0.4	3.2				0.0				0.0			
8.0			0.0				0.0				0.0			

8.1	**0.0**	**0.0**	**0.0**
8.2	**0.0**	**0.0**	**0.0**
8.3	**0.0**	**0.0**	**0.0**
8.4	**0.0**	**0.0**	**0.0**
8.5	**0.0**	**0.0**	**0.0**
8.6	**0.0**	**0.0**	**0.0**
8.7	**0.0**	**0.0**	**0.0**
8.8	**0.0**	**0.0**	**0.0**
8.9	**0.0**	**0.0**	**0.0**
9.0	**0.0**	**0.0**	**0.0**
9.1	**0.0**	**0.0**	**0.0**
9.2	**0.0**	**0.0**	**0.0**
9.3	**0.0**	**0.0**	**0.0**
9.4	**0.0**	**0.0**	**0.0**
9.5	**0.0**	**0.0**	**0.0**
9.6	**0.0**	**0.0**	**0.0**
9.7	**0.0**	**0.0**	**0.0**
9.8	**0.0**	**0.0**	**0.0**
9.9	**0.0**	**0.0**	**0.0**
10.0	**0.0**	**0.0**	**0.0**

Appendix B

ID/IG Ratio for Grootegeluk Char

0.817215	**0.980919**	**0.934859**	**0.706037**	**0.996089**	**0.955031**	**0.652962**
0.877143	0.786641	0.749444	0.822403	0.840476	0.852927	0.932969
0.761932	0.758061	0.952003	0.756862	0.804988	0.891459	0.837959
0.977824	0.848467	0.797345	0.825913	0.929098		0.838038
0.859918	0.69891	0.95085	0.878814	0.8482	0.776111	0.82763
0.724253		0.810459	0.867494	1.09737	0.740462	0.673432
0.862322	0.833222	0.607278		0.809965	0.773242	0.756862

IV/IG Ratio for Grootegeluk char

0.798705	1.091695	1.023392	2.306253	0.811916	0.943618	0.799921
1.251162	0.705878	0.688601	0.737781	0.837033	0.800452	0.946619
1.068179	0.717089	0.904243	0.615369	1.081411	1.243582	0.717242
0.865486	0.998978	0.83722	0.972308	0.815729		0.661457
0.627879	1.27071	0.969617	0.826314	0.846122	0.907753	0.748977
0.872567		1.057735	0.973645	0.955325	1.228581	0.7634
0.724361	0.746088	1.160475		0.753085	0.891575	0.615369

ID/IG ratio for New Vaal Char

1.330441	1.434369	1.391787	1.62867	1.377717	0.99007	1.367921
1.323016	1.272014	1.302326	1.219747	1.317636	1.150451	1.386522
1.473403	1.221254	1.360621	1.320656	1.268913	1.379274	1.220736
1.209601	1.315254	1.408005	1.292058	0.971682	1.169516	0.979139
1.207464	1.071642	1.071167	1.346875	1.23286	1.184062	1.305777
1.457016	0.985017	1.047079	1.438223	1.43886	0.971892	1.15006
0.995502	0.896486	1.076995	1.198987	1.2094	1.05488	1.192121

IV/IG ratio for New Vaal Char

0.730712	0.798773	0.794068	1.017322	0.743811	0.676831	0.923568
0.6951	0.709349	0.741875	0.720464	0.886105	0.812047	0.62005
0.81905	0.803465	0.738403	0.636363	0.73411	0.916939	0.839286
0.720857	0.962186	0.808245	0.791452	0.657805	0.925915	0.622407
0.706319	0.816756	0.590428	0.982137	0.915874	0.953071	1.000126
0.812118	0.630065	0.708447	0.919247	0.850071	0.680613	0.793357
0.639951	0.593094	0.691593	0.746116	0.75523	0.759155	0.732513

Appendix C List of Publications

(i) **B.O Oboirien**, A.D Engelbrecht, B.C North, Vivien M. Du Cann and R Falcon (2011). Textural properties of chars as determined by petrographic analysis: Comparison between air-blown, oxygen-blown and oxygen-enriched gasification. Fuel (*In press*).

(ii) **B.O Oboirien**, A.D Engelbrecht, B.C North, R Erasmus and R Falcon (2011). Mineral-char interaction during the gasification of high ash coals in a fluidised bed gasifier. *Energy Fuels,*25, 5189-5199

(iii) **B.O Oboirien**, A.D Engelbrecht, B.C North, Vivien M. Du Cann, S Veryn and R Falcon (2011). Study on structure and gasification characteristics of selected South African bituminous coal in fluidised bed gasification. *Fuel Processing Technology.* 92, 735-742.

(iv) **B.O. Oboirien,** A.D. Engelbrecht, B.C North and R. Falcon (2011) Mineral-char interaction during the gasification of high ash coals in a fluidised bed gasifier: Redistribution of mineral phases within the char matrix Paper to be presented to the International Conference of Coal Science and Technology. Oviedo, Spain. October, 2011.

(v) **B.O Oboirien,** A.D Engelbrecht, B.C North, V.M. Du Cann, S. Verryn and R Falcon. (2010). Textural Properties of Chars as Determined by Petrographic Analysis: Comparison between air-blow, oxygen-blown and oxygen-enriched gasification. Paper presented to the 8th European Conference on Coal research and its Applications: ECCRIA 2010. Leeds, United Kingdom. September 2010.

(vi) **B.O Oboirien**, A.D Engelbrecht, B.C North, Vivien M. Du Cann and R Falcon (2009). Study on structure and gasification characteristics of selected South African bituminous coal in fluidised bed gasification. International Conference on Coal Science and Technology, 26-29th October, 2009, Cape Town.

(vii) **B.O Oboirien**, A.D Engelbrecht, B.C North, Vivien M. Du Cann and R Falcon (2009). Characterisation of coal and char in fluidised bed gasification.14th South African Coal Science and Technology Conference, 11-12th March, 2009, Johannesburg.